UNIVERSIDADE FEDERAL DE MINAS GERAIS
FACULDADE DE FARMÁCIA
PROGRAMA DE PÓS-GRADUAÇÃO EM CÊNCIAS FARMACÊUTICAS

ELIZA ROCHA GOMES

EXOSSOMAS FUNDIDOS COM LIPOSSOMAS pH-SENSÍVEIS DE CIRCULAÇÃO PROLONGADA CONTENDO DOXORRUBICINA: PREPARO, CARACTERIZAÇÃO, AVALIAÇÃO DA TOXICIDADE AGUDA E DA ATIVIDADE ANTITUMORAL

Belo Horizonte
2022

ELIZA ROCHA GOMES

EXOSSOMAS FUNDIDOS COM LIPOSSOMAS pH-SENSÍVEIS DE CIRCULAÇÃO PROLONGADA CONTENDO DOXORRUBICINA: PREPARO, CARACTERIZAÇÃO, AVALIAÇÃO DA TOXICIDADE AGUDA E DA ATIVIDADE ANTITUMORAL

Tese apresentada ao Programa de Pós-Graduação em Ciências Farmacêuticas da Faculdade de Farmácia da Universidade Federal de Minas Gerais, como requisito parcial à obtenção do grau de Doutora em Ciências Farmacêuticas.

Orientadora: Profa. Dra. Mônica Cristina de Oliveira

Belo Horizonte

2022

Gomes, Eliza Rocha.
G633e Exossomas fundidos com lipossomas pH-sensíveis de circulação prolongada contendo doxorrubicina: preparo, caracterização, avaliação da toxicidade aguda e da atividade antitumoral [recurso eletrônico] / Eliza Rocha Gomes. – 2022.
1 recurso eletrônico (98 f. : il.) : pdf

Orientadora: Mônica Cristina de Oliveira.

Tese (doutorado) – Universidade Federal de Minas Gerais, Faculdade de Farmácia, Programa de Pós-Graduação em Ciências de Farmacêuticas.

Exigências do sistema: Adobe Acrobat Reader.

1. Câncer de mama – Teses. 2. Lipossomas – Teses. 3. Doxorrubicina – Teses. 4. Metástase – Teses. I. Oliveira, Mônica Cristina de. II. Universidade Federal de Minas Gerais. Faculdade de Farmácia. III. Título.

CDD: 616.994

Elaborado por Aline Guimarães Amorim – CRB-6/2292

UNIVERSIDADE FEDERAL DE MINAS GERAIS
FACULDADE DE FARMÁCIA
PROGRAMA DE PÓS-GRADUAÇÃO EM CIÊNCIAS FARMACÊUTICAS

ATA DA DEFESA DE TESE DA ALUNA ELIZA ROCHA GOMES

Realizou-se, no dia 18 de agosto de 2022, às 13:30 horas, em formato remoto, a 167ª defesa de tese, intitulada *EXOSSOMAS FUNDIDOS COM LIPOSSOMAS pH-SENSÍVEIS DE CIRCULAÇÃO PROLONGADA CONTENDO DOXORRUBICINA: PREPARO, CARACTERIZAÇÃO, AVALIAÇÃO DA TOXICIDADE AGUDA E DA ATIVIDADE ANTITUMORAL*, apresentada por ELIZA ROCHA GOMES, número de registro 2018710014, graduada no curso de FARMÁCIA, como requisito parcial para a obtenção do grau de Doutora em CIÊNCIAS FARMACÊUTICAS, à seguinte Comissão Examinadora: Prof(a). Mônica Cristina de Oliveira - Orientadora (UFMG), Prof(a). Sávia Caldeira de Araújo Lopes (Hospital de Aeronáutica de Lagoa Santa), Prof(a). Lucas Antônio Miranda Ferreira (UFMG), Prof(a). Frederic Jean Georges Frezard (UFMG), Prof(a). Izabella Thaís da Silva (UFSC).

A Comissão considerou a tese:

(X) Aprovada

( ) Reprovada

Finalizados os trabalhos, lavrei a presente ata que, lida e aprovada, vai assinada por mim e pelos membros da Comissão.
Belo Horizonte, 18 de agosto de 2022.

Documento assinado eletronicamente por **Monica Cristina de Oliveira**, **Membro**, em 19/08/2022, às 10:39, conforme horário oficial de Brasília, com fundamento no art. 5º do Decreto nº 10.543, de 13 de novembro de 2020.

Documento assinado eletronicamente por **Frederic Jean Georges Frezard**, **Professor do Magistério Superior**, em 19/08/2022, às 11:31, conforme horário oficial de Brasília, com fundamento no art. 5º do Decreto nº 10.543, de 13 de novembro de 2020.

Documento assinado eletronicamente por **Savia Caldeira de Araújo Lopes**, **Usuário Externo**, em 19/08/2022, às 14:11, conforme horário oficial de Brasília, com fundamento no art. 5º do Decreto nº 10.543, de 13 de novembro de 2020.

Documento assinado eletronicamente por **Izabella Thais da Silva**, **Usuário Externo**, em 19/08/2022, às 14:32, conforme horário oficial de Brasília, com fundamento no art. 5º do Decreto nº 10.543, de 13 de novembro de 2020.

Documento assinado eletronicamente por **Lucas Antonio Miranda Ferreira**, **Professor do Magistério Superior**, em 19/08/2022, às 15:52, conforme horário oficial de Brasília, com fundamento no art. 5º do Decreto nº 10.543, de 13 de novembro de 2020.

A autenticidade deste documento pode ser conferida no site https://sei.ufmg.br/sei/controlador_externo.php?acao=documento_conferir&id_orgao_acesso_externo=0, informando o código verificador **1666206** e o código CRC **BD10CF04**.

AGRADECIMENTOS

A Deus por me abençoar, iluminar meu caminho e me dar força perante as dificuldades.

Aos meus pais, por tudo que representam, pelo amor, apoio incondicional em todas as minhas decisões e por se orgulharem tanto de mim.

Aos meus irmãos e ao Márcio, pelo apoio, carinho e amizade. Ao Arthur, pelos momentos de alegria e diversão.

À Professora Mônica, pela orientação, disponibilidade e ensinamentos oferecidos ao longo desses anos. Agradeço pelo seu exemplo de profissionalismo e pela honra de ter sido orientada por uma professora de tamanha competência. Muito obrigada por todo carinho e respeito durante todo esse tempo.

Aos colaboradores, Thiago, Luiza, Andrea Teixeira e Fernanda e aos Professores André e Geovanni, muito obrigada pela ajuda indispensável com os experimentos.

Aos membros da banca examinadora pela disponibilidade em participar e pelas valiosas considerações para o enriquecimento do trabalho.

À equipe LTF, alunos e professores, obrigada pelo carinho da convivência diária, pela troca de experiências e pela disposição em ajudar sempre.

Às minhas sis, Marjorie e Marina, pelos anos de amizade, pelas trocas de experiência e desabafos e, por participarem dessa trajetória junto comigo.

À Jaque, Cibele e Edu muito obrigada pelos anos de convivência no lab e fora dele.

Às amigas, desde a graduação, Kel, Rúbia, Mari e Lela, muito obrigada por tantos momentos especiais durante todos esses anos.

Aos funcionários da FAFAR-UFMG, em especial Adelaide, Batista, Fernanda, Nazaré, e Marton, pela gentileza e auxílio sempre que necessário.

À FAPEMIG, CAPES e CNPq pelo apoio financeiro e bolsas de estudo concedidas.

Agradeço a todos que participaram direta e indiretamente para a conclusão deste trabalho. Muito obrigada!

RESUMO

A doxorrubicina (DOX) apresenta uma potente ação antineoplásica e vem sendo utilizada no tratamento de diversos tumores. Entretanto, graves efeitos tóxicos têm limitado seu uso, principalmente a cardiotoxicidade. Recentemente, nanocarreadores híbridos obtidos pela fusão das membranas lipídicas de exossomas e lipossomas vêm sendo estudados, a fim de aumentar a eficácia antitumoral, minimizar os efeitos adversos e contornar os problemas relacionados a resistência de quimioterápicos. A proposta desse estudo consistiu na fusão de exossomas derivados de células de mama tumorais com lipossomas pH-sensíveis de circulação prolongada contendo DOX para tratamento de câncer de mama (ExoSpHL-DOX). O diâmetro médio das vesículas foi de 100,8 ± 7,8 nm, o índice de polidispersão igual a 0,122 ± 0,004 e o teor de DOX encapsulado foi de 83,5 ± 2,5%. A fusão de exossomas com lipossomas pH-sensíveis de circulação prolongada foi confirmada por espectroscopia de infravermelho com transformada de Fourier, espectroscopia Raman e nanocitometria de fluxo. A avaliação da estabilidade de armazenamento dos ExoSpHL-DOX a 4°C comprovou a manutenção das características físico-químicas da formulação por 60 dias. O estudo de liberação de DOX a partir de ExoSpHL-DOX em meios de diluição apresentando diferentes valores de pH, comprovou a característica de pH-sensibilidade do nanossistema. A formulação mostrou-se citotóxica para células tumorais 4T1 de mama murina. A toxicidade aguda foi determinada pela avaliação da mortalidade e morbidade dos animais, análises hematológicas, bioquímicas e histopatológicas, após uma única administração intravenosa de ExoSpHL-DOX. O intervalo de dose letal mediana (LD50) encontrado após o tratamento com ExoSpHL-DOX (17,5 - 20 mg/kg) é maior do que o encontrado com DOX livre (12,5 - 15 mg/kg). Além disso, ExoSpHL-DOX não apresentou sinais de nefrotoxicidade mesmo na dose mais elevada de DOX, indicando que o nanocarreador híbrido pode alterar a distribuição de DOX e reduzir o dano renal. Em relação à atividade antitumoral, ExoSpHL-DOX inibiu em aproximadamente 50% o crescimento do tumor comparado ao grupo controle. Além disso, o nanocarreador híbrido de exossomas-lipossomas reduziu o número de focos metastáticos nos pulmões. Esses resultados indicam que ExoSpHL-DOX pode ser um nanocarreador promissor para o tratamento do câncer de mama, reduzindo a toxicidade e inibindo a metástase, principalmente nos pulmões.

Palavras-chave: câncer de mama; lipossomas; exossomas; doxorrubicina; metástase.

ABSTRACT

Doxorubicin (DOX) has a potent antineoplastic action and has been used in the treatment of several tumors. However, serious toxic effects have limited its use, especially cardiotoxicity. Recently, hybrid nanocarriers obtained by fusion of lipid membranes of exosomes and liposomes have been studied in order to increase antitumor efficacy, minimize adverse effects and overcome problems related to chemotherapy resistance. Thus, the purpose of this study was the fusion of exosomes derived from breast tumor cells with long-circulating and pH-sensitive liposomes containing DOX (ExoSpHL-DOX) for the treatment of breast cancer. The mean diameter of ExoSpHL-DOX was 100.8 ± 7.8 nm, the polydispersity index was 0.122 ± 0.004, and the encapsulated DOX content was equal to 83.5 ± 2.5%. The fusion of exosomes with long-circulating and pH-sensitive liposomes was confirmed by Fourier transform infrared spectroscopy, Raman spectroscopy, and nano-flow cytometry. The physicochemical characteristics of ExoSpHL-DOX were maintained for 60 days, at 4°C. The study of the release of DOX from ExoSpHL-DOX in dilution media with different pH values showed the pH-sensitivity of the nanosystem. The cytotoxic study against the 4T1 breast cancer cell line demonstrated that ExoSpHL-DOX treatment significantly reduced the cancer cell viability. Acute toxicity was determined by evaluating the mortality and morbidity of the animals, hematological, biochemical, and histopathological analyses, after a single intravenous administration of ExoSpHL-DOX. The results of the study indicated that the median lethal dose range (LD50) of the ExoSpHL-DOX treatment (17.5 - 20 mg/kg) is higher than that found for treatment with free DOX (12.5 - 15 mg/kg). In addition, ExoSpHL-DOX treatment showed no signs of nephrotoxicity even at the highest dose of DOX, indicating that the presence of hybrid nanocarrier may alter the distribution of DOX and reduce kidney damage. Regarding to the antitumor activity, ExoSpHL-DOX treatment inhibited close to 50% the tumor growth compared to control group. Furthermore, the hybrid nanocarrier of tumor-derived exosomes fused with long-circulating and pH-sensitive liposomes reduced the number of metastatic foci in the lungs. These results indicate that ExoSpHL-DOX may be a promising nanocarrier for the treatment of breast cancer, reducing toxicity and inhibiting metastasis, mainly in the lungs.

Keywords: breast cancer; liposomes; exosomes; doxorubicin; metastasis.

LISTA DE FIGURAS

Figura 1 - Distribuição proporcional dos dez tipos de câncer mais incidentes estimados para 2020-2022 por sexo, no Brasil..... 14
Figura 2 - Anatomia da mama humana feminina..... 16
Figura 3 - Estrutura química da doxorrubicina..... 18
Figura 4 - Representação esquemática da estrutura de lipossomas..... 20
Figura 5 - Representação esquemática dos principais fosfolípides..... 21
Figura 6 - Classificação de lipossomas de acordo com o tamanho e o número de lamelas..... 22
Figura 7 - Estrutura química da distearoilfosfatidiletanolamina acoplada ao polietilenoglicol 2000 (DSPE-PEG_{2000})..... 23
Figura 8 - Representação esquemática das principais características de lipossomas como carreadores de fármacos para o tratamento do câncer e sua evolução..... 24
Figura 9 - Representação esquemática das mudanças de fases em lipossomas pH-sensíveis compostos por DOPE e CHEMS..... 25
Figura 10 - Biogênese dos exossomas..... 27
Figura 11 - Representação esquemática da fusão de lipossomas com exossomas..... 31

CAPÍTULO 1

Figure 1 - CryoTEM photomicrographs of exosomes (A), SpHL (B) and ExoSpHL (C)..... 45
Figure 2 - Raman spectra of exosomes, SpHL, ExoSpHL and exosomes+SpHL physical mixture..... 46
Figure 3 - FTIR spectra of exosomes, SpHL, ExoSpHL and exosomes+SpHL physical mixture..... 47
Figure 4 - Exosomes isolation and fusion with long-circulating and pH-sensitive liposomes evaluated by nano-flow cytometry..... 48
Figure 5 - ExoSpHL-DOX size, PDI (A), and concentration of DOX (B) up to 60 days at 4 °C..... 49
Figure 6 - Release profile of ExoSpHL-DOX at pH 5.0 and 7.4 at different times..... 50

Figure 7 - Evaluation of the vesicle diameter of ExoSpHL-DOX at pH 5.0 and 7.4 at different times..... 51

CAPÍTULO 2

Appendix A - Treatment scheme used to assess the median lethal dose (LD50) after treatment with free DOX..... 61

Appendix B - Treatment scheme used to assess the median lethal dose (LD50) after treatment with SpHL-DOX or ExoSpHL-DOX..... 62

Figure 1 - Histological sections of female Balb/c mice liver (A-B) and spleen (C-D). (A) Represents the control group (HBS) and the groups treated with SpHL-DOX and ExoSpHL-DOX at dose of 15 mg/kg. (B) Represents the groups treated with both doses of free DOX (10 and 12.5 mg/kg) and the groups treated with SpHL-DOX and ExoSpHL-DOX at dose of 17.5 mg/kg. (C) Represents the control group (HBS) and the groups treated with both tested doses of SpHL-DOX and ExoSpHL-DOX (15 and 17.5 mg/kg). (D) Represents the groups treated with both tested doses of free DOX (10 and 12.5 mg/kg)..... 68

Figure 2 - Histological sections of female Balb/c mice kidney (A-B). (A) Represents the control group (HBS), the groups treated with both doses of ExoSpHL-DOX (15 and 17.5 mg/kg), and SpHL-DOX at dose of 15 mg/kg. (B) Represents the groups treated with both tested doses of free DOX (10 and 12.5 mg/kg) and SpHL-DOX at dose of 17.5 mg/kg..... 69

Figure 3 - Histological sections of female Balb/c mice heart. (A) Represents the control group (HBS). (B) Represents the group treated with free DOX at dose of 10 mg/kg. Arrow indicates the areas of cardiomyocyte vacuolization. (C) Represents the group treated with free DOX at dose of 12.5 mg/kg. Arrow indicates the areas of cardiomyocyte vacuolization more intense than B. (D) Represents the groups treated with both doses of SpHL-DOX and ExoSpHL-DOX..... 70

Figure 4 - Antitumor efficacy evaluation of female Balb/c mice with 4T1 breast tumor. (A) Variation of the mice breast cancer tumor volume after treatment with HBS, DOX, SpHL-DOX, and ExoSpHL-DOX. Animals received intravenously five times, every 2 days, HBS (control), DOX at cumulative dose of 25 mg/kg, SpHL-DOX at cumulative dose of 25 mg/kg, or ExoSpHL-DOX at cumulative dose of 25 mg/kg. (B) Percentage of body weight variation, on day 10, after

administration of HBS (control), DOX at cumulative dose of 25 mg/kg, SpHL-DOX at cumulative dose of 25 mg/kg, or ExoSpHL-DOX at cumulative dose of 25 mg/kg treatments…… 72

Figure 5 - Representative photomicrographs of histological sections of primary tumor of female Balb/c mice bearing 4T1 breast tumor treated with (A) HBS or ExoSpHL. (B) DOX, SpHL-DOX or ExoSpHL-DOX at cumulative dose of 25mg/kg..... 73

Figure 6 - Representative photomicrographs of metastatic foci in lung (A) and liver (B) of female Balb/c mice bearing 4T1 breast tumor treated with HBS (control), ExoSpHL (control), DOX at cumulative dose of 25mg/kg, SpHL-DOX at cumulative dose of 25mg/kg or ExoSpHL-DOX at cumulative dose of 25mg/kg. Hematoxylin-eosin staining, amplification of 40X..... 74

Figure 7 - Histological sections of spleen (A-B) and heart (C-D) of female Balb/c mice bearing 4T1 breast tumor. (A) Represents the groups treated with SpHL-DOX and ExoSpHL-DOX. Normal spleen. (B) Represents the groups treated with HBS, ExoSpHL and DOX. (C) Represents the groups treated with HBS and ExoSpHL. Normal heart. (D) Represents the groups treated with DOX, SpHL-DOX and ExoSpHL-DOX…… 76

LISTA DE TABELAS

CAPÍTULO 1

Table 1 - NTA measurements of exosomes and ExoSpHL-DOX…….. 44

Table 2 - Quantification of total proteins in samples of SpHL, exosomes, and ExoSpHL……. 45

Table 3 - IC_{50} values for DOX, SpHL-DOX and ExoSpHL-DOX against 4T1 breast cancer cells..... 51

CAPÍTULO 2

Table 1 - Hematological parameters for healthy Balb/c mice treated with different doses of free DOX, SpHL-DOX or ExoSpHL-DOX……..... 66

Table 2 - Biochemical parameters for healthy Balb/c mice treated with different doses of free DOX, SpHL-DOX or ExoSpHL-DOX..... 67

Table 3 - Relative tumor volume and tumor growth inhibition after administration of HBS, free DOX, SpHL-DOX and ExoSpHL-DOX by intravenous route……..…… 73

Table 4 - Number of metastatic foci in the lungs of female Balb/c mice bearing 4T1 breast tumor treated with HBS, ExoSpHL, free DOX, SpHL-DOX or ExoSpHL-DOX. Animals received each treatment intravenously five times, every 2 days, at a dose of 5 mg/kg…….. 75

SUMÁRIO

1 INTRODUÇÃO..... 11
2 REVISÃO DA LITERATURA..... 13
2.1 Câncer..... 13
2.1.1 *Câncer de mama*..... 14
2.2 Tratamento do câncer de mama..... 16
2.2.1 *Doxorrubicina*..... 17
2.3 Lipossomas..... 19
2.3.1 *Lipossomas contendo doxorrubicina*..... 26
2.4 Exossomas..... 27
2.4.1 Aplicações de exossomas..... 29
2.4.2 Carreador híbrido de exossoma-lipossoma..... 30
3 OBJETIVOS..... 33
3.1 Objetivos geral..... 33
3.2 Objetivos específicos..... 33
CAPÍTULO 1 35
1 Introduction..... 37
2 Material and Methods..... 38
3 Results..... 43
4 Discussion..... 52
5 Conclusion..... 54
CAPÍTULO 2 55
1 Introduction..... 57
2 Material and Methods..... 58
3 Results..... 64
4 Discussion..... 76
5 Conclusion..... 79
4 DISCUSSÃO GERAL..... 80
5 CONCLUSÃO GERAL..... 85
6 PERSPECTIVAS..... 87
7 REFERÊNCIAS BIBLIOGRÁFICAS..... 88
PRODUÇÕES RELACIONADAS À TESE..... 95

1 INTRODUÇÃO

O câncer é uma das principais causas de morte no mundo e, portanto, um problema de saúde pública. De acordo com os dados do GLOBOCAN, os tipos de câncer mais incidentes no mundo são os de mama (2,26 milhões), pulmão (2,21 milhões), próstata (1,41 milhão) e cólon (1,15 milhão) (SUNG, 2021). Para o Brasil, a estimativa para cada ano do triênio 2020-2022 é de 625 mil novos casos de câncer, sendo que 66 mil novos casos são de câncer de mama (INCA, 2022; WHO, 2022). Além da grande incidência e prevalência, o câncer de mama é umas das principais causas de morbidade e mortalidade nas mulheres e, dessa maneira, novas estratégias terapêuticas tornam-se necessárias, visando o aumento da sobrevida das pacientes após a terapia (NÚÑEZ *et al*., 2016; SUNG, 2021). O tratamento do câncer de mama pode ser feito mediante cirurgia, radioterapia, terapia hormonal, imunoterapia e quimioterapia (TRAYES; COKENAKES, 2021). Diversas classes de quimioterápicos são empregadas no tratamento do câncer de mama e, dentre elas, os antibióticos antitumorais, como a doxorrubicina (DOX), apresentam grande importância (ZHAO; WOODLE; MIXSON, 2018; ACS, 2022). Os principais mecanismos de ação da DOX são geração de espécies reativas de oxigênio, que resulta em danos na membrana celular e ao DNA e inibição da topoisomerase II (AL-MALKY; AL-HARTHI; OSMAN, 2020). Entretanto, a elevada toxicidade, principalmente cardíaca, relacionada a DOX, bem como os mecanismos de resistência desenvolvidos pelas células a esse fármaco têm limitado o seu uso (JAMIALAHMADI; ZAHEDIPOUR; KARIMI, 2021). Com a intenção de minimizar os efeitos adversos da DOX a partir do direcionamento para a região tumoral, bem como contornar os problemas relacionados a resistência, vários nanossistemas carreadores de DOX têm sido desenvolvidos (ZHAO; WOODLE; MIXSON, 2018; FRAIX *et al.*, 2020; GHANDHARIYOUN *et al.*, 2020).

Dentre os diversos nanossistemas disponíveis, os lipossomas são sistemas versáteis que permitem a veiculação de substâncias hidrofílicas, lipofílicas e anfifílicas, bem como podem apresentar propriedades de direcionamento de fármacos para a região tumoral, podendo consequentemente aumentar a eficácia terapêutica e reduzir a toxicidade (GUIMARÃES; PAULO, NOGUEIRA, 2021). Recentemente, tais lipossomas têm sido fundidos com exossomas, obtendo nanocarreadores híbridos de exossoma-lipossoma, para melhorar a entrega de fármacos, aumentar a eficácia

antitumoral, inibir metástases e superar a resistência quimioterápica no tratamento de câncer (BUNGGULAWA *et al.*, 2018; LV *et al.*, 2020; SUN *et al.*, 2021).

Os exossomas são vesículas secretadas naturalmente por vários tipos de células, que contêm lípides, proteínas e ácidos nucleicos, e são responsáveis pela comunicação intercelular (GURUNATHAN; KANG; KIM, 2021). Recentemente, começaram a ser explorados para o uso como veículo de entrega de ácidos nucleicos, proteínas e fármacos. A entrega do fármaco às células é facilitada devido a presença de tetraspaninas e integrinas na superfície dos exossomas, que facilitam as interações de membrana e são responsáveis pelo direcionamento e entrada seletiva de exossomas nas células receptoras (LIANG *et al.*, 2021).

Diante disso, o uso de exossomas derivados de células tumorais de mama, fundidos com lipossomas pH-sensíveis de circulação prolongada contendo DOX pode ser uma alternativa promissora para o aumento da eficácia antitumoral, redução da toxicidade sistêmica e contornar os problemas relacionados a resistência ao fármaco, uma vez que essas vesículas favorecem o direcionamento, reconhecimento, fusão e liberação preferencial do seu conteúdo nas células tumorais.

2 REVISÃO DA LITERATURA

2.1 Câncer

Câncer é um conjunto de doenças caracterizadas por um crescimento descontrolado de células anormais, as quais ultrapassam seus limites usuais e possuem a capacidade de invadir e/ou se espalhar para outros tecidos e órgãos, por um processo chamado de metástase (INCA, 2022; WHO, 2022).

O surgimento do câncer (carcinogênese) se dá a partir de alterações em genes que regulam a multiplicação e a diferenciação das células. Em geral, o processo da carcinogênese ocorre lentamente e pode ser dividido em iniciação, promoção e progressão (VINCENT; GATENBY, 2008).

A aquisição de mutações, durante o processo de transformação neoplásica, faz com que as células adquiram capacidades funcionais como autossuficiência para os sinais de crescimento, insensibilidade aos sinais de inibição de crescimento, angiogênese sustentada, invasão tecidual e metástase, potencial ilimitado de replicação, resistência à morte celular, desregulação energética celular e evasão ao sistema imune. Além disso, as células cancerígenas possuem características habilitantes, que são instabilidade genômica e inflamação induzida pelos tumores. Outras características funcionais e habilitantes, ainda emergentes, são desbloqueio da plasticidade fenotípica, reprogramação epigenética não mutacional, microbiomas polimórficos e senescência celular (HANAHAN, 2022).

As causas do câncer são diversas, podendo ser externas e internas ao organismo, estando ambas inter-relacionadas. As causas externas referem-se ao meio ambiente e aos hábitos ou costumes próprios do indivíduo e, estão associadas a 80% dos casos de câncer. Os principais fatores de riscos são: tabagismo, alcoolismo, má alimentação, sedentarismo, alto índice de massa corporal, hábitos sexuais, fatores ocupacionais, exposição solar, radiação e medicamentos. As causas internas são, na maioria das vezes, geneticamente pré-determinadas, e são raros os casos de câncer que se devem exclusivamente a fatores hereditários (INCA, 2022).

O câncer é um enorme problema de saúde pública em todas as regiões e grupos socioeconômicos (WHO, 2022). Em 2020, ocorreram 19,3 milhões de novos casos de

câncer e 9,96 milhões de óbitos no mundo. Para 2040, são esperados um total de 28,9 milhões de novos casos de câncer e 16,2 milhões de óbitos (SUNG, 2021).

No Brasil, a estimativa é de 625 mil novos casos de câncer para cada ano do triênio 2020-2022. De acordo com o sexo, os tipos de câncer mais incidentes, à exceção do câncer de pele do tipo não melanoma (cerca de 177 mil novos casos), são o câncer de próstata, em homens e o câncer de mama, entre as mulheres (aproximadamente 66 mil casos cada) **(Figura 1)**. Ambos representam cerca de 30% do total de casos estimados para cada sexo em 2020-2022 (INCA, 2022). Diante disso, é de extrema importância a busca por novas alternativas terapêuticas para o câncer de mama, foco desse trabalho.

Figura 1 - Distribuição proporcional dos dez tipos de câncer mais incidentes estimados para 2020-2022 por sexo, no Brasil

Localização primária	Casos	%
Próstata	65.840	29,2%
Cólon e Reto	20.520	9,1%
Traqueia, Brônquio e Pulmão	17.760	7,9%
Estômago	13.360	5,9%
Cavidade Oral	11.180	5,0%
Esôfago	8.690	3,9%
Bexiga	7.590	3,4%
Linfoma não Hodgkin	6.580	2,9%
Laringe	6.470	2,9%
Leucemias	5.920	2,6%

Localização primária	Casos	%
Mama feminina	66.280	29,7%
Cólon e Reto	20.470	9,2%
Colo do útero	16.590	7,4%
Traqueia, Brônquio e Pulmão	12.440	5,6%
Glândula Tireoide	11.950	5,4%
Estômago	7.870	3,5%
Ovário	6.650	3,0%
Corpo do útero	6.540	2,9%
Linfoma não Hodgkin	5.450	2,4%
Sistema Nervoso Central	5.220	2,3%

As estatísticas não consideraram câncer de pele não melanoma. Os números foram arredondados para múltiplos de 10.
Fonte: adaptado de Instituto Nacional do Câncer (INCA), 2022.

2.1.1 Câncer de mama

O câncer de mama é o tipo de câncer mais incidente em mulheres no mundo, com cerca de 2,26 milhões de casos por ano e mais de 680 mil óbitos anuais (SUNG, 2021). Os principais fatores de risco para o desenvolvimento da doença são idade, obesidade e sobrepeso, história familiar de câncer de ovário ou mama, alteração genética, consumo de bebida alcoólica, tabagismo, sedentarismo e uso de contraceptivos hormonais (BRASILEIRO-FILHO, 2014; ACS, 2022).

O câncer de mama é considerado uma doença heterogênea, com uma variedade de características morfológicas e moleculares (NASCIMENTO; OTONI, 2020). A classificação da doença objetiva entender o comportamento clínico e a escolha do

melhor tratamento (TSANG; TSE, 2020). O tipo e o grau do tumor são definidos com base na classificação histológica da OMS (WHO, 2019). Aproximadamente, 85% dos casos de câncer de mama tem início nos ductos, que transportam o leite para o mamilo. Os outros 15%, surgem nos lóbulos mamários, responsáveis pela produção do leite **(Figura 2)**. Se diagnosticado no estádio inicial, quando o crescimento das células cancerígenas se restringe aos ductos ou lóbulos (*in situ*), o carcinoma é facilmente curável (NÚÑEZ *et al*., 2016, WHO, 2021). A progressão do carcinoma *in situ*, invadindo o tecido mamário adjacente, dá origem ao chamado carcinoma invasivo. O tipo de câncer de mama invasivo mais incidente é o carcinoma ductal invasivo, que corresponde a cerca de 40% a 75% dos casos. Geralmente, apresenta uma grande variação morfológica e de comportamento clínico. O segundo tipo mais incidente, com cerca de 5% a 15% dos casos, é classificado como carcinoma lobular invasivo e acomete principalmente mulheres em idades avançada. O restante dos casos de câncer de mama invasivo se divide em carcinoma medular, carcinoma metaplástico, carcinoma apócrino, carcinoma mucinoso, carcinoma cribriforme, carcinoma tubular, entre outros (NASCIMENTO; OTONI, 2020). No carcinoma invasivo, as células podem se espalhar para os linfonodos próximos ou para outros órgãos do corpo, originando metástases (WHO, 2021). As metástases originárias do câncer de mama atingem principalmente os ossos, pulmões, fígado e cérebro (KIM, 2021).

Figura 2 – Anatomia da mama humana feminina

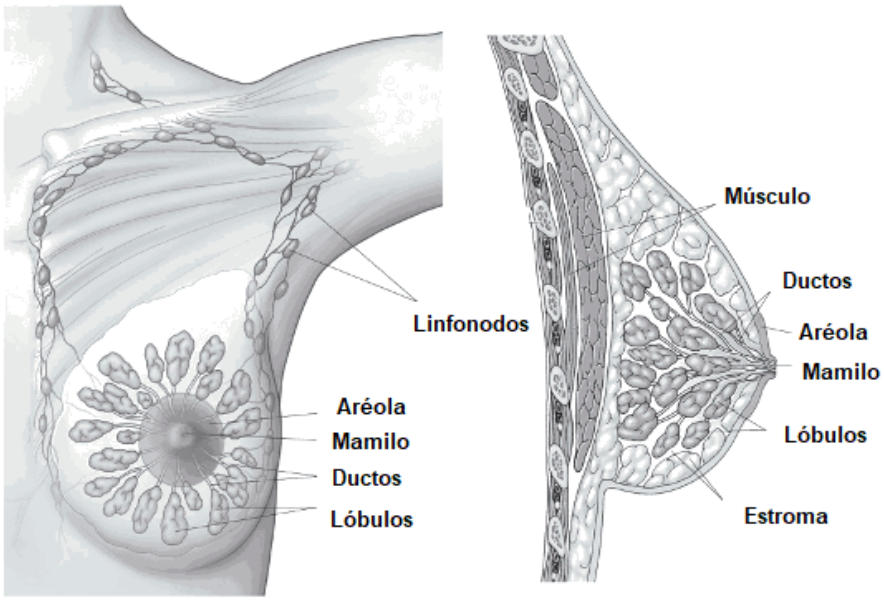

Fonte: adaptado de American Cancer Society (ACS), 2022.

Do ponto de vista molecular, o câncer de mama é classificado de acordo com a expressão de receptor de estrógeno (ER), receptor de progesterona (PR) e receptor do fator de crescimento epidermal humano 2 (HER2). ER e PR são expressos em aproximadamente 75% dos casos de câncer de mama e, normalmente podem ser tratados com terapia hormonal. O tipo duplo positivo (ER^+/PR^+) é pouco agressivo e corresponde à maioria dos casos. Os fenótipos compostos por apenas um receptor positivo (ER^+/PR^- ou ER^-/PR^+) são a minoria, mais agressivos e respondem menos à terapia hormonal. Aproximadamente 15% dos casos de câncer expressam HER2, e estão associados a um curso clínico agressivo, prognóstico ruim, porém preditivo a uma resposta com tratamento direcionado a HER2. O fenótipo triplo negativo, que não expressa nenhum dos marcadores, corresponde entre 10% a 15% dos casos e está associado a uma maior taxa de recorrência, menor sobrevida global e não responde à terapia hormonal direcionada (TSANG; TSE, 2020).

2.2 Tratamento do câncer de mama

O tratamento do câncer de mama pode ser realizado mediante cirurgia (lumpectomia ou mastectomia), radioterapia, terapia hormonal, imunoterapia e quimioterapia (TRAYES; COKENAKES, 2021). A escolha do tratamento depende do estádio do

câncer de mama, classificação histológica e molecular (MAUGHAN; LUTTERBIE; HAM, 2010). A combinação de duas ou mais dessas modalidades tem maximizado as chances de cura ou controle da doença (FISUSI; AKALA, 2019).

A cirurgia é considerada a forma mais eficaz de tratamento, principalmente quando o câncer de mama está em estádio inicial e não apresenta metástases. A radioterapia é frequentemente combinada com a cirurgia com o objetivo de aumentar a eficiência do tratamento e diminuir a recorrência do tumor (FISUSI; AKALA, 2019).

Em estádios mais avançados da doença, as opções terapêuticas são terapia hormonal ou imunoterapia, quando o câncer de mama expressa receptores de estrógeno, progesterona ou HER2 (TRAYES; COKENAKES, 2021). Inibidor de aromatase (anastrozol), agonista do hormônio liberador de gonadotrofina (gosserrelina) e modulador seletivo de receptor de estrógeno (tamoxifeno) são utilizados para o tratamento de câncer de mama receptor de hormônio positivo (MAUGHAN; LUTTERBIE; HAM, 2010). O uso de anticorpo monoclonal (trastuzumabe) tem resultado em aumento da sobrevida de pacientes com câncer de mama HER2 positivo (FISUSI; AKALA, 2019).

A quimioterapia pode ser administrada como terapia neoadjuvante (antes da cirurgia), terapia adjuvante (após a cirurgia) e é a única opção de tratamento quando o câncer é triplo negativo (TRAYES; COKENAKES, 2021). Dentre os agentes quimioterápicos, destacam-se taxanos (paclitaxel e docetaxel), antraciclinas (DOX e epirrubicina), agentes da platina (cisplatina e carboplatina), 5-fluorouracil e ciclofosfamida. Combinações de dois ou três desses fármacos têm sido utilizadas, devido a vantagens de aumento da eficácia do tratamento, redução da toxicidade e redução do desenvolvimento de resistência ao tratamento (FISUSI; AKALA, 2019; YIN *et al.*, 2020).

2.2.1 Doxorrubicina

A DOX **(Figura 3)** é um antibiótico antitumoral que pertence à classe das antraciclinas, produzido pela bactéria *Streptomyces peucetius var. caesius (*AL-MALKY; AL-HARTHI; OSMAN, 2020). Frequentemente, a DOX tem sido utilizada no tratamento de cânceres hematológicos (leucemias e linfomas de Hodgkin e não Hodgkin) e tumores sólidos (câncer de mama, pulmão, bexiga, ovário, tireoide, sarcoma,

osteossarcoma, entre outros) (ZHAO; WOODLE; MIXSON, 2018; AL-MALKY; AL-HARTHI; OSMAN, 2020).

Figura 3 – Estrutura química da doxorrubicina

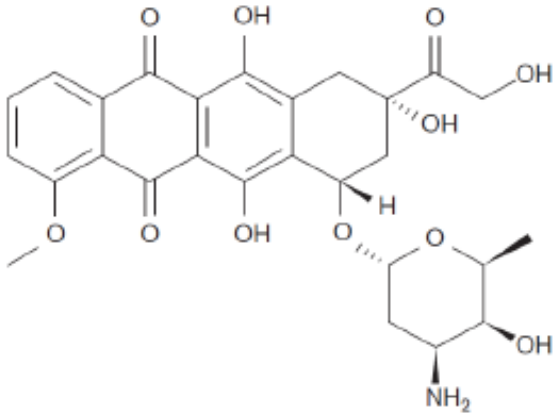

Apesar do extenso uso da DOX na clínica, seus mecanismos de ação não estão completamente elucidados. Dentre alguns já propostos, os dois mais importantes são geração de espécies reativas de oxigênio, que resulta em danos na membrana celular e ao DNA e inibição da topoisomerase II, que impossibilita o reparo da dupla fita de DNA, ambos resultando em apoptose *(*AL-MALKY; AL-HARTHI; OSMAN, 2020). Outros mecanismos propostos são inibição da síntese de DNA e RNA, produção de espécies reativas de oxigênio mitocondrial e ativação do gene supressor de tumor p53 (MEREDITH; DASS, 2016; AL-MALKY; AL-HARTHI; OSMAN, 2020).

Embora seja um fármaco com alta eficácia para o tratamento de diversos tumores, o uso da DOX é limitado devido à toxicidade. Essa toxicidade afeta, frequentemente, coração, cérebro, fígado e rins (CARVALHO *et al.*, 2009). O efeito adverso mais grave, relacionado à administração de DOX, é a toxicidade cardíaca dose-dependente. Uma dose cumulativa de DOX de 400-700 mg/m^2 em adultos e de 300 mg/m^2 em crianças, pode causar insuficiência cardíaca congestiva (ICC) (SONGBO *et al.*, 2019). A cardiotoxicidade aguda ocorre rapidamente após uma única dose de DOX ou ao longo da quimioterapia, podendo ser controlada clinicamente e é normalmente reversível (RAWAT *et al.*, 2021). Os efeitos agudos incluem alterações eletrocardiográficas, arritmias e hipotensão (CARVALHO *et al.*, 2009). A cardiotoxicidade crônica

geralmente se desenvolve no primeiro ano após o término do tratamento ou pode ter início tardio. Os efeitos crônicos são dose-dependente, normalmente irreversíveis, envolvendo cardiomiopatia dilatada e ICC (SONGBO *et al.*, 2019; RAWAT *et al.*, 2021).

Outra limitação ao uso de DOX para o tratamento de câncer de mama é a resistência ao fármaco relacionada principalmente ao aumento do efluxo de DOX, devido à expressão elevada de transportadores da família ABC, glicoproteína P (gpP), proteína-1 de resistência a múltiplas drogas (MRP1) e proteína de resistência ao câncer de mama (BCRP1). Outros mecanismos de resistência envolvem redução da apoptose, devido à desregulação na expressão de p53 e oncogenes, inibição de autofagia, ativação anormal de vias de sinalização e parada de ciclo celular (JAMIALAHMADI; ZAHEDIPOUR; KARIMI, 2021).

A fim de direcionar a DOX para a região tumoral, aumentar a eficácia terapêutica, diminuir a cardiomiopatia e outros efeitos adversos, bem como contornar os problemas relacionados a resistência, a encapsulação deste fármaco em nanoestruturas, como lipossomas, tem sido considerada uma importante estratégia (ZHAO; WOODLE; MIXSON, 2018; FRAIX *et al.*, 2020; GHANDHARIYOUN *et al.*, 2020).

2.3 Lipossomas

Os lipossomas são vesículas esféricas, formadas por fosfolípides, que em meio aquoso se organizam espontaneamente em bicamadas lipídicas circundando um compartimento aquoso. Devido à propriedade anfifílica dos fosfolípides, os lipossomas são capazes de incorporar substâncias hidrofílicas no núcleo aquoso, substâncias lipofílicas na bicamada lipídica e substâncias anfifílicas na interface entre o núcleo aquoso e a bicamada lipídica **(Figura 4)** (GUIMARÃES; PAULO, NOGUEIRA, 2021).

Figura 4 - Representação esquemática da estrutura de lipossomas

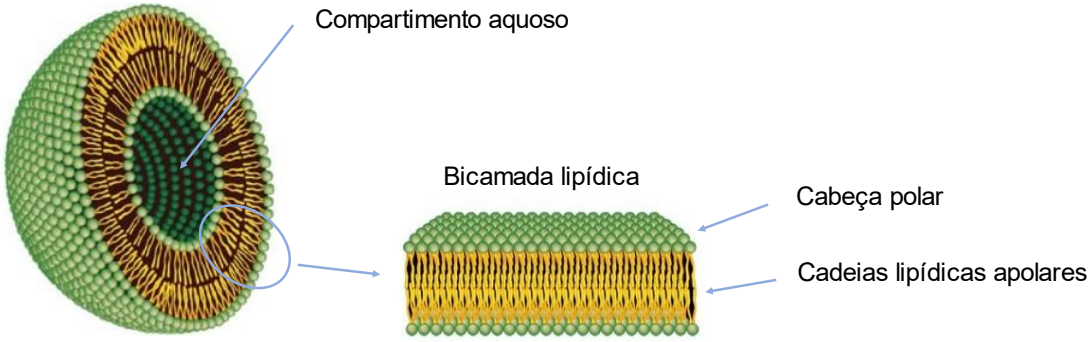

Fonte: adaptado de BOZZUTO; MOLINARI, 2015.

O uso de lipossomas para entrega de fármacos foi primeiramente proposto em 1973. Essas vesículas são consideradas um importante sistema de carreamento devido a sua capacidade de acomodar moléculas de diferentes solubilidades, além de serem biodegradáveis, não-tóxicas, biocompatíveis e não-imunogênicas (FRANCO *et al.*, 2021; GUIMARÃES; PAULO, NOGUEIRA, 2021).

O componente principal dos lipossomas é o fosfolípide, que consiste em um glicerol ligado a um grupo fosfato e duas cadeias longas de ácidos graxos. O grupo fosfato pode ser ligado a moléculas como colina, etanolamina, serina e glicerol, originando os glicerofosfolípides fosfatidilcolina (PC), fosfatidiletanolamina (PE), fosfatidilserina (PS) e fosfatidilglicerol (PG), respectivamente **(Figura 5)** (MONTEIRO e*t al.*, 2014).

Figura 5 – Representação esquemática dos principais fosfolípides

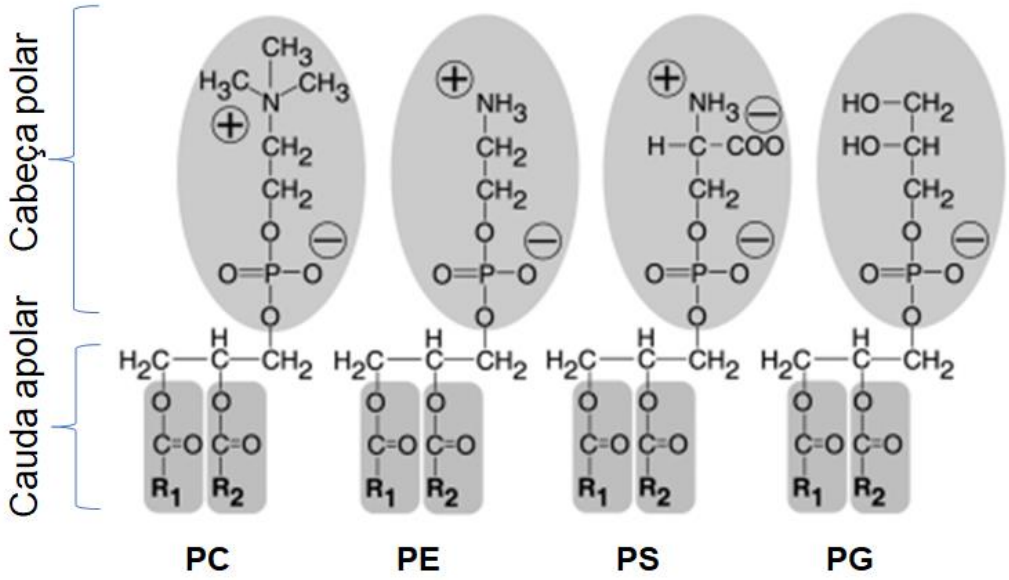

Fonte: adaptado de KRAFT e*t al.*, 2014.

De acordo com o diâmetro e o número de lamelas, os lipossomas podem ser classificados em unilamelar (SUV OU ULV, vários tamanhos), multilamelar (MLV, maior que 500 nm) e multivesicular (MVV, maior que 1000 nm). Os lipossomas unilamelares são formadas por uma única bicamada lipídica e possuem uma maior capacidade de encapsular substâncias hidrofílicas. Podem ser classificados em vesículas unilamelares pequenas (SUV, entre 20 a 100 nm), vesículas unilamelares grandes (LUV, maior que 100 nm) e vesículas gigantes unilamelares (GUV, maior que 1000 nm). Os lipossomas do tipo MLV são formados por várias bicamadas lipídicas concêntricas separadas por compartimentos aquosos e são ideais para encapsular substâncias lipofílicas. Os lipossomas do tipo MVV são formados por várias vesículas pequenas não concêntricas aprisionadas dentro de uma única bicamada lipídica e possuem capacidade de encapsular grande volume de substâncias hidrofílicas **(Figura 6)** (GUIMARÃES; PAULO, NOGUEIRA, 2021).

Figura 6 - Classificação de lipossomas de acordo com o tamanho e o número de lamelas

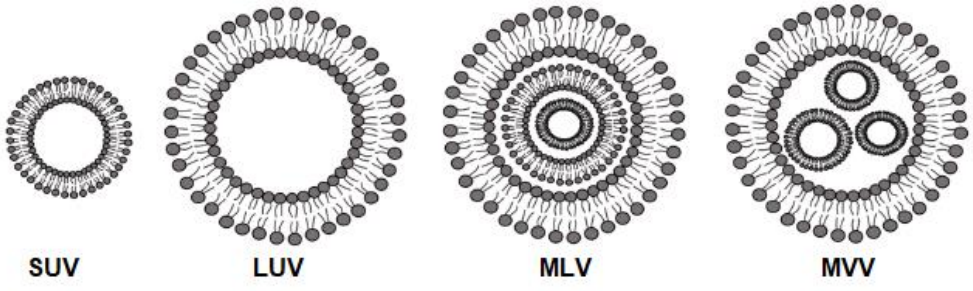

Fonte: adaptado de GUIMARÃES; PAULO, NOGUEIRA, 2021.

De acordo com a composição e a funcionalização, os lipossomas podem ser classificados como convencionais, de circulação prolongada, lipossomas sítio-específicos e lipossomas responsivos a estímulos (GUIMARÃES; PAULO, NOGUEIRA, 2021).

Os lipossomas convencionais são considerados estruturalmente mais simples, constituídos por fosfolípides neutros ou carregados positivamente ou negativamente, geralmente combinados com o colesterol. Após administração por via endovenosa, esses lipossomas são reconhecidos como partículas estranhas pelas opsoninas, e consequentemente, capturados pelo sistema fagocitário mononuclear (SFM), e acumulados rapidamente no fígado e baço (TORCHILIN, 2005; NSAIRAT *et al*., 2022).

Com o objetivo de aumentar o tempo de circulação sanguínea, o polietilenoglicol (PEG), um polímero hidrofílico biocompatível, foi incorporado na superfície dos lipossomas, funcionando como uma barreira estérica para a adesão das opsoninas, dando origem aos lipossomas de circulação prolongada (TORCHILIN, 2005; GUIMARÃES; PAULO, NOGUEIRA, 2021). O diestearoilfosfatidiletanolamina acoplada ao polietilenoglicol 2000 (DSPE-PEG_{2000}) **(Figura 7)** é um fosfolípide conjugado ao PEG que vem sendo muito utilizado como constituinte de lipossomas para esse propósito (KIM *et al.*, 2009).

Figura 7 - Estrutura química da distearoilfosfatidiletanolamina acoplada ao polietilenoglicol 2000 (DSPE-PEG$_{2000}$)

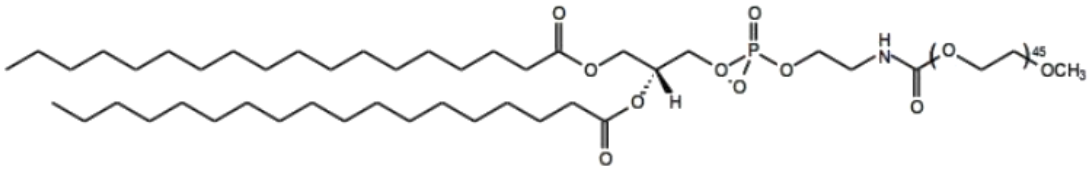

Em 1974, o uso de lipossomas foi proposto para o tratamento de câncer, baseado em sua capacidade de se acumular passivamente na região tumoral. Esse acúmulo foi explicado pela vasculatura permeável e a redução da drenagem linfática no tumor, que é conhecido como efeito de permeabilidade e retenção aumentadas (EPR) (FRANCO *et al.*, 2021). Recentemente foi descoberto que também o acúmulo de nanopartículas no tumor pode ocorrer por transporte transcelular através das células endoteliais (SINDHWANI *et al.*, 2020; SHETH *et al.*, 2021).

Na tentativa de direcionar os lipossomas ativamente para a região de interesse, foram projetados os lipossomas sítio-específicos, funcionalizados com peptídeos, proteínas (incluindo anticorpos), carboidratos, ácidos nucleicos ou vitaminas (NSAIRAT *et al*., 2022). Esses lipossomas permitem entrega direcionada de compostos nos tecidos desejados, promovendo maior eficácia terapêutica e menos danos para as células saudáveis (GUIMARÃES; PAULO, NOGUEIRA, 2021).

A fim de aumentar a liberação do fármaco no sítio-alvo, foram desenvolvidos os lipossomas responsivos a estímulos, que liberam seu conteúdo somente quando expostos a estímulos físicos extracorporal como temperatura, luz, ultrassom, campos elétricos e magnéticos ou estímulos fisiológicos presentes na região tumoral, como a presença de baixo pH, enzimas, hipóxia, entre outros (FRANCO *et al*., 2021).

A **Figura 8** resume a evolução da estratégia de uso de lipossomas como carreadores de fármacos para o tratamento do câncer.

Figura 8 – Representação esquemática das principais características de lipossomas como carreadores de fármacos para o tratamento do câncer e sua evolução

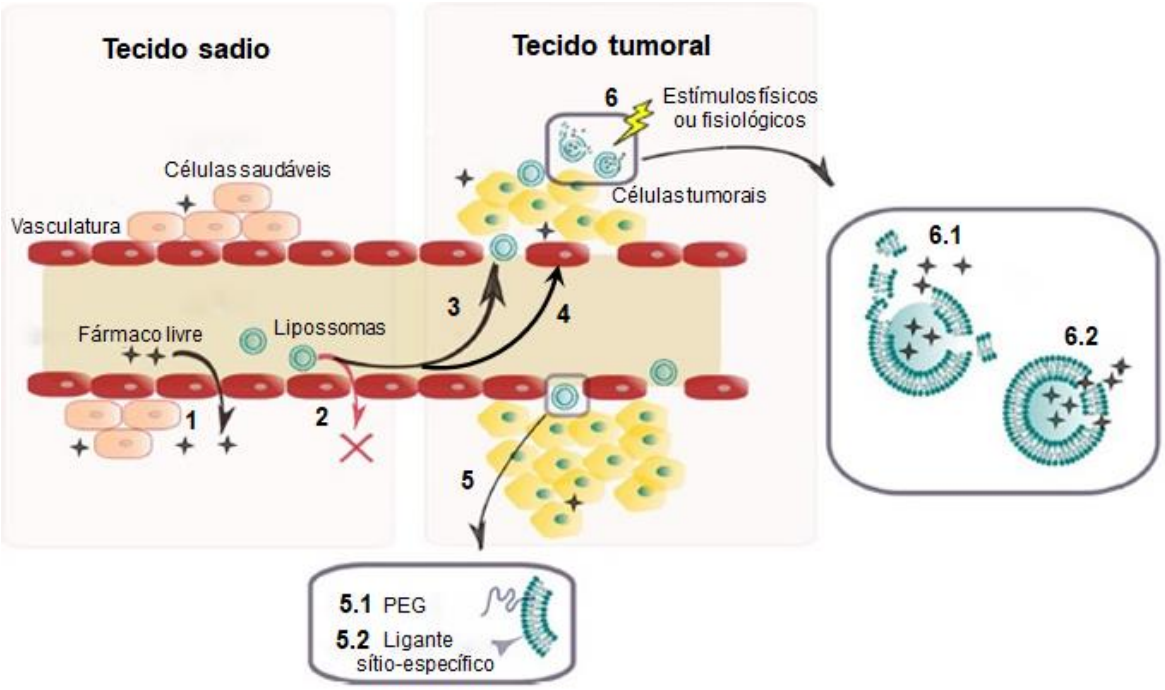

As células endoteliais justapostas permitem a passagem do fármaco livre do vaso sanguíneo para o tecido saudável (1). No entanto, devido ao tamanho, os lipossomas não passam através das junções estreitas nos vasos sanguíneos de tecidos saudáveis (2), acumulando-se preferencialmente no tecido tumoral, onde os vasos apresentam fenestrações entre as células endoteliais (3) em um processo conhecido como efeito EPR. Além disso, os lipossomas entram no tumor, a partir de mecanismos trans endoteliais ativos (4). Moléculas podem ser incorporadas na superfície de lipossomas para melhorar suas características (5). A incorporação do PEG aumenta o tempo de circulação sanguínea dos lipossomas (5.1). A funcionalização com ligantes sítio-específicos, permite direcionar os lipossomas para as células tumorais (5.2). Diferentes estímulos físicos extracorporal e fisiológicos podem desencadear a liberação do fármaco na região tumoral (6). Esse estímulo pode romper completamente a membrana do lipossoma (6.1) ou aumentar sua permeabilidade (6.2).

Fonte: adaptado de FRANCO *et al.*, 2021.

A inclusão do fosfolípide fusogênico, a dioleilfosfatidiletanolamina (DOPE), e do agente estabilizante hemisuccinato de colesterila (CHEMS) na superfície dos lipossomas, resultou nos chamados lipossomas pH-sensíveis, que quando em contato com um meio ácido, como em tecidos tumorais e no interior dos endossomas, liberam o material encapsulado **(Figure 9)** (FERREIRA *et al., 2*013; FRANCO *et al.*, 2021). Em pH neutro ou fisiológico, a molécula de DOPE não é capaz de se organizar em bicamadas lipídicas. Isso acontece porque a molécula de DOPE possui uma cabeça polar pequena e pouco hidratada, que ocupa um pequeno volume comparado às duas cadeias longas de ácidos graxos, resultando assim, em uma organização geométrica

molecular do tipo cone, que favorece fortes interações entre os grupos amino e fosfato da cadeia polar, justificando a forte tendência das moléculas de DOPE em se organizarem sob a forma hexagonal invertida (H_{II}). A inserção das moléculas de CHEMS, em meio neutro, resulta em uma repulsão eletrostática entre os grupos fosfato e carboxilato das moléculas de DOPE e CHEMS, respectivamente, o que favorece a organização do sistema em bicamadas lipídicas. Por sua vez, quando em contato com um meio ácido, ocorre protonação das moléculas de CHEMS, levando a desestabilização das vesículas, uma vez que as moléculas da DOPE retomam a forma H_{II}, liberando o conteúdo dos lipossomas pH-sensíveis (FERREIRA *et al., 2*013; FRANCO *et al.*, 2021).

Figura 9 - Representação esquemática das mudanças de fases em lipossomas pH-sensíveis compostos por DOPE e CHEMS

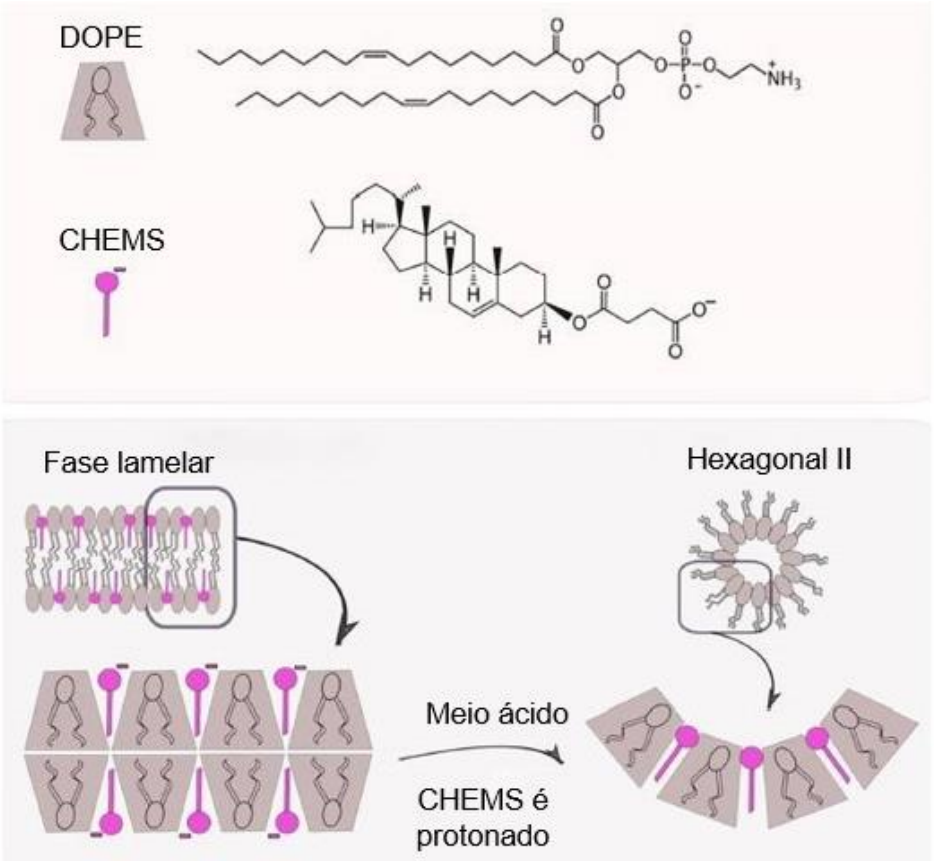

Sozinhas, as moléculas de DOPE se organizam em uma fase hexagonal invertida devido à sua geometria cônica. Quando combinadas com moléculas de CHEMS em pH fisiológico ou neutro, é possível se organizar em bicamada lipídica (Fase lamelar). Uma vez exposto ao meio ácido (região tumoral ou interior de endossomas), ocorre a protonação do grupo carboxilato das moléculas de CHEMS levando à desestabilização do lipossoma, que retorna à fase hexagonal invertida (Hexagonal II), seguida da liberação dos fármacos encapsulados.

Fonte: adaptado de FRANCO *et al.*, 2021.

2.3.1 Lipossomas contendo doxorrubicina

Alguns lipossomas contendo DOX foram investigados e aprovados para o uso no tratamento do câncer. Desde a década de 1990, a primeira formulação lipossomal de circulação prolongada, conhecida como Caelyx®/Doxil®, na Europa e Estados Unidos, respectivamente, vem sendo utilizada e, a partir de 2004 seu uso foi aprovado para o tratamento de câncer de mama metastático. Lipo-Dox®, também peguilado, teve seu uso aprovado em 1998, na China. A principal diferença entre Lipo-Dox® e Caelyx®/Doxil® é o fosfolípide que compõe a bicamada das vesículas. O Caelyx®/Doxil® é composto por fosfatidilcolina de soja hidrogenada (HSPC) e o Lipo-Dox® contém distearoilfosfatidilcolina (DSPC) (NGAN; GUPTA, 2016). Uma formulação lipossomal não-peguilada também é comercializada, sob o nome Myocet®, cuja composição é fosfatidilcolina de ovo e colesterol (ZHAO; WOODLE; MIXSON, 2018). ThermoDox® é um lipossoma termossensível, que foi desenvolvido para liberar DOX mediante estímulo de calor. Seu uso está sendo avaliado em um estudo de fase III, como terapia adjuvante associada a ablação por radiofrequência, para tratamento de câncer de fígado primário (TAK *et al.*, 2018). ThermoDox® é composto por dipalmitoilfosfatidilcolina (DPPC), lisofosfatidilcolina (LPC) e DSPE-PEG_{2000} (HAUCK *et al.*, 2006). Os pacientes tratados com formulações lipossomais de DOX apresentam redução de efeitos adversos como cardiotoxicidade, náuseas, vômitos e mielossupressão, comparado ao tratamento convencional com DOX livre. Além disso, os lipossomas peguilados aumentam a sobrevida dos pacientes com câncer que apresentam alto risco de cardiomiopatia. Porém, não há um ganho em relação à eficácia terapêutica dos lipossomas comparado à DOX convencional (ZHAO; WOODLE; MIXSON, 2018). Diante disso, estudos vêm sendo feitos a fim de desenvolver um nanocarreador que além de aumentar a segurança, aumente a eficácia do tratamento com DOX. Lipossomas pH-sensíveis contendo DOX inibiram significativamente o crescimento do tumor em modelo animal de câncer de mama, quando comparado ao tratamento com DOX livre (SILVA, *et al.*, 2019). Na tentativa de aumentar a eficácia de entrega do fármaco à região tumoral, lipossomas pH-sensíveis de circulação prolongada podem ser fundidos com vesículas liberadas por células tumorais.

2.4 Exossomas

Os exossomas são vesículas secretadas por uma variedade de células para o meio extracelular, que apresentam tamanho entre 30-150 nm (CHEN *et al.*, 2022). A biogênese dos exossomas se inicia com a formação do endossoma inicial através de uma invaginação natural da membrana plasmática celular. Em seguida, os endossomas iniciais se transformam em endossomas tardios que contêm proteínas e ácidos nucleicos. A invaginação das membranas endossomais tardias, resulta na formação de vesículas intraluminais (VIL). O acúmulo das VIL, dentro dos endossomas tardios, forma os corpos multivesiculares (CMV). OS CMV formados podem se fundir com o lisossomo para degradar seu conteúdo ou fundir com a membrana plasmática para liberar as VIL para o meio extracelular, que então são denominadas exossomas **(Figura 10)** (GURUNATHAN; KANG; KIM, 2021).

Figura 10 – Biogênese dos exossomas

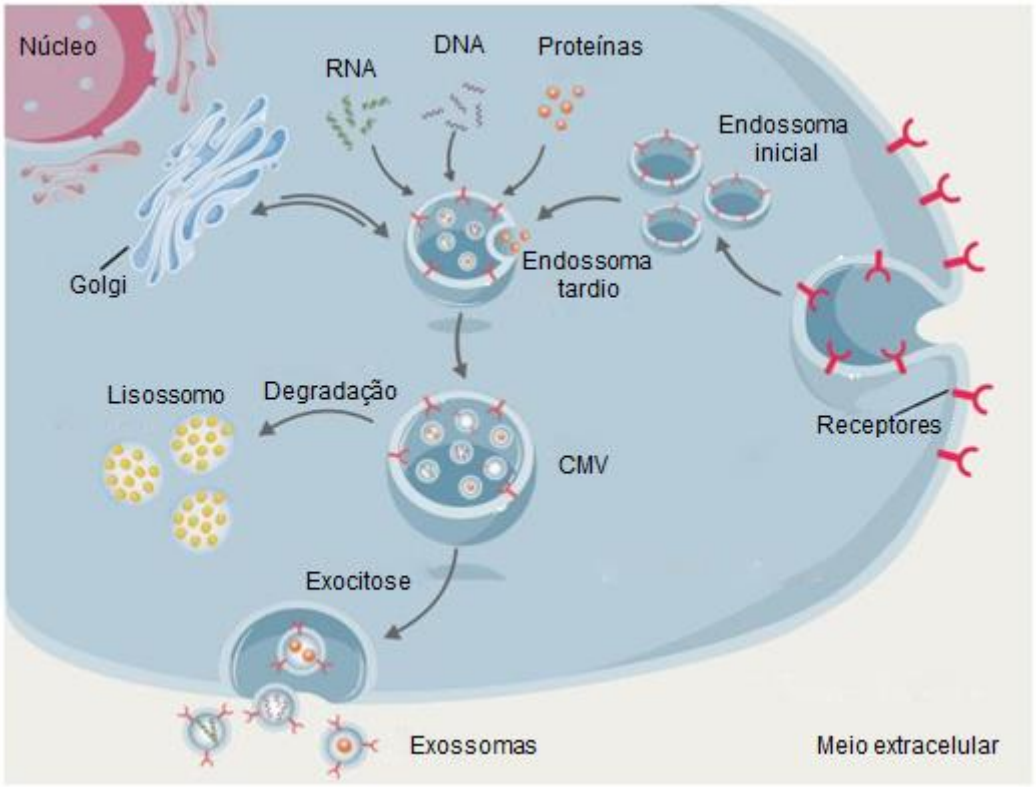

Fonte: adaptado de GURUNATHAN; KANG; KIM, 2021.

Os exossomas são internalizados na célula receptora por fusão direta com a membrana plasmática, interações entre ligante/receptor, fagocitose, macropinocitose

e endocitose (MUKHERJEE *et al.*, 2022). Os principais componentes dos exossomas são lípides, proteínas e ácidos nucleicos (GURUNATHAN; KANG; KIM, 2021). Esses constituintes variam de acordo com o tipo, origem e estado fisiopatológico da célula de origem (LIU *et al.*, 2021). Um total de 9769 proteínas, 3408 mRNAs, 2838 miRNAs e 1116 lípides já foram identificados em exossomas de diferentes tipos de células e espécies animais e são listados em uma base de dados de conteúdo de exossomas – ExoCarta (MUKHERJEE *et al.*, 2022). Proteínas comumente encontradas em exossomas são as tetraspaninas (CD9, CD63, CD81 e CD82), proteínas de choque térmico (Hsp70 e Hsp90), proteínas de transporte e fusão (Rab2, Rab7, anexinas e flotilina) e integrinas (CHEN *et al.*, 2022; MUKHERJEE *et al.*, 2022). As tetraspaninas, uma família de proteínas transmembranas, são responsáveis pelo direcionamento e entrada seletiva dos exossomas nas células receptoras (LIANG *et al.*, 2021). As proteínas de choque térmico, anexinas e proteínas da família Rab estão envolvidas na síntese e transporte de exossomas. As integrinas são importantes na adesão de exossomas às células receptoras (MUKHERJEE *et al.*, 2022). Essas proteínas são consideradas marcadores moleculares para detecção de exossomas (CHEN *et al.*, 2022). Vários ácidos nucleicos são encontrados em exossomas, como micro RNAs (miRNAs), RNA mensageiro (mRNAs), DNA mitocondrial (mtDNA), RNA longo não-codificante (lncRNAs), RNA ribossomal (rRNA) e RNA transportador (rRNA). Esses ácidos nucleicos podem afetar a síntese de proteínas nas células receptoras. A bicamada lipídica dos exossomas é composta principalmente por colesterol, fosfatidilcolina, esfingomielina, fosfatidiletanolamina, ceramida, diglicerídeo, ácido fosfatídico e triglicerídeos (LIANG *et al.*, 2021; LIU *et al.*, 2021). As moléculas lipídicas estão envolvidas na manutenção da estabilidade e rigidez estrutural dos exossomas (LIANG *et al.*, 2021).

Exossomas têm sido encontrados em diversos fluidos biológicos, como sangue, plasma, saliva, urina, sêmen, líquido epididimal, líquido cefalorraquidiano, líquido sinovial, líquido amniótico, e leite materno (GURUNATHAN *et al.*, 2019). Seu papel é como uma ferramenta de comunicação intercelular, transportando proteínas, lípides e RNAs entre as células, podendo induzir alterações fenotípicas e moleculares nas células receptoras (KALLURI; LEBLEU, 2020). Os exossomas podem estar envolvidos em uma série de processos celulares incluindo inflamação, angiogênese, respostas

imunes, coagulação e regeneração neuronal, além de processos fisiológicos (ALZHRANI *et al.*, 2021).

A caracterização dos exossomas inclui medidas de tamanho, concentração de partículas, avaliação da morfologia, identificação de proteínas de superfície, entre outros. Várias técnicas têm sido utilizadas para caracterizar o diâmetro dos exossomas, como análise de rastreamento de nanopartículas (NTA, do inglês *nanoparticle tracking analysis*) e espalhamento dinâmico da luz (DLS, do inglês *dynamic light scattering*). Adicionalmente, NTA permite uma análise de concentração e distribuição de tamanho das partículas. Outra técnica amplamente utilizada para caracterizar o tamanho e morfologia dos exossomas é a criomicroscopia eletrônica de transmissão (cryoTEM, do inglês *cryo-transmission electron microscopy*) (ALZHRANI *et al.*, 2021). A quantificação total de proteínas em exossomas pode ser feita utilizando método do ácido bicinconínico (BCA), que se caracteriza pela redução de Cu^{2+} a Cu^{1+} pelas proteínas em meio alcalino (reação de Biureto). Duas moléculas de BCA ligam-se ao cobre reduzido, formando um produto de intensa coloração púrpura, que exibe uma absorbância forte a 562 nm (HUANG; LONG; HUO, 2010; REZAKHANI *et al.*, 2021). Informações sobre o tamanho, granulosidade e composição dos exossomas podem ser coletadas por citometria de fluxo utilizando o CytoFLEX, um citômetro de alta sensibilidade desenvolvido para análise de nanopartículas biológicas (ALZHRANI *et al.*, 2021). Além disso, informações sobre a estrutura química dos exossomas podem ser obtidas usando a espectroscopia Raman (GURUNATHAN *et al.*, 2019) e a composição de exossomas em termos de conteúdo proteico, lipídico e genético pode ser determinada por espectroscopia de infravermelho com transformada de Fourier (FTIR) (ROMANÒ *et al.*, 2020).

2.4.1 *Aplicações de exossomas*

Os exossomas exibem características de superfície que fornecem informações sobre o estado patológico de suas células de origem, podendo conter marcadores diferenciais entre indivíduos saudáveis e doentes e serem usados para diagnóstico, avaliação da progressão da doença, desenvolvimento de terapia alvo específica e de agente teranóstico (KIM e*t al*., 2018; MUKHERJEE *et al.*, 2022). Os exossomas são biocompatíveis, não imunogênicos e possuem especificidade de entrega. Recentemente, começaram a ser explorados para o uso como veículo de entrega de

ácidos nucleicos, proteínas e fármacos (WANG; ZHENG; ZHAO, 2016; MUKHERJEE *et al.*, 2022).

Os exossomas de origem tumoral contêm proteínas e lípides semelhantes às células que os secretam e fundem-se preferencialmente com células tumorais de mesma origem (QIAO *et al*., 2020). Exossomas podem reconhecer células específicas mediante os receptores de membrana, e assim a internalização de exossomas pelas células pode ser cerca de dez vezes maior que de lipossomas do mesmo tamanho, indicando a maior especificidade para a terapia do câncer (KIM e*t al*., 2018). Além disso, exossomas derivados de pacientes podem evitar o reconhecimento imunológico melhor que os lipossomas peguilados formulados *in vitro* (HADLA e*t al.*, 2016). Estudos recentes têm mostrado o potencial de exossomas contendo DOX para redução do tamanho do tumor e redução da cardiotoxicidade em modelo animal portador de tumor de mama e ovário, quando comparado ao fármaco livre (HADLA *et* al., 2016; GONG *et al.*, 2019).

Para melhorar a entrega de fármacos por exossomas, recentemente tem sido estudada a fusão desses com lipossomas, gerando os conhecidos nanocarreadores híbridos de exossoma-lipossoma (BUNGGULAWA *et al.*, 2018; MUKHERJEE *et al.*, 2022).

2.4.1.2 Nanocarreador híbrido de exossoma-lipossoma

Nanocarreadores híbridos de exossoma-lipossoma são obtidos pela fusão das membranas lipídicas de lipossoma e exossoma **(Figura 11)**. Os principais métodos empregados para preparo dessa nova geração de nanossistemas são incubação, congelamento-descongelamento e sonicação (MUKHERJEE *et al.*, 2022).

Figura 11 – Representação esquemática da fusão de lipossomas com exossomas

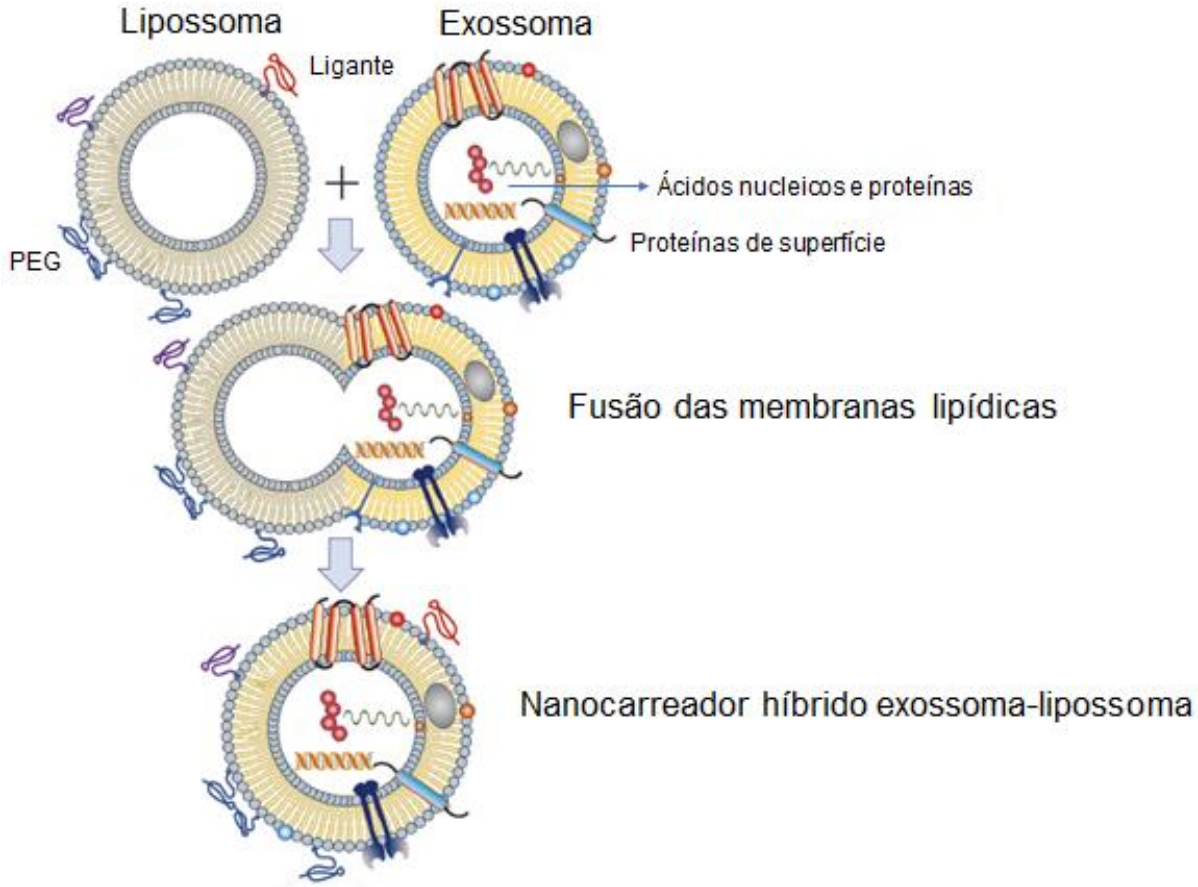

Fonte: adaptado de MUKHERJEE *et al.*, 2022.

Os exossomas possuem a vantagem de direcionamento, por serem um nanocarreador de origem endógena e, limitações como, baixo rendimento e dificuldade de modificação de superfície. Os lipossomas, por sua vez, podem ter sua superfície modificada facilmente, porém tem como desvantagem a ausência de funcionalidade endógena (RAYAMAJHI *et al.*, 2019). Os benefícios adicionais do nanocarreador híbrido são maior tempo de circulação sanguínea, melhor perfil farmacocinético, aumento de estabilidade coloidal e menor imunogenicidade (MUKHERJEE *et al.*, 2022).

Exossomas de origem tumoral foram incubados com Doxil® e as nanovesículas híbridas obtidas aumentaram em 2,3 vezes a concentração de DOX no tumor de mesma origem celular das células secretoras, comparado ao Doxil®. Além disso, as

nanovesículas híbridas apresentaram maior eficácia na inibição do crescimento do tumor em um modelo tumoral animal (QIAO *et al*., 2020).

Diante do exposto, o desenvolvimento de nanocarreador híbrido de exossoma-lipossoma obtido pela fusão de exossomas secretados por células tumorais de mama com lipossomas pH-sensíveis de circulação prolongada contendo DOX, pode ser uma alternativa promissora para o aumento da eficácia de tratamento do câncer de mama, redução da toxicidade sistêmica e contornar problemas relacionados a resistência a DOX. Por terem características das células tumorais de origem, essas vesículas poderiam favorecer o direcionamento, reconhecimento, fusão e liberação preferencial do seu conteúdo nessas células.

3 OBJETIVOS

3.1 Objetivos geral

Desenvolver, caracterizar, avaliar a toxicidade e o potencial terapêutico de exossomas fundidos com lipossomas pH-sensíveis de circulação prolongada contendo doxorrubicina (ExoSpHL-DOX) para o tratamento de câncer de mama.

3.2 Objetivos específicos

- Isolar os exossomas a partir de sobrenadante celular da linhagem tumoral de mama murina 4T1.

- Preparar os ExoSpHL-DOX.

- Caracterizar os ExoSpHL-DOX mediante a determinação do diâmetro, potencial zeta (PZ) e índice de polidispersão (IP).

- Determinar o teor de encapsulação de DOX em ExoSpHL-DOX.

- Caracterizar os exossomas e ExoSpHL-DOX mediante a determinação do diâmetro, concentração de partículas e distribuição de tamanho por NTA.

- Caracterizar os exossomas e ExoSpHL-DOX por criomicroscopia eletrônica de transmissão.

- Quantificar o total de proteínas presentes em exossomas e em exossomas fundidos com lipossomas pH-sensíveis de circulação prolongada brancos (ExoSpHL).

- Caracterizar os ExoSpHL por espectroscopia Raman e infravermelho.

- Identificar a proteína de superfície CD9 em exossomas e ExoSpHL por nanocitometria de fluxo.

- Avaliar a estabilidade química, físico-química e biológica da formulação de ExoSpHL-DOX.

- Avaliar a liberação de DOX, em pH 5 e 7,4, a partir da formulação de ExoSpHL-DOX.

- Determinar a citotoxicidade de ExoSpHL-DOX em linhagem tumoral de mama 4T1.

- Avaliar a atividade antitumoral de ExoSpHL-DOX em fêmeas de camundongos Balb/c portadores de tumor de mama 4T1.

- Avaliar a toxicidade aguda sistêmica de ExoSpHL-DOX em fêmeas de camundongos Balb/c sadios.

CAPÍTULO 1

Fusion of tumor-derived exosomes with long-circulating and pH-sensitive liposomes loaded with doxorubicin for the treatment of breast cancer

Eliza Rocha Gomes, Andréa Teixeira Carvalho, Tiago Campolina Barbosa, Luiza de Lazari Ferreira, Hallen Daniel Rezende Calado, Adriano de Paula Sabino, Mônica Cristina Oliveira

Artigo publicado em AAPS PharmSciTec, v.23, 255, 2022.

ABSTRACT

Doxorubicin (DOX) is a chemotherapeutic agent that has been used in the treatment of breast cancer. However, serious toxic effects, have limited its use, mainly cardiotoxicity. To minimize the adverse effects, liposomal preparations containing DOX have been developed. These preparations can reach the target in the tumor region as well as bypass the resistance-related problems. An alternative to increase therapeutic efficacy may be the fusion of liposomes with exosomes released from tumor cells to facilitate membrane and fusion interactions, achieving greater cell uptake. Thus, the purpose of this study was the fusion of exosomes derived from breast tumor cells with long-circulating and pH-sensitive liposomes loading DOX (ExoSpHL-DOX) for the treatment of breast cancer. The mean diameter of ExoSpHL-DOX was 100.8 ± 7.8 nm, the polydispersity index was 0.122 ± 0.004, and the encapsulated DOX content was equal to 83.5 ± 2.5%. The fusion of exosomes with long-circulating and pH-sensitive liposomes was confirmed by Fourier transform infrared spectroscopy, Raman spectroscopy, and nano-flow cytometry. The physicochemical characteristics of ExoSpHL-DOX were maintained for 60 days, at 4°C. The study of the release of DOX from ExoSpHL-DOX in dilution media with different pH values showed the pH-sensitivity characteristic of the nanosystem, since 96.6 ± 0.2% of DOX was released from ExoSpHL-DOX at pH 5.0, while at pH 7.4 the release was 70.1 ± 1.7% in the medium. The cytotoxic study against the breast cancer cell line demonstrated that ExoSpHL-DOX treatment significantly reduced the cancer cell viability.

Keywords: breast cancer, liposomes, exosomes, fusion, doxorubicin

1 Introduction

Anthracycline antibiotics, such as doxorubicin (DOX), are of great importance being used in the treatment of breast cancer (ZHAO; WOODLE; MIXSON, 2018; ACS, 2020). However, the high toxicity, mainly cardiac, related to DOX, as well as the resistance mechanisms developed by cells to this drug, have limited its use (KIZEK *et al.*, 2012; YANG, *et al.*, 2014; TACAR; SRIAMORNSAK; DASS, 2013; ZHAO; WOODLE; MIXSON, 2018). To minimize the adverse effects of DOX, nanocarriers, such as liposomes, are in development for delivering the antitumor drug (TACAR; SRIAMORNSAK; DASS, 2013; NÚÑEZ, T. *et al*., 2016; ZHAO; WOODLE; MIXSON, 2018).

Since the 1990s, long-circulating liposomes containing DOX, known as Caelyx®/Doxil®, in Europe and the United States, respectively, have been used. Their use for the treatment of metastatic breast cancer has been approved since 2004. Lipo-Dox®, also pegylated, was approved for use in China in 1998. The main difference between Lipo-Dox® and Caelyx®/Doxil® is the phospholipid that makes up the bilayer of the vesicles. Caelyx®/Doxil® contain hydrogenated soy phosphatidylcholine (HSPC) and Lipo-Dox® is composed of distearoylphosphatidylcholine (DSPC) (NGAN; GUPTA, 2016). Myocet®, a non-pegylated liposomal formulation, is composed of egg phosphatidylcholine and cholesterol (ZHAO; WOODLE; MIXSON, 2018). Patients treated with liposomal formulations of DOX have presented a reduced cardiotoxicity, nausea, vomiting, and myelosuppression, compared to conventional treatment with DOX. In addition, pegylated liposomes increase the survival of cancer patients who are at high risk for cardiomyopathy. This decrease of the toxicity can be explained by the retention of liposomes in the tumor region due to the EPR effect. However, there is no increase in the therapeutic efficacy of liposomes compared to conventional DOX (TARDI; BOMAN; CULLIS, 1996; GABIZON *et al.*, 2002). Therefore, studies have been carried out to develop a nanocarrier that, in addition to increasing safety, can improve the effectiveness of treatment with DOX. Long-circulating and pH-sensitive liposomes loading DOX significantly inhibited tumor growth in an animal model of breast cancer when compared to treatment with free DOX (SILVA *et al.,* 2019*)*. In an attempt to further increase therapeutic efficacy, liposomes can be fused with vesicles released by tumor cells, aiming at greater cell targeting and uptake (BUNGGULAWA, 2018).

Exosomes are vesicles naturally secreted by different types of cells, which contain various proteins, DNA, and RNAs, and are responsible for intercellular communication (GYORGY *et al.*, 2011; BUNGGULAWA, 2018). Recently, they have been explored for use as a delivery vehicle for nucleic acids, therapeutic proteins, and small active molecules. Drug delivery to cells is facilitated by the presence of adhesive proteins (tetraspanins and integrins) on the surface of exosomes, which facilitate membrane and fusion interactions (KIM *et al*., 2018).

Therefore, the fusion of tumor-derived exosomes with long-circulating and pH-sensitive liposomes can be a promising alternative to increase anticancer efficacy and reduce toxicity, since these vesicles have characteristics of tumor cells of origin that favor specific targeting, and due to their pH-sensitivity they can promote a preferential release of their content in tumor cells. In view of findings, the proposals of this study were to develop and physiochemically characterize a formulation composed of breast tumor-derived exosomes fused with long-circulating and pH-sensitive liposomes loading DOX.

2 Materials and methods

2.1 Chemicals

1,2-dioleoyl-sn-glycero-3-phosphoethanolamine (DOPE) and 1,2-distearoyl-sn-glycero-3-phosphoethanolamine-N-[amino(polyethyleneglycol)-2000 (DSPE-PEG2000) were supplied by Lipoid GmbH (Ludwigshafen, Germany). Cholesterol hemisuccinate (CHEMS), doxorubicin (DOX), phosphate-buffered saline (PBS), sodium hydroxide, 4-(2-hydroxyethyl)piperazine-1-ethanesulfonic acid (HEPES), and sodium bicarbonate were obtained from Sigma Aldrich (St. Louis, USA). Total exosome isolation reagent and BCA protein assay kit were obtained from Thermo Fisher Scientific (Waltham, USA). FITC anti-mouse CD9 monoclonal was obtained from BioAlbra Biotecnologia (Viçosa, Brazil). Sodium chloride and methanol were purchased from Merck (Frankfurt, Germany).

2.2 Cells

The 4T1 murine breast cancer cells were obtained from American Type Culture Collection (ATCC) (Manassas, USA). The Roswell Park Memorial Institute (RPMI) 1640 Medium and fetal bovine serum (FBS) were obtained from Gibco Life

Technologies (Carlsbad, USA). Sulforhodamine B (SRB), tris(hydroxymethyl)aminomethane (tris base), and trypsin were obtained from Sigma-Aldrich (St. Louis, USA).

2.3 Isolation of exosomes

4T1 breast cancer cells were grown in RPMI-1640, supplemented with 10% of ultracentrifuged FBS, and maintained at 37°C and 5% CO_2 in a humidified atmosphere. The cell supernatant was removed from the cell culture flask T-75 when 4T1 cells reached an approximate confluence of 80%. To the cell supernatant, total exosome isolation reagent was added (2:1 v/v ratio, respectively) and maintained at 2° to 8°C for 15h. Then, the mixture was centrifuged at 10,000xg, for 1h, at 4°C, using a centrifuge Thermo Scientific, model Heraeus Multifuge X 1R. The exosome pellet obtained was resuspended in PBS or in a mixture of methanol and chloroform (1:1 v/v ratio, respectively).

2.4 Preparation of ExoSpHL-DOX

ExoSpHL-DOX were prepared by the lipid film hydration method (BANGHAM; STANDISH; WATKINS, 1965), followed by size calibration. Firstly, lipids were solubilized in chloroform. DOPE, CHEMS, and DSPE-PEG_{2000} (molar ratio of 5.7:3.8:0.5, respectively) were transferred to a round bottom flask. Then exosomes dissolved in a mixture of methanol and chloroform (1:1 v/v) were added. For each mL of liposome, it was added the exosome pellet obtained from 2 mL of cell supernatant (concentration of 3.6×10^{10} particles/mL). A lipid film, with total lipid concentration of 20 mM, was obtained by evaporating the chloroform and methanol under reduced pressure. Next, NaOH 0.228 M solution was added to the lipidic film to ionize CHEMS molecules and allow the formation of vesicles. Then, an ammonium sulfate solution (300 mM, pH 7.4) was used for hydration of the lipidic film. The size of the vesicles was calibrated by the extrusion method in the Lipex Biomembranes extruder, Model T001 (Vancouver, Canada). The vesicles were submitted to ultracentrifugation (Ultracentrifuge Optima® L-80XP, Beckman Coulter, Brea, USA) to remove external ammonium sulfate (SILVA *et al.,* 2019*)*. The pellet obtained was resuspended with HEPES buffered saline (HBS). The dispersion was incubated with a DOX solution for 2h, at room temperature. The non-encapsulated DOX was removed from the vesicles by ultracentrifugation. The purified pellet was resuspended with HBS. DOX-loaded

long-circulating and pH-sensitive liposomes (SpHL-DOX) were prepared in the same way without exosomes.

2.5 ExoSpHL-DOX characterization

2.5.1 Determination of the diameter, polydispersity index, and zeta potential

The size and polydispersity index (PDI) of ExoSpHL-DOX were measured by dynamic light scattering (DLS). The zeta potential was evaluated by DLS associated with electrophoretic mobility. Sample preparation was performed by diluting 50 µL of vesicles in 1 mL of HBS. The equipment used was the Zetasizer Nano ZS90 (Malvern Instruments Ltd, Worcestershire, UK).

2.5.2 Determination of DOX concentration

The DOX concentration in ExoSpHL-DOX was determined by high-performance liquid chromatography (HPLC). The eluent system consisted of methanol:phosphate buffer pH 3.0 (65:35 v/v), at a flow of 1.0mL/min. The column ACE® C8, 25 cm x 4.6 mm, 5 µm (Merck, Darmstadt, Germany) was used in an elution time of 8 min. A fluorescence detector model 2475 (Waters Instruments, Milford, MA, USA) was used. The excitation and emission wavelengths were 470 nm and 555 nm, respectively (FERREIRA *et al*., 2016). For sample preparation, the vesicles were disrupted with isopropyl alcohol (1:2 v/v ratio, respectively) and diluted in methanol:phosphate buffer pH 3.0 (65:35 v/v). The DOX encapsulation percentage (EP) was determined according to the following equation:

$$DOX\ encapsulation\ percentage\ (\%) = \frac{[DOX]\ in\ purified\ liposomes}{[DOX]\ in\ non-purified\ liposomes} \text{ x } 100$$

2.5.3 Nanoparticle tracking analysis (NTA)

NanoSight NS300 (Malvern Instruments Ltd., UK) was used to NTA measurements. Samples were diluted in filtered HBS buffer, and were manually introduced into the equipment. Each sample was evaluated 5 times, capturing 60s videos, at 25 °C. The NTA 3.1 software was used to perform the analysis of concentration, size and diameter distribution of the particles.

2.6 Transmission electron cryomicroscopy (CryoTEM)

The morphology of blank SpHL, exosomes, and blank ExoSpHL was evaluated by means of CryoTEM. The samples were prepared by rapid freezing in liquid ethane in the Automatic Plunge Freezer EM GP2 equipment (Leica Microsystems, Morrisville, USA). The temperature and relative humidity of the chamber were 25°C and 99%, respectively. For each sample, a volume of 3 µL was pipetted and deposited on the surface of the carbon film of the copper grids (300 mesh) of the ultra-thin lacey-carbon (EMS) type, previously ionized by oxygen plasma (glow discharge). The sample was kept on the surface of the film for 20s and the excess sample was removed in an automated way by contacting the back of the carbon film with absorbent paper for 5s (blotting). After blotting, the sample was kept for 20s on the carbon film before freezing. After immersing the sample in liquid ethane, the grid was stored in liquid nitrogen, and kept frozen during the analysis in the Tecnai G2-12 Spirit Biotwin FEI at 120 kV (Centro de Microscopia da Universidade Federal de Minas Gerais, Belo Horizonte, Minas Gerais, Brazil).

2.7 Determination of protein concentration of ExoSpHL

The Pierce BCA Protein Assay kit (Thermo) was used to measure protein concentration in ExoSpHL and exosomes. The vesicles were added in 96-well plates and diluted with the work reagent. Color was developed for 30 min at 37°C, and absorbance at 562 nm was measured in the Spectra Max Plux 384 (Molecular Devices®, San Jose, USA). The results were analyzed using Softmax Pro 6.51® software.

2.8 Raman spectroscopy

The Raman spectra of SpHL, exosomes, and ExoSpHL, were measured using a Raman microscope (Alpha300R, WITec, Ulm, Germany). A 532 nm laser of 1 mW was used for excitation, and 50× objective lens were used to focus the laser beam. The spectra were captured for a total time of 10s, and spectral data were accumulated six times with a resolution of 2 cm^{-1} and a power of 1mW. The measurements were carried out on a microscope slide, at room temperature. The background signal (water) was excluded to obtain the real Raman intensity of the lipids.

2.9 Fourier transform infrared spectroscopy (FTIR)

The infrared spectra were performed by the Frontier spectrophotometer FTIR (Perkin Elmer, Waltham, USA), at CTNano-UFMG. The samples were analyzed in the attenuated total reflectance (ATR) mode in the spectral range of 650 to 4000 cm^{-1}, with the acquisition of 32 scans.

2.10 Nano-flow cytometry

Briefly, 10 µL of samples was incubated with 10 µL of FITC-conjugated anti-CD9 monoclonal antibody (BioAlbra Biotecnologia, Brazil) for 30 min at room temperature in the dark. The volume was made up to 400 µL using HBS. Nano-flow cytometry was performed using the CytoFLEX S cytometer (Beckman Coulter, Brea, USA) in the flow cytometry facility at FIOCRUZ-Minas. Over 200,000 events were acquired by each sample using a flow rate setting of 30 uL/min, and the sample acquisition time was 2 min/sample. Data analysis was performed by FlowJo software v.10.x (BD, USA).

2.11 Stability assay

2.11.1 Storage stability

The storage stability of ExoSpHL-DOX was evaluated for 60 days. The vesicles were maintained at 4°C in HBS buffer. Over time, parameters such as mean diameter, PDI, zeta potential, and DOX retention percentage were evaluated and the results were compared with those obtained at time zero.

2.11.2 *In vitro* biological stability

ExoSpHL-DOX were added in HBS pH 7.4 and RPMI culture media supplemented with 10% (v/v) of FBS to estimate vesicle behavior in biological assays (*in vitro* and *in vivo*). ExoSpHL-DOX were diluted in HBS or RPMI (volume ratio 1:4) and incubated at 37°C for 24h. Aliquots were collected before incubation and in intervals of 24h to measure the size, PDI, and zeta potential, as previously described.

2.12 Release study

Briefly, dialysis bags (10 kDa Sigma, USA) containing 300 µL of ExoSpHL-DOX were immersed into a flask with 100 mL of HBS at pH 7.4 or 5.0. The dialysis flasks were maintained in agitation (156 rpm), at 37°C in an incubator model KS 4000i Control (IKA, Shangai, China). The release study of ExoSpHL-DOX was evaluated at different

time intervals (1, 2, 4, 8, 12, and 24h). At each time, the samples were evaluated for mean diameter and amount of DOX.

2.13 Sulforhodamine B assay

4T1 cells were plated at a density of 5 x 10^3 cells/well in 96-well plates and incubated for 24h, at 37°C and 5% CO_2. After the incubation time, solutions of free DOX, SpHL-DOX, ExoSpHL-DOX, or ExoSpHL (blank exosome-liposome hybrid nanocarrier) were added to the wells. After incubation time (48h), 100 µL of 10% trichloroacetic acid (TCA) was incubated for 1 h at 4°C. After 1h, plates were washed with water four times and 100 µL of sulforhodamine was incubated for 30 min. Then, the plates were washed four times with 1% (v/v) acetic acid. Finally, 100 µL of 10 mM Tris-Base solution (pH 10.5) was added to solubilize dye that has bound to proteins. The absorbance of the wells was determined at 510 nm using a spectrophotometer Spectra Max Plux 384 (Molecular Devices, Sunnyvale, USA) (VICHAI; KIRTIKARA, 2006). The IC_{50} values were calculated using GraphPad Prism 6.0 (Graph Pad software, La Jolla, California, USA).

2.14 Statistical analyses

Statistical analyzes were performed using the GraphPad Prism software (version 6.00, La Jolla, California, USA). The normality and homoscedasticity of variance were tested by D`Agostino and Shapiro-Wilk, respectively. The comparison between the experimental groups was made by analysis of variance (one-way ANOVA followed by Tukey's test). If the data were not normal, the Kruskal-Wallis test with Dunn's post-test were used. For statistical analyses, the differences were considered statistically significant when $p < 0.05$.

3 Results

3.1 ExoSpHL-DOX characterization

3.1.1 Determination of the diameter, PDI, zeta potential, and the DOX entrapment

ExoSpHL-DOX presented a mean diameter of 100.8 ± 7.8 nm and a PDI value of 0.122 ± 0.044, which indicates a monodisperse distribution of the vesicles. The mean value of zeta potential was near neutrality (-5.1 ± 0.9 mV), due to the presence of PEG in the formulation. The concentration of DOX in ExoSpHL-DOX was 1.67 ± 0.05 mg/mL. This

value represents a high percentage of encapsulation (83.5 ± 2.5 %), achieved by using the ammonium sulfate gradient method.

3.1.2 NTA

Results of the NTA measurements of particle concentration, mean size, and diameter distribution are shown in **Table 1**. The mean diameter of exosomes was 115.8 ± 21.8 nm. ExoSpHL-DOX presented a mean diameter of 99.1 ± 3.9 nm and particle concentration of $1.89 \times 10^{13} \pm 5.26 \times 10^{12}$ particles/mL. The diameter observed by the NTA technique was similar to that obtained using the DLS technique (shown in 3.1.1).

Table 1: NTA measurements of exosomes and ExoSpHL-DOX

Properties	Exosomes	ExoSpHL-DOX
Vesicle diameter	115.8 ± 21.8	99.1 ± 3.9
Particle concentration (particles/mL)	$3.59 \times 10^{10} \pm 2.08 \times 10^{9}$	$1.89 \times 10^{13} \pm 5.26 \times 10^{12}$
D10 (nm)	100.5 ± 9.5	88.4 ± 1.8
D50 (nm)	146.7 ± 17.6	110.5 ± 3.4
D90 (nm)	267.4 ± 32.0	182.9 ± 30.2

D10, D50, and D90 mean diameter below which 10%, 50% and 90%, respectively, of the particles are contained. Data expressed as mean ± standard deviation (SD) (n = 3).

3.2 CryoTEM

The morphology of the vesicles was evaluated by CryoTEM. It was possible to confirm the exosome isolation, which had a typical size of 60-140 nm **(Figure 1A)**. In addition, as shown in **Figure 1B and 1C**, respectively, SpHL and ExoSpHL are spherical, predominantly unilamellar, monodisperse and without fusion. The vesicles were predominantly smaller than 200 nm. This result was similar to those found using the DLS and NTA techniques.

Figure 1: CryoTEM photomicrographs of exosomes (A), SpHL (B) and ExoSpHL (C)

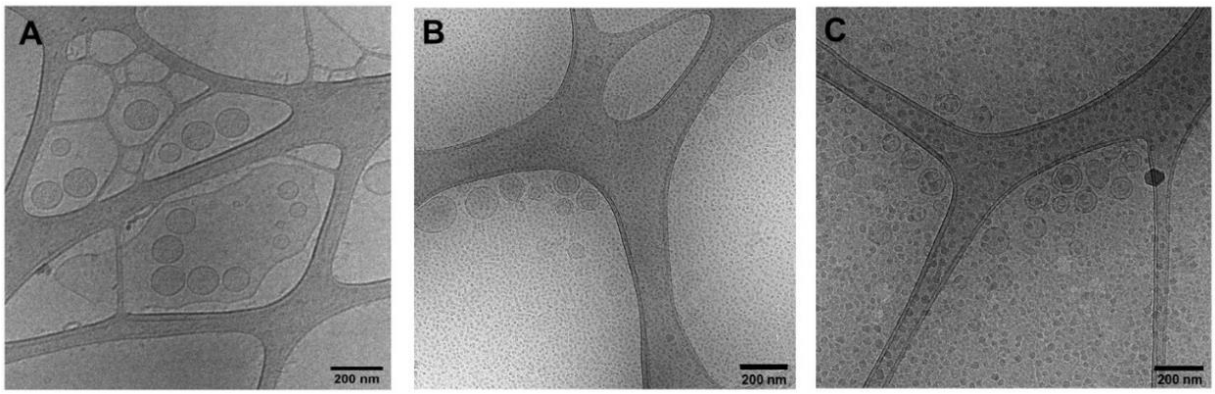

3.3 Determination of protein content of ExoSpHL using BCA

BCA assays were performed to measure the exosome protein level. The results are shown in **Table 2**. The presence of proteins was also confirmed in ExoSpHL and the average concentration in SpHL was clearly lower than the concentration of proteins in ExoSpHL.

Table 2: Quantification of total proteins in samples of SpHL, exosomes, and ExoSpHL

Samples	Protein content (µg/mL)
SpHL	68.4 ± 4.7
Exosomes	293.5 ± 30.1 ****
ExoSpHL	253.2 ± 10.9 ****

Asterisks mean significant difference compared to SpHL ($p < 0.05$). Data expressed as mean ± standard deviation (SD) (n = 3).

3.4 Raman spectroscopy

Raman spectra of SpHL, exosomes, and ExoSpHL are presented in **Figure 2**. The SpHL Raman spectrum exhibited numerous signals in the high-wavenumber spectral region (2700 - 3100 cm^{-1}), referring to the CH stretch regions, two of which attributed to the hydrocarbon chains of the DOPE molecules and of the CHEMS molecules at 2855 cm^{-1} and 2890 cm^{-1}, respectively (FARIED *et al*., 2019). Other known signals were present at 700 cm^{-1} (C-N stretch), 1030-1150 cm^{-1} (C-C stretch), 1300 cm^{-1} (CH_2 twisting of the lipid acyl chains), 1442 cm^{-1} (CH_2 deformation of lipids), and 1736 cm^{-1} (C = O stretch) (FOX; UIBEL; HARRIS, 2007; FARIED *et al*., 2019). Some Raman

peaks that are present in the exosome spectrum already have their attributions related to known biomolecules, such as those at 620 cm^{-1} and 1050-1160 cm^{-1} (proteins), and at 1260-1270 cm^{-1} and 1650-1670 cm^{-1} (lipids) (KRUGLIK e*t al.*, 2019). ExoSpHL exhibited Raman spectrum signal characteristics of the SpHL sample at 1442 cm^{-1} and 2700-3050 cm^{-1}, and of the exosome sample at 450 cm^{-1}, 620 cm^{-1}, and 3100 cm^{-1}. Exosomes+SpHL physical mixture exhibited Raman spectrum signals different of ExoSpHL mainly in the regions at 1200-1600 cm^{-1} and 2600-2900 cm^{-1}.

Figure 2: Raman spectra of exosomes, SpHL, ExoSpHL and exosomes+SpHL physical mixture

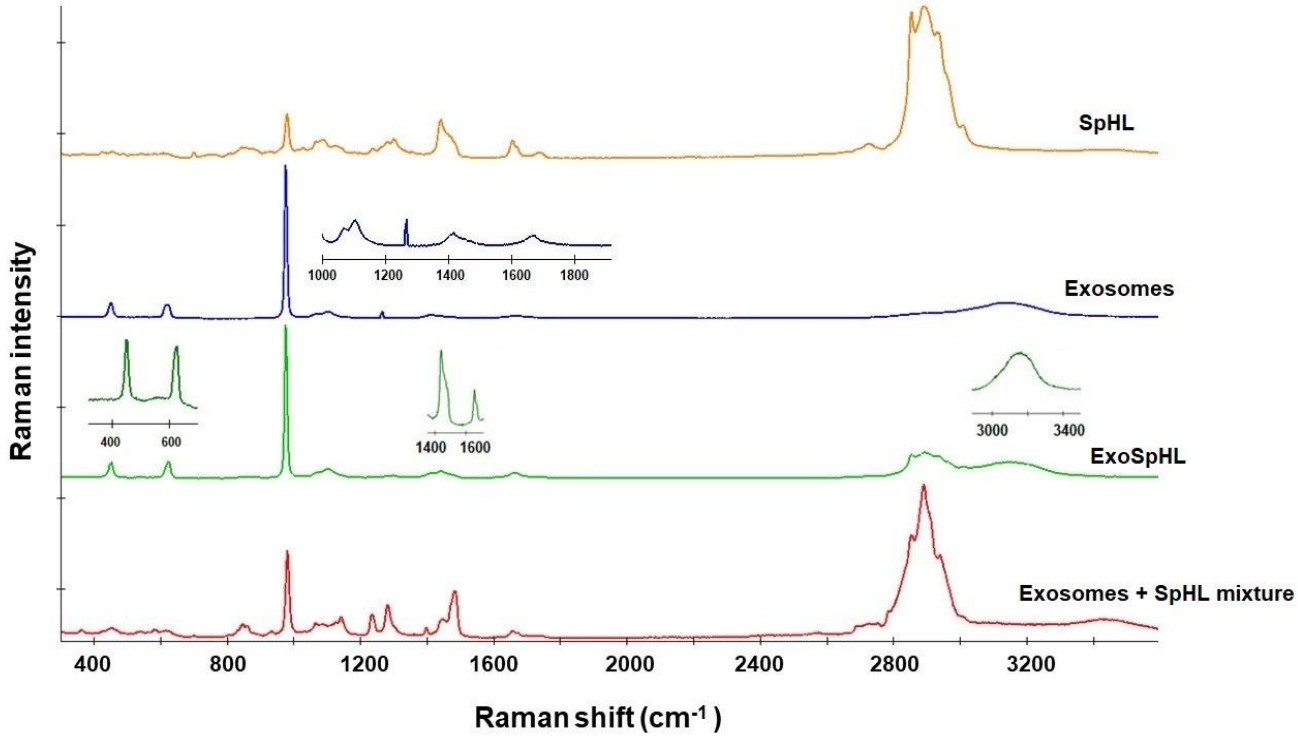

3.5 Fourier transform infrared spectroscopy

FTIR spectra of SpHL, exosomes, and ExoSpHL are presented in **Figure 3**. The SpHL sample exhibited bands at 3219 cm^{-1} (C-N stretch), 2921 cm^{-1} and 2856 cm^{-1} (C-H stretch), 1740 cm^{-1} (C=O stretch), 1653 cm^{-1} (C=C stretch), 1446 (CH_3 stretch), and 1076 cm^{-1} (C-O stretch) (LOPES; FASCIO, 2004). In the FTIR spectrum of exosomes, bands similar to the SpHL spectrum were observed in the region from 4000 cm^{-1} to 1700 cm^{-1}. This is expected, since exosomes are made up of lipids as well as liposomes. Additionally, exosomes exhibited bands at 1628 cm^{-1} (titled amide I, related to C=O stretching vibrations of the proteins), 1444 cm^{-1} (belonging to CH_2 scissoring

vibration of lipid acyl), 1082 cm^{-1} and 976 cm^{-1} (related to phosphodiester groups stretching vibrations and C-O-C stretching vibrations of cholesterol esters, phospholipids and triglycerides) (MIHÁLY *et al.*, 2016; HURVITZ *et al.*, 2019; MARTINS *et al.*, 2020). The FTIR spectrum of ExoSpHL showed the characteristic bands of exosomes at 976 cm^{-1} and the characteristic bands of SpHL at 1740 cm^{-1} and 1653 cm^{-1}. Exosomes+SpHL physical mixture exhibited FTIR spectrum different from ExoSpHL mainly in the regions at 2700-3000 cm^{-1}.

Figure 3: FTIR spectra of exosomes, SpHL, ExoSpHL and exosomes+SpHL physical mixture

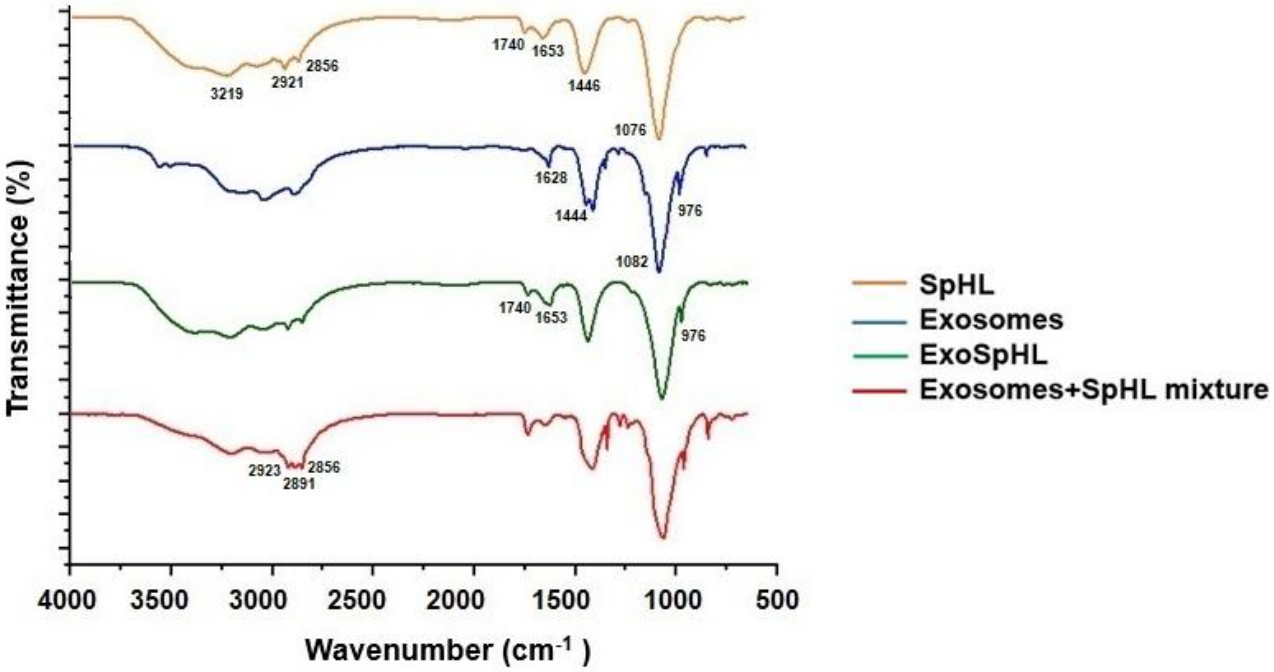

3.6 Nano-flow cytometry

The data demonstrated that exosome and ExoSpHL groups showed increased percentage of nanoparticles positive for CD9 when compared to SpHL **(Figure 4)**. These results confirm the isolation of exosomes from 4T1 cells and the fusion between long-circulating and pH-sensitive liposomes and tumor-derived exosomes, since a typical exosome marker was detected on the surface of exosomes and ExoSpHL by nanoscale flow cytometry.

Figure 4: Exosomes isolation and fusion with long-circulating and pH-sensitive liposomes evaluated by nano-flow cytometry. A) The mean percentages of the positive fluorescent nanoparticles of all experimental groups are presented in bar plot as follows: orange=SpHL, blue=Exossomes, green=ExoSpHL bars. The samples were labelled with FITC-conjugated anti-CD9. B) Representative density plots considering FSC-A *vs* Violet-SSC-A parameters are presented for each group.

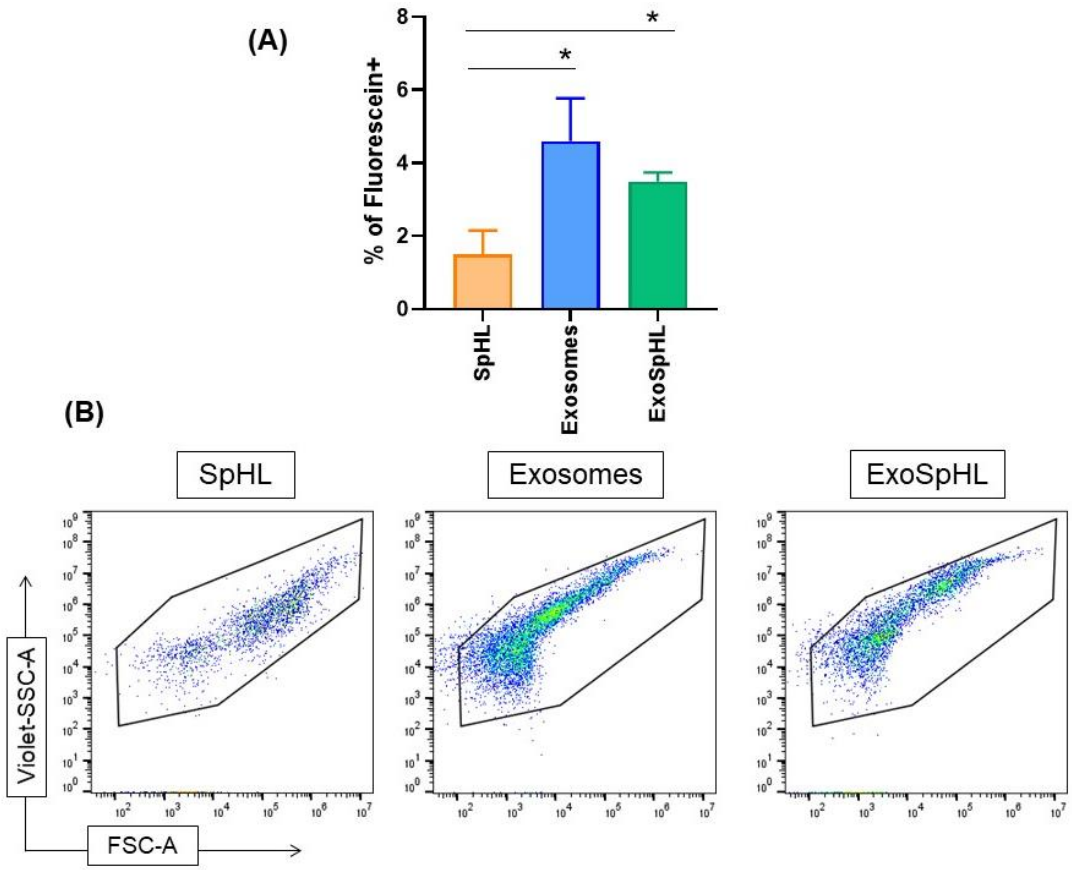

Asterisk means a significant difference compared to SpHL (p< 0.05).

3.7 Stability assay

3.7.1 Storage stability

It was observed good stability for ExoSpHL-DOX. No notable changes were observed in vesicle size, PDI **(Figure 5A)**, and DOX content **(Figure 5B)** during 60 days at 4°C. Also, there was no change in the zeta potential values (data not shown).

Figure 5: ExoSpHL-DOX size, PDI (A), and concentration of DOX (B) up to 60 days at 4 °C

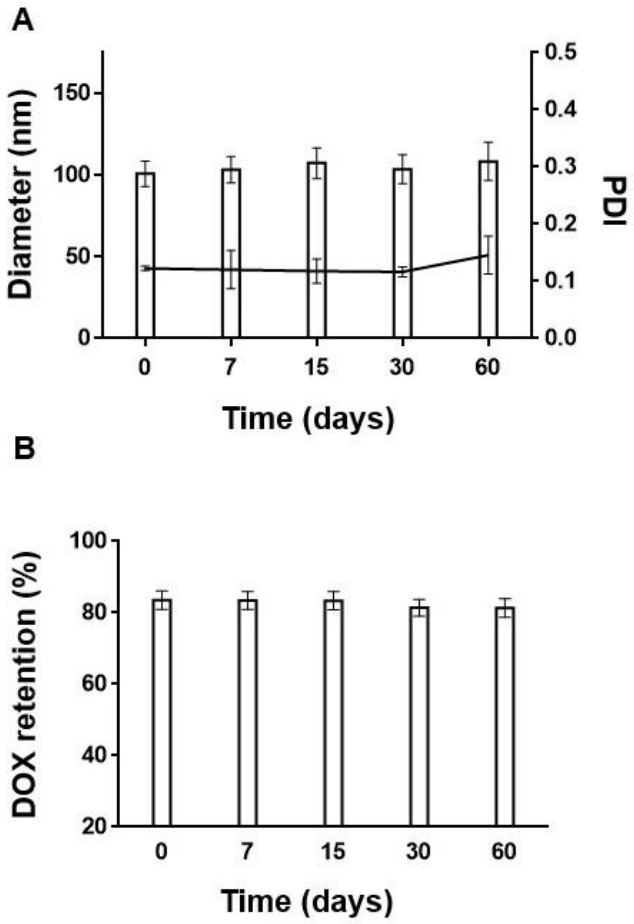

3.7.2 *In vitro* biological stability

The size, PDI, and zeta potential of ExoSpHL-DOX were evaluated again after incubation in HBS and RPMI. ExoSpHL-DOX showed suitable stability in simulated biological conditions (pH, temperature, and protein content) until 24 h after incubation. There was no change in the size of vesicles, PDI**,** and zeta potential, which remained near neutrality (data not shown).

3.8 Release study

The release study of ExoSpHL-DOX was evaluated at different pH (7.4 and 5.0) **(Figure 6)**. After 1h, ExoSpHL-DOX incubated at pH 5.0 already showed greater release of DOX compared to pH 7.4. After 24h, 96.6 ± 0.2% of DOX was released from ExoSpHL-DOX at pH 5.0, while only 70.1 ± 1.7% of DOX was released at pH 7.4. Significant changes in the diameter of the vesicles at pH 5.0 were also observed

(Figure 7). At pH 7.4, the vesicle size was not altered for 24h, while an increase was observed in the diameter size of vesicles at pH 5.0 (105.8 nm at time 0 and 162.0 nm at time 24 h).

Figure 6: Release profile of ExoSpHL-DOX at pH 5.0 and 7.4 at different times

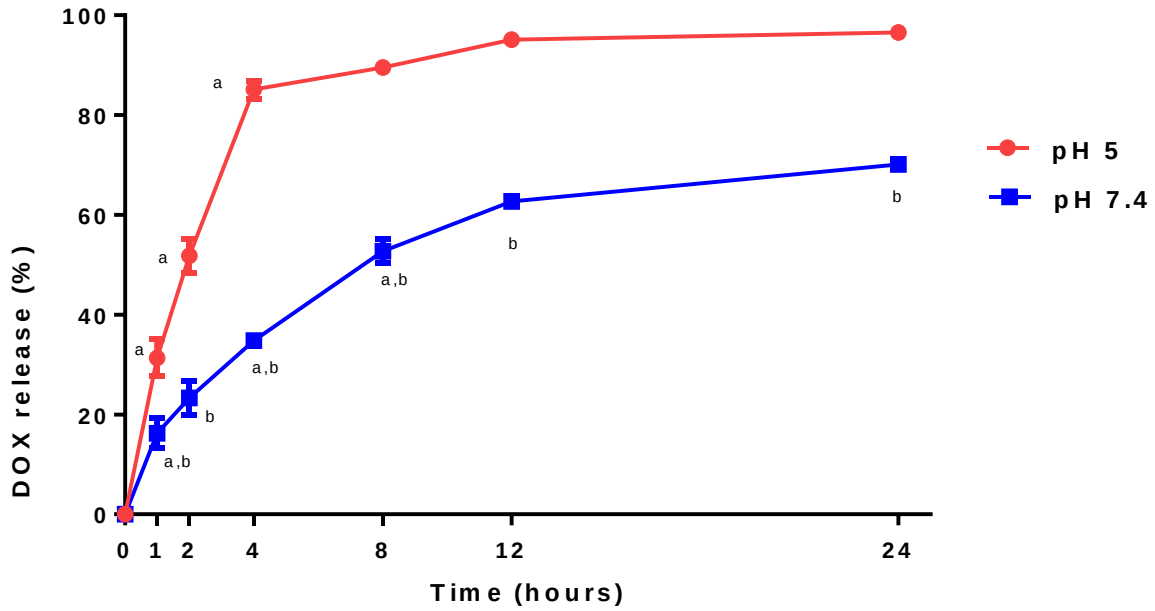

[a]Represents statistical differences between 1h, 2h, 4h or 8 h and the previous time at the same pH. [b]Represents statistical differences between pH 5.0 and 7.4 at the same time.

Figure 7: Evaluation of the vesicle diameter of ExoSpHL-DOX at pH 5.0 and 7.4 at different times

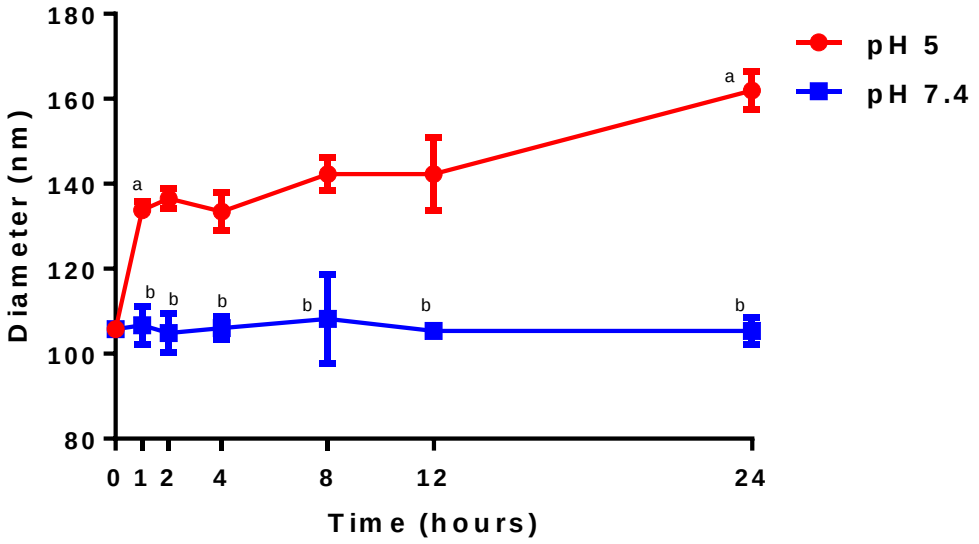

[a]Represents statistical differences between 1h or 24 h and the previous time at the same pH.
[b]Represents statistical differences between pH 5.0 and 7.4 at the same time.

3.9 Evaluation of the cytotoxicity

The IC_{50} values, summarized in **Table 3**, were determined for each treatment to which the 4T1 cell line was submitted. The free DOX, SpHL-DOX, and ExoSpHL-DOX treatments presented the same cytotoxicity against the 4T1 cell line. There is no significant difference between IC_{50} values for the three treatments. The blank ExoSpHL treatment showed no cytotoxic effect.

Table 3: IC_{50} values for DOX, SpHL-DOX and ExoSpHL-DOX against 4T1 breast cancer cells

Treatments	IC_{50} (µM)
DOX	0.164 ± 0.105
SpHL-DOX	0.174 ± 0.085
ExoSpHL-DOX	0.203 ± 0.066

IC_{50} values are given in µM. Data expressed as mean ± SD (n = 3).

4 Discussion

Extracellular vesicles (EV) derived from the 4T1 breast cancer cell supernatant were successfully isolated using the exosome extraction kit (TANG *et al*., 2017). These purified vesicles were analyzed by CryoTEM and showed typical characteristics of exosomes shape and size distribution. When these vesicles were characterized using NTA, the mean diameter was equal to 115.8 ± 21.8 nm, which is within the range of exosome diameters (30-150 nm) (BUNGGULAWA, 2018). Additionally, a BCA protein assay kit and flow cytometry, respectively, were used to measure protein concentrations and characterize CD9 exosomal surface protein on isolated exosomes (GURUNATHAN *et al.*, 2019). Recently, many studies have shown that the hybrid nanoparticles, formed by the fusion of membranes of exosomes and liposomes, have increased drug delivery, prevented clearance by the mononuclear phagocytic system (LV *et al.*, 2020), increased antitumor efficacy (WANG *et al.*, 2020), reduced the number of lung metastasis lesions (NIE *et al.*, 2020), and overcome cisplatin-resistant ovarian cancer (LI *et al.*, 2022). Thinking about these findings, in this study, long-circulating and pH-sensitive liposomes fused with tumor-derived exosomes containing DOX (ExoSpHL-DOX) were prepared by the Bangham method or lipid film hydration, which is a simple technique widely used for liposome preparation (BANGHAM; STANDISH; WATKINS, 1965). The lipids are first dissolved in an organic solvent and transferred to a flask for evaporation of the solvent in rotavapor, thus obtaining the lipidic film, which after being dispersed in an aqueous medium forms the liposomes. ExoSpHL-DOX presented the mean diameter of vesicles and PDI values suitable for intravenous administration. Due to the known enhanced permeability and retention effect (EPR), vesicles of this size are able to preferentially accumulate in the tumor region (FRANCO *et al*., 2021). Both DLS and NTA techniques, were used to obtain the mean diameter value for ExoSpHL-DOX and the results obtained were similar. This diameter value of ExoSpHL-DOX was also confirmed by CryoTEM analysis. The mean value of zeta potential was near neutrality, due to the presence of PEG in the formulation. In addition to reducing the electrophoretic mobility of the particles, PEG molecules prevent the aggregation of vesicles due to the steric barrier generated (GOMES *et al*., 2018). The presence of PEG molecules may justify the stability of ExoSpHL-DOX over 60 days (GOMES *et al*., 2018; FRANCO *et al*., 2021). The method used to encapsulate DOX was the ammonium sulphate gradient, which proved to be

efficient for encapsulation in long-circulating and pH-sensitive liposomes (83.5%), similarly to the results obtained by other studies of our research group (SILVA *et al.*, 2018; NOVAIS *et al*., 2021). This method allows high value for DOX entrapment percentage. A gradient is created between the HBS and the inside of the vesicles with the ammonium sulfate buffer. Once inside the vesicles, DOX reacts with the sulfate forming an insoluble salt, which precipitates inside the vesicles. This DOX precipitation could also explain the great stability of ExoSpHL-DOX for 60 days (NOVAIS *et al*., 2021). The mean diameter, PDI, and zeta potential of the vesicles were evaluated after incubation in HBS and biological medium (RPMI). ExoSpHL-DOX showed suitable stability in simulated biological conditions (pH, temperature, and protein content) until 24h after incubation. Therefore, ExoSpHL-DOX could be considered suitable for *in vitro* and *in vivo* assays. BCA assays were also performed to measure the protein level in ExoSpHL. The presence of proteins was confirmed in these vesicles, which suggests the fusion between membranes of tumor-derived exosomes and long-circulating and pH-sensitive liposomes. ExoSpHL were characterized by Raman spectroscopy and FTIR and compared to SpHL, exosomes, and a physical mixture of exosomes and SpHL. ExoSpHL showed Raman signals and FTIR characteristic bands of SpHL and exosomes, which were different from the exosomes+SpHL mixture, suggesting again the fusion between membranes of tumor-derived exosomes and long-circulating and pH-sensitive liposomes, during the preparation of ExoSpHL. The characterization of exosomes is commonly performed by the identification of CD9, CD63, and CD81, which are members of the tetraspanin family, abundantly expressed on the surface of exosomes (PADDA *et al.*, 2019). The presence of CD9, a typical exosome marker, was detected on the surface of ExoSpHL using nanoscale flow cytometry, which confirmed the presence of exosomes in the membrane of the vesicles. The release of DOX from ExoSpHL-DOX was performed using a dialysis method at pH 5.0 and 7.4 and showed a higher percentage of release of DOX in acidic medium relative to neutral pH. Significant change in the vesicle diameter at pH 5.0 over 24h could be observed, while it was not observed at pH 7.4, suggesting that the pH-sensitivity of liposomes to acid pH medium was preserved, even with the fusion of tumor-derived exosomes. These findings suggest ExoSpHL-DOX as a potential system for DOX delivery to the tumor region since these vesicles will be able to release their content when in contact with the acidic microenvironment of the tumor area (SILVA *et al.*, 2018; FRANCO *et al*., 2021). In pH-sensitive liposomes, the carboxyl

group of CHEMS molecules is protonated when exposed to an acid environment, such as endosomes (pH values between 4.5–6.5), leading to a lamellar to hexagonal phase transition, and consequently, the release of the encapsulated drug (FRANCO *et al*., 2021). Regarding the cytotoxic effects, the IC_{50} values presented for the 4T1 cell line were similar for the treatments with ExoSpHL-DOX, free DOX and SpHL-DOX, which indicate that the cytotoxic effect of DOX against the murine breast cancer cell line is not impaired when liposomes are fused with exosomes.

5 Conclusion

The results of this study shown that the developed ExoSpHL-DOX remained stable over 60 days. The release of DOX from the vesicles is pH-dependent, being higher in acidic medium. The analyses by Raman, FTIR, and nano-flow cytometry confirmed the fusion between lipid membranes. The cytotoxic study against the breast cancer cell line demonstrated that ExoSpHL-DOX treatment significantly reduced the cancer cell viability. Therefore, the present results suggest that the fusion of tumor-derived exosomes with long-circulating and pH-sensitive liposomes using the lipid film hydration method represents a new strategy to yield advanced drug delivery systems.

CAPÍTULO 2

Investigation of the antitumor activity and toxicity of tumor-derived exosomes fused with long-circulating and pH-sensitive liposomes containing doxorubicin

Eliza Rocha Gomes, Fernanda Rezende Souza, Geovanni Dantas Cassali, Adriano de Paula Sabino, André Luís Branco de Barros, Mônica Cristina Oliveira

ABSTRACT

Exosome-liposome hybrid nanocarriers containing chemotherapeutic agent have been developed to enhance drug delivery, improve efficacy of the treatment of metastatic cancer, and overcome chemoresistance of cancer therapy. Thus, the objectives of this study were to investigate the toxicological profile of exosomes fused with long-circulating and pH-sensitive liposomes containing doxorubicin (ExoSpHL-DOX) in healthy mice and the antitumor activity of ExoSpHL-DOX in Balb/c female mice bearing 4T1 breast tumor. Acute toxicity was determined by evaluating the mortality and morbidity of the animals, hematological, biochemical, and histopathological analyses, after a single intravenous administration of ExoSpHL-DOX. The results of the study indicated that ExoSpHL-DOX treatment is less toxic than free doxorubicin (DOX) treatment. ExoSpHL-DOX showed no signs of nephrotoxicity even at the highest dose of DOX, indicating that the hybrid nanosystem may alter the distribution of DOX and reduce the kidney damage. Regarding the antitumor activity, ExoSpHL-DOX showed an antitumor effect compared to the control group. Furthermore, the hybrid nanocarrier of tumor-derived exosomes fused with long-circulating and pH-sensitive liposomes reduced the number of metastatic foci in the lungs. These results indicate that ExoSpHL-DOX may be a promising nanocarrier for the treatment of breast cancer, reducing toxicity and inhibiting metastasis, mainly in the lung.

Keywords: acute toxicity, breast cancer, metastasis, exosomes, liposomes, doxorubicin

1 Introduction

Cancer is one of the leading causes of death and an important barrier to increasing life expectancy in the world. Annually, more than 19 million people develop cancer and approximately 10 million people die from the disease. Breast cancer is the most commonly diagnosed cancer in women, with 2.3 million new cases (SUNG *et al.*, 2021). Doxorubicin (DOX) is a chemotherapeutic drug used as the first-line treatment for breast cancer. However, this drug causes serious toxic effects, mainly dose-dependent cardiotoxicity, which has limited its clinical use (ZHAO; WOODLE; MIXSON, 2018; JAMIALAHMADI; ZAHEDIPOUR; KARIMI, 2021). To minimize the adverse effects caused by DOX, liposomes have been used in the treatment of patients (NGAN; GUPTA, 2016; ZHAO; WOODLE; MIXSON, 2018). However, there is no increase in the therapeutic efficacy, mainly in DOX-resistant cancer, of liposomal formulations compared to conventional DOX (ZHAO; WOODLE; MIXSON, 2018). In order to improve the therapeutic efficacy of DOX, liposomes can be fused with exosomes released by breast cancer cells. Tetraspanins and integrins present on the surface of exosomes can facilitate fusion and membrane interactions, achieving greater cell uptake of fused vesicles (LIANG *et al.*, 2021; MUKHERJEE, *et al.*,2022).

Considering the potential strategy of liposomes and exosome fusion, Gomes and coworkers (GOMES *et al*., 2022) developed and characterized a hybrid nanocarrier of tumor-derived exosomes fused with long-circulating and pH-sensitive liposomes containing DOX (ExoSpHL-DOX) for the treatment of breast cancer. The developed formulation can be administered intravenously, since its mean diameter was equal to 100.8 ± 7.8 nm and the polydispersity index (PDI) was of 0.122 ± 0.004. The encapsulated DOX content was equal to 83.5 ± 2.5%. Besides ExoSpHL-DOX showed to be stable at 4°C for 60 days. The study of the release of DOX from ExoSpHL-DOX in dilution media with different pH values confirmed the pH-sensitivity characteristic of the nanosystem, and the cytotoxic study against 4T1 murine breast cancer cell line, demonstrated that ExoSpHL-DOX treatment significantly reduced the cancer cell viability. Herein, we investigated the toxicological profile of ExoSpHL-DOX in healthy mice and the antitumor activity of ExoSpHL-DOX on Balb/c female mice bearing 4T1 breast tumor.

2 Materials and methods

2.1 Chemicals

1,2-dioleoyl-sn-glycero-3-phosphoethanolamine (DOPE) and 1,2-distearoyl-sn-glycero-3-phosphoethanolamine-N-[amino(polyethyleneglycol)-2000 (DSPE-PEG_{2000}) were supplied by Lipoid GmbH (Ludwigshafen, Germany). Cholesterol hemisuccinate (CHEMS), DOX, phosphate-buffered saline (PBS), sodium hydroxide, 4-(2-hydroxyethyl)piperazine-1-ethanesulfonic acid (HEPES), and sodium bicarbonate were obtained from Sigma Aldrich (St. Louis, USA). Total exosome isolation reagent was obtained from Thermo Fisher Scientific (Waltham, USA).

2.2 Cells

The 4T1 murine breast cancer cells were purchased from American Type Culture Collection (ATCC) (Manassas, USA). The Roswell Park Memorial Institute (RPMI) 1640 Medium and fetal bovine serum (FBS) were obtained from Gibco Life Technologies (Carlsbad, USA). Trypsin was obtained from Sigma-Aldrich (St. Louis, USA). Mycoplasma test using Hoechst fluorescence staining was performed on the cell line.

2.3 Isolation of exosomes

4T1 cells were grown in RPMI-1640 supplemented with 10% of ultracentrifuged FBS, and maintained at 37°C and 5% CO_2 in a humidified atmosphere. When 4T1 cells reached an approximate confluence of 80%, the supernatant was removed from the cell culture flask T-75. The exosome isolation reagent was added to the supernatant (1:2 v/v ratio, respectively) and kept in refrigerator for 15h. After that time, the mixture was centrifuged at 10,000xg, for 1h, at 4°C, using a centrifuge Thermo Scientific, model Heraeus Multifuge X 1R. The pellet was dissolved in a mixture of chloroform and methanol (1:1 v/v ratio).

2.4 Preparation of ExoSpHL-DOX

ExoSpHL-DOX was prepared using the Bangham method (BANGHAM; STANDISH; WATKINS, 1965), followed by extrusion for size calibration. Chloroform aliquots of DOPE, CHEMS, and DSPE-PEG_{2000} (5.7 : 3.8 : 0.5, molar ratio, respectively) and exosomes in a mixture of chloroform and methanol were added to a round bottom flask

to obtain a lipid film. For each mL of liposome, it was added the exosome pellet obtained from 2 mL of cell supernatant (concentration of 3.6 x 10^{10} particles/mL). After evaporation of the solvents, NaOH 0.228 M solution was added to ionize CHEMS molecules, and subsequently, promote the formation of vesicles. Hydration of the lipid film was carried out under agitation with an ammonium sulfate solution (300 mM, pH 7.4). The vesicles obtained were calibrated by extrusion using the Lipex Biomembranes extruder, Model T001 (Vancouver, Canada) (SILVA *et al.*, 2019). The external ammonium sulfate was removed by ultracentrifugation (Ultracentrifuge Optima® L-80XP, Beckman Coulter, Brea, USA) at 150,000xg, 4°C, for 120 min. The pellet was resuspended with HEPES buffered saline (HBS). The vesicles were incubated with a DOX solution for 2h, in the dark and at room temperature. The non-encapsulated DOX was removed by ultracentrifugation using the same method described above. The final pellet was resuspended with HBS. Blank breast tumor-derived exosomes fused with long-circulating and pH-sensitive liposomes (ExoSpHL) and long-circulating and pH-sensitive liposomes containing DOX (SpHL-DOX) were prepared in the same way without the addition of DOX and exosomes, respectively.

2.5 ExoSpHL-DOX characterization

2.5.1 Determination of the diameter, polydispersity index, and zeta potential

The mean diameter and polydispersity index (PDI) of ExoSpHL-DOX were measured by dynamic light scattering (DLS). The zeta potential value was determined by DLS associated with electrophoretic mobility. To perform both analysis, 50 µL of ExoSpHL-DOX were diluted in 1 mL of HBS, and the Zetasizer Nano ZS90 equipment was used (Malvern Instruments Ltd, Worcestershire, UK).

2.5.2 Determination of the content of DOX

The DOX content was measured by high-performance liquid chromatography (HPLC). The mobile phase consisted of methanol:phosphate buffer pH 3.0 (65:35 v/v). Samples were injected (20 µL) and separation was performed with an ACE® C8 column, 25 cm x 4.6 mm, 5 µm (Merck, Darmstadt, Germany) at a flow rate of 1.0 mL/min. Detection was performed in model 2475 fluorescence mode (Waters Instruments, Milford, MA, USA) with excitation and emission wavelengths of 470 nm and 555 nm, respectively (FERREIRA *et al.,* 2016). ExoSpHL-DOX was opened with isopropyl alcohol (1:2 v/v,

respectively), and diluted in the mobile phase. The encapsulation percentage (EP) of DOX in ExoSpHL-DOX was calculated according to the following equation:

$$DOX\ encapsulation\ percentage\ (\%) = \frac{[DOX]\ in\ purified\ vesicles}{[DOX]\ in\ non-purified\ vesicles} \text{ x } 100$$

2.6 Animals

Healthy female Balb/c mice of 8-10 weeks and approximately 18 g were obtained from Central Biotery, Universidade Federal de Minas Gerais – UFMG, (Belo Horizonte, Brazil). The mice were kept in plastic cages with free access to food and water and under standardized light/dark cycle conditions. All protocols were approved by the Ethics Committee for Animal Experiments from the Universidade Federal de Minas Gerais (CEUA/UFMG - Protocol number 265/2019).

2.7 Acute toxicity

Acute toxicity was assessed according to the recommendations of the Organization for Economic Cooperation and Development (OECD) 423 (OECD, 2002), adapted for intravenous administration, as previously done by our research group (SILVA *et al.*, 2018). The animals were divided into five groups. Each group received intravenously a single dose of HBS, ExoSpHL, free DOX, SpHL-DOX or ExoSpHL-DOX. Mice were observed for 14 days regarding their behavior, weight, and mortality. After observation period, the animals were anesthetized with a mixture of xylazine (15 mg/kg) and ketamine (80 mg/kg) intraperitoneally. The blood was collected by puncture of the brachial plexus for hematological and biochemical analyzes. The organs were collected for histopathological analyzes.

In previous studies, our research group evaluated toxicity of 10 mg/kg and 15 mg/kg of free DOX and SpHL-DOX in mice. Weight loss around 5%, prostration, and intense piloerection were observed in animals treated with free DOX (15 mg/kg). No significant signs of toxicity were observed in animals treated with SpHL-DOX (15 mg/kg). Based on the findings of this study, the initial doses proposed in this study were 10 mg/kg of free DOX and 15 mg/kg of SpHL-DOX and ExoSpHL-DOX (SILVA *et al.*, 2018). According to the OECD guideline (OECD, 2002), initially, each group of treatment was composed of 3 animals. If the dose tested was capable of causing the death of 2 or more animals in the group, dosing of 3 additional animals at the previous lowest dose level was required. However, if the tested dose was able to cause one or no death, the

next step is dosing of 3 additional animals, with the same dose. In the case of confirmation of the results of one or no death, it was necessary dosing of 3 additional animals at the next higher dose level. The doses scheme used to assess the median lethal dose (LD50), after treatments with free DOX and formulations (SpHL-DOX and ExoSpHL-DOX), respectively, is presented in **Appendices A** and **B**. LD50 means the single dose of DOX that is required to cause death in 50 percent of animals tested.

Appendix A: Treatment scheme used to assess the median lethal dose (LD50) after treatment with free DOX

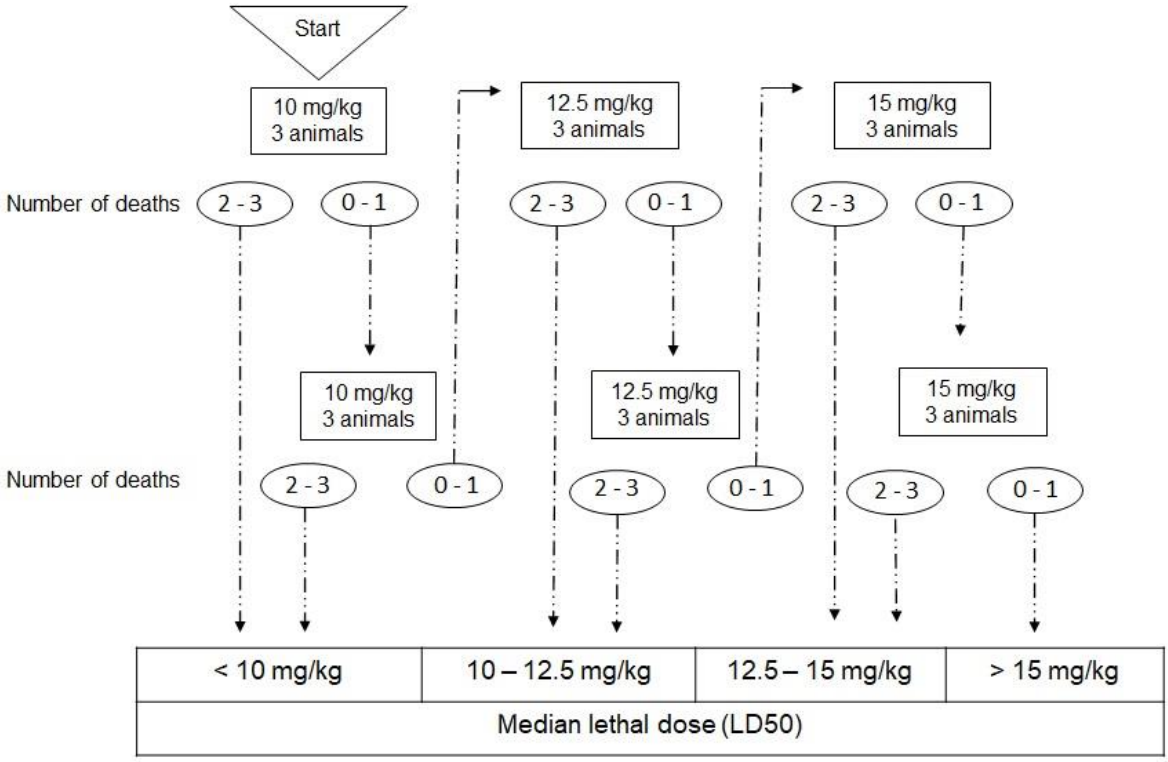

Appendix B: Treatment scheme used to assess the median lethal dose (LD50) after treatment with SpHL-DOX or ExoSpHL-DOX

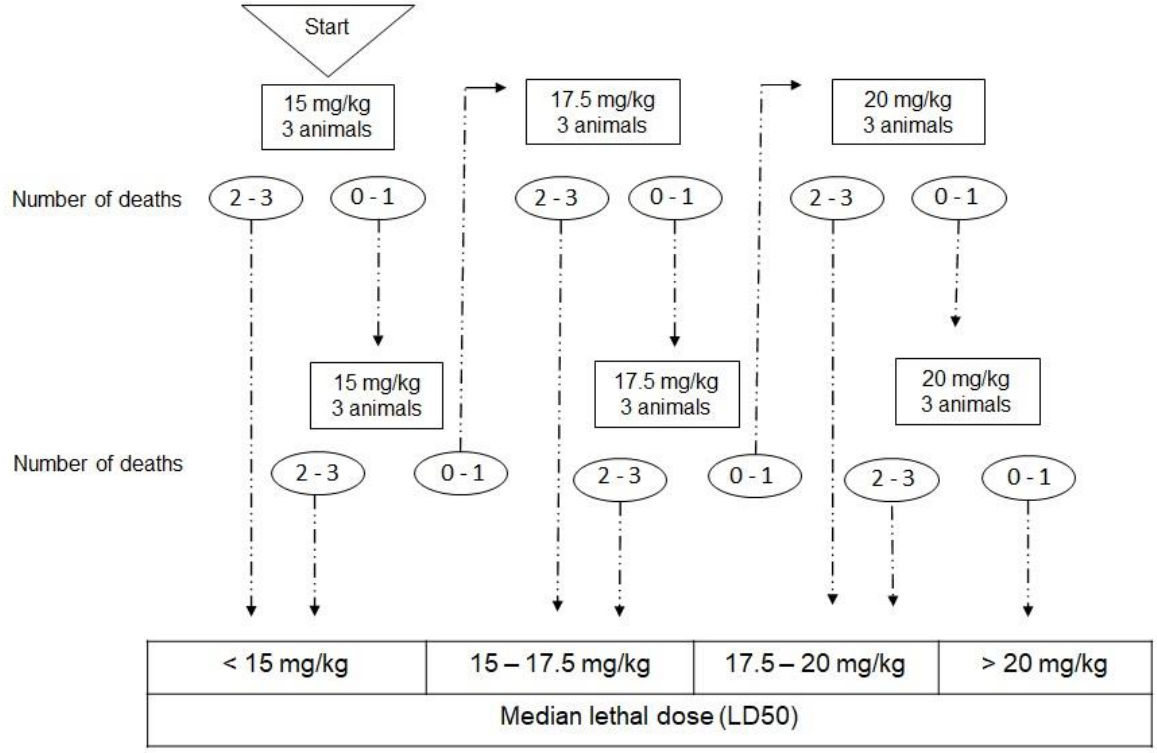

2.7.1 Hematology and biochemistry analyzes

For hematological analysis, the blood was collected in tubes containing anticoagulant (EDTA 0.1M) and inserted into the automated hematological analyzer HEMOVET 2300 (Hemovet, São Paulo, Brazil). Hematological parameters related to red and white blood cells were evaluated for each group of treatment. For biochemical analysis, the blood was centrifuged (3000 rpm, 15 min) and the plasma obtained was collected. The tests were performed in the Bioplus BIO-2000 semiautomatic analyzer (Bioplus, São Paulo, Brazil) using commercial kits (Labtest, Lagoa Santa, Brazil). Renal, liver, and cardiac functions were evaluated for each group of treatment.

2.7.2 Histopathological Analysis

Liver, kidneys, spleen, sternum, lung, and heart were harvested and fixed in formalin [10% w/v in phosphate-buffered saline (PBS), pH 7.4] and included in paraffin blocks. Consecutive histological sections were prepared and stained by the hematoxylin and eosin routine method. The slides were evaluated by trained pathologists and images

of histological sections were captured using a digital camera connected to an optical microscope Olympus BX-40 (Olympus, Tokyo, Japan).

2.8 Evaluation of the antitumor activity

The 4T1 breast cancer cells were injected in the right flank of female Balb/c mice (1.0 x 10^6 cells in 100 µL PBS). When tumor volume reached approximately 100 mm^3, the animals were randomly divided into five groups of treatment, each containing six animals. Each group received intravenously, five administrations of HBS, ExoSpHL, free DOX, SpHL-DOX or ExoSpHL-DOX. The cumulative dose of DOX was 25 mg/kg. The dose used in this study was based on previous study of our research group (LAGES *et al.*, 2020). The antitumor activity was evaluated based on the tumor volume (TV) calculated as previously described (ROLLAND *et al.*, 2009), where TV = 0.52 x (d1 x $d2^2$), being d1 and d2, the largest and the smallest perpendicular diameters, respectively. Six measurements of the diameters of the tumors were made during ten days of treatment using a caliper MIP/E-103 (Mitutoyo, Suzano, São Paulo, Brazil). The TV at day 0 was considered as 100% and changes in the TV every two days were determined by calculating the percentages of TV increase or decrease. Relative tumor volume (RTV) and inhibition percentage of tumor growth (TGI) were calculated according to the following equations:

$$RTV = \frac{TV\ on\ day\ 10}{TV\ on\ day\ 0}$$

$$TGI = 1 - \frac{RTV\ of\ each\ treatment}{RTV\ of\ the\ control\ group} \text{x}\ 100$$

On day 10, the animals were anesthetized with a mixture of xylazine (15 mg/kg) and ketamine (80 mg/kg) intraperitoneally. Liver, kidneys, spleen, lung, heart, and tumor were collected for histopathological analysis.

2.9 Statistical analyses

To confirm the normality and homoscedasticity of variance, D'Agostino and Shapiro-Wilk tests were applied, respectively. The differences between the experimental groups were tested by analysis of variance (one-way ANOVA followed by Tukey's test). If the data were not normal or homoscedastic, the Kruskal-Wallis test with Dunn's post-

test was used for the same purpose. The Two-way ANOVA test with Tukey's post-test was also used to relate two different independent variables over one dependent variable. Values of $p < 0.05$ were considered significant. The analyzes were performed using the GraphPad Prism software (version 6.00, La Jolla, California, USA).

3 Results

3.1 ExoSpHL-DOX characterization

ExoSpHL-DOX presented a mean diameter of 105.4 ± 2.9 nm and PDI value of 0.132 ± 0.010, indicating the presence of monodisperse vesicles. The zeta potential value was near neutrality (-6.4 ± 1.2 mV), as expected by vesicles that contain PEG in their composition. The encapsulation percentage of DOX was 88.5 ± 2.4 %, achieved by using the ammonium sulfate gradient method.

3.2 Acute toxicity study

3.2.1 Evaluation of animal mortality and morbidity

HBS and ExoSpHL treatments did not show significant difference in relation to mortality and morbidity. These findings indicate no toxicity of the treatments of mice in control groups. The LD50 assessment by animals treated with free DOX started with 10 mg/kg, and for both formulations (SpHL-DOX and ExoSpHL-DOX) with 15 mg/kg. For free DOX treatment, the 10 mg/kg dose showed no significant signs of toxicity in the first 3 animals tested. Thus, the next step was dosing of 3 additional animals with the same dose. The results remained the same in all animals, so the next higher dose level was injected in 3 animals. After 8 days of application of 12.5 mg/kg of DOX, piloerection and ascites in the animals were observed. It is worth mentioning that the most notable result was weight loss of 13 % observed at day 12 post-administration. However, no deaths were observed. Therefore, the next step was dosing of 3 additional animals, with the same dose. The previous observations were confirmed and there was 1 death on day 13. According to **Appendix A**, the next step was dosing of 3 additional animals at the next higher dose level (15 mg/kg). For the first 3 mice evaluated, there was 1 death on day 10 and 1 death on day 12 of the study. In addition, intense piloerection was observed in all animals. Also, it was observed loss of weight of the animals between 7 % and 20 % during the days after treatment. Therefore, according to OECD 423 guideline (OECD, 2002), the LD50 value for free DOX treatment is between 12.5

and 15 mg/kg for this experimental model. Thus, 15 mg/kg was the last dose tested for the treatment with free drug.

The studies carried out with SpHL-DOX and ExoSpHL-DOX treatments started with a dose of 15 mg/kg. For both treatments, there was no death and weight loss in all 6 animals tested. After treatment with a dose of 17.5 mg/kg, no deaths were also observed. Although, there was a 5 % weight loss in the animals. According to these results, we repeated the experiments for groups treated with SpHL-DOX and ExoSpHL-DOX at dose of 17.5 using 3 more animals per treatment, and the previous observations were confirmed. We followed the treatment scheme **(Appendix B)**, increasing the dose to 20 mg/kg for SpHL-DOX and ExoSpHL-DOX treatments. After treatments with the 20 mg/kg dose, it was observed 2 deaths on day 6 and 1 death on day 8 for the SpHL-DOX treatment group. For ExoSpHL-DOX treatment occurred 1 death on day 6, 1 death on day 8 and 1 death on day 10. In addition, during the days after treatment, animals treated with ExoSpHL-DOX and SpHL-DOX had weight loss of 10 % and 20 %, respectively. Therefore, according to OECD 423 guideline (OECD, 2002), the LD50 value for SpHL-DOX and ExoSpHL-DOX treatments is between 17.5 and 20 mg/kg for this experimental model. Thus, 20 mg/kg was the last dose tested for both formulations.

3.2.2 Hematological analysis

Hematological parameters of mice treated with DOX, SpHL-DOX and ExoSpHL-DOX are shown in **Table 1**. HBS and ExoSpHL treatment groups showed no significant difference, therefore, only HBS treatment group was expressed as a control. The evaluation of white blood cells (WBC) showed that there was an increase in WBC after treatment with DOX at dose of 12.5 mg/kg when compared to the control group (HBS). The other treatments did not change the WBC count when compared to HBS. The same increase was observed to granulocytes (neutrophils, eosinophils and basophils) and agranulocytes (lymphocytes and monocytes) in the treatment with DOX at dose of 12.5 mg/kg when compared to HBS. The other treatments did not change the granulocytes and agranulocytes count when compared to HBS. Regarding red blood cells, the number of red blood cells (RBC), amount of hemoglobin (HGB) and, hematocrit (HCT) showed a decrease in mice treated with DOX at dose of 12.5 mg/kg and did not change with the other treatments when compared to the control. The platelets count showed no difference in all treatments.

Table 1: Hematological parameters for healthy Balb/c mice treated with different doses of free DOX, SpHL-DOX or ExoSpHL-DOX

Blood components	Control	Free DOX		SpHL-DOX		ExoSpHL-DOX	
		10 mg/kg	12.5 mg/kg	15 mg/kg	17.5 mg/kg	15 mg/kg	17.5 mg/kg
WBC (10^3/ mm^3)	4.95 ± 1.13	4.55 ± 1.62[b]	9.53 ± 2.12[a]	4.20 ± 1.18[b]	4.85 ± 0.41[b]	5.83 ± 1.40[b]	4.48 ± 0.82[b]
AGRANULOCYTES (10^3 / mm^3)	3.68 ± 0.99	3.15 ± 1.25[b]	7.15 ± 2.58[a]	2.58 ± 0.95[b]	2.87 ± 0.30[b]	3.77 ± 0.97[b]	3.00 ± 0.60[b]
GRANULOCYTES (10^3 / mm^3)	1.27 ± 0.27	1.40 ± 0.41[b]	2.80 ± 1.05[a]	1.34 ± 0.46[b]	1.98 ± 0.36[b]	2.07 ± 0.59[b]	1.48 ± 0.26[b]
RBC (10^6 / mm^3)	6.26 ± 0.72	5.95 ± 0.45[b]	4.18 ± 0.36[a]	6.06 ± 0.25[b]	5.79 ± 0.18[b]	5.30 ± 0.26[b]	6.10 ± 0.14[b]
HGB (g/dL)	12.68 ± 2.26	11.43 ± 1.06[b]	8.40 ± 1.35[a]	11.72 ± 0.64[b]	11.53 ± 0.45[b]	10.23 ± 0.43	12.10 ± 0.41[b]
HCT (%)	30.90 ± 3.47	30.00 ± 2.05[b]	21.55 ± 1.52[a]	29.68 ± 1.30[b]	28.87 ± 1.01[b]	26.82 ± 2.03[b]	30.04 ± 0.86[b]
PLT (10^3 / mm^3)	338.20 ± 22.66	254.2 ± 24.70	335.50 ± 78.57	351.80 ± 57.90	333.80 ± 61.90	314.20 ± 40.51	314.00 ± 79.53

WBC: white blood cells; RBC: red blood cells; HGB: hemoglobin; HCT: hematocrit; PLT: platelet. The results are presented as mean ± standard deviation from the mean (n = 6, except for free DOX treatment at dose of 12.5 mg/kg n=5). [a] Statistical significance compared to control (HBS) (p<0.05); [b] Statistical significance compared to free DOX treatment at dose of 12.5 mg/kg (p<0.05). Data were evaluated by One-way ANOVA (Tukey's post-test). If the data were abnormal, the Kruskal-Wallis test with Dunn's post-test was used.

3.2.3 Biochemical analysis

Biochemical parameters of mice treated with DOX, SpHL-DOX, and ExoSpHL-DOX are shown in **Table 2**. HBS and ExoSpHL treatment groups showed no significant difference, therefore, only HBS treatment group was expressed as a control. Renal function was evaluated by measuring creatinine and urea. There was no change in creatinine values in all treatments when compared to the control. For the quantification of the urea, only DOX treatment at dose of 12.5 mg/kg presented an increase in relation to the control group. Hepatic function was evaluated by determining alanine aminotransferase (ALT) and aspartate aminotransferase (AST) activity and the doses used did not cause liver damage, since there was no significant difference in serum levels of ALT and AST in all treatments when compared to the control group. Cardiac injury was assessed by measuring creatine kinase – MB (CK-MB) activity. DOX treatment at dose of 12.5 mg/kg and SpHL-DOX and ExoSpHL-DOX treatments at dose of 17.5 mg/kg showed high level of CK-MB in relation to the control group. Furthermore, the increase in CK-MB level by DOX treatment at dose of 12.5 mg/kg was greater than that of SpHL-DOX and ExoSpHL-DOX at dose of 17.5 mg/kg.

Table 2: Biochemical parameters for healthy Balb/c mice treated with different doses of free DOX, SpHL-DOX or ExoSpHL-DOX

Biochemical parameters	Control	Free DOX		SpHL-DOX		ExoSpHL-DOX	
		10 mg/kg	12.5 mg/kg	15 mg/kg	17.5 mg/kg	15 mg/kg	17.5 mg/kg
Creatinine (mg/dL)	0.30 ± 0.09	0.22 ± 0.07	0.29 ± 0.12	0.19 ± 0.04	0.20 ± 0.03	0.31 ± 0.06	0.22 ± 0.04
Urea (mg/dL)	35.54 ± 3.92	40.51 ± 18.06^{b}	149.10 ± 14.89^{a}	34.82 ± 9.91^{b}	39.20 ± 13.33^{b}	31.16 ± 1.73^{b}	30.63 ± 1.37^{b}
ALT (U/L)	44.09 ± 7.34	52.97 ± 15.68	48.01 ± 9.34	45.54 ± 11.21	56.39 ± 10.01	47.72 ± 5.86	51.67 ± 7.71
AST (U/L)	124.30 ± 24.72	93.78 ± 25.79	127.80 ± 10.44	109.20 ± 41.60	128.00 ± 26.19	110.70 ± 30.26	126.30 ± 24.95
CK-MB (U/L)	28.31 ± 6.36	33.46 ± 13.55^{bc}	89.34 ± 8.03^{a}	33.90 ± 10.33^{b}	52.49 ± 13.51^{ab}	25.99 ± 7.47^{bcd}	49.11 ± 6.58^{ab}

The results are presented as mean ± standard deviation from the mean (n = 6, except for free DOX treatment at dose of 12.5 mg/kg n=5). [a] Statistical significance compared to control group (HBS) (p<0.05); [b] Statistical significance compared to free DOX treatment at dose of 12.5 mg/kg (p<0.05); [c] Statistical significance compared to SpHL-DOX treatment at dose of 17.5 mg/kg (p<0.05). [d] Statistical significance compared to ExoSpHL-DOX treatment at dose of 17.5 mg/kg (p<0.05). Data were evaluated by One-way ANOVA (Tukey's post-test). If they were abnormal, the Kruskal-Wallis test with Dunn's post-test was used.

3.2.4 Histological analysis

Histological analyses of different organs were performed at the end of the treatment period. Mice treated with HBS and ExoSpHL presented the same histopathological profile, and therefore, only the HBS treatment group photomicrography was presented as the control group. Liver analysis showed no changes for the SpHL-DOX (15 mg/kg) and ExoSpHL-DOX (15 mg/kg) treatment groups compared to the control group **(Figure 1A)**. In contrast, diffuse hydropic degeneration was observed in animals treated with DOX (10 and 12.5 mg/kg), SpHL-DOX (17.5 mg/kg), and ExoSpHL-DOX (17.5 mg/kg) **(Figure 1B)**. For splenic analysis, no changes were observed after treatments with both doses of SpHL-DOX and ExoSpHL-DOX (15 and 17.5 mg/kg) **(Figure 1C)**. In animals treated with DOX (10 and 12.5 mg/kg), it was observed a splenic congestion. Red pulp sinusoids have a large number of erythrocytes **(Figure 1D)**.

Figure 1: Histological sections of female Balb/c mice liver (A-B) and spleen (C-D). (A) Represents the control group (HBS) and the groups treated with SpHL-DOX and ExoSpHL-DOX at dose of 15 mg/kg. (B) Represents the groups treated with both doses of free DOX (10 and 12.5 mg/kg), and the groups treated with SpHL-DOX and ExoSpHL-DOX at dose of 17.5 mg/kg. (C) Represents the control group (HBS) and the groups treated with both tested doses of SpHL-DOX and ExoSpHL-DOX (15 and 17.5 mg/kg). (D) Represents the group treated with both tested doses of free DOX (10 and 12.5 mg/kg)

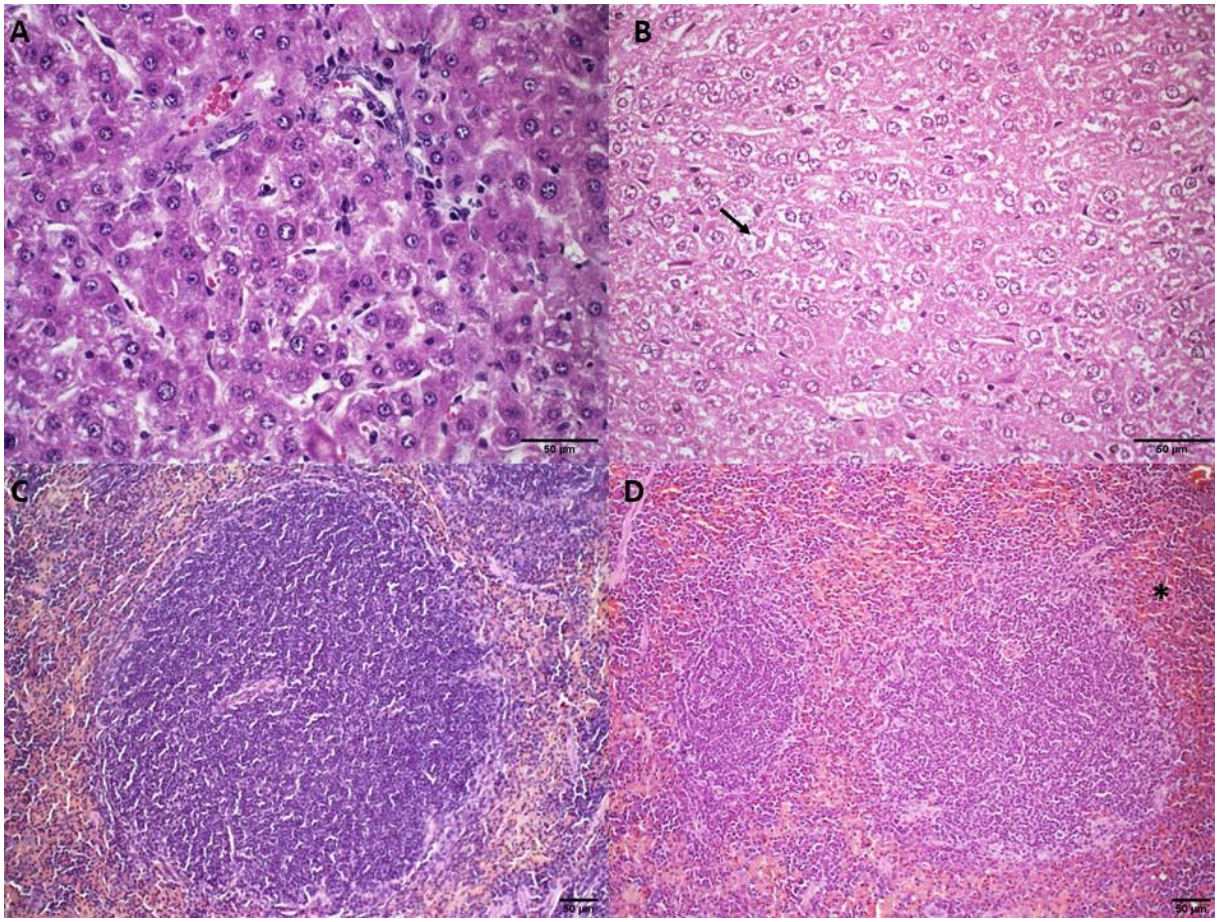

Arrow indicates the regions of diffuse hydropic degeneration in the liver and asterisk indicates the increase of erythrocytes in the red pulp of the spleen. HE, scale bar = 50 µm.

The histopathological analysis of the kidney revealed no changes for SpHL-DOX 15 mg/kg, ExoSpHL-DOX (15 and 17.5 mg/kg) treatment groups compared to the control group **(Figure 2A)**. Animals treated with DOX (10 and 12.5 mg/kg) and SpHL-DOX 17.5 mg/kg presented tubule dilation and hyalinization of the glomeruli **(Figure 2B)**.

Figure 2: Histological sections of female Balb/c mice kidney. (A) Represents the control group (HBS), the groups treated with both doses of ExoSpHL-DOX (15 and 17.5 mg/kg), and SpHL-DOX at dose of 15 mg/kg. (B) Represents the groups treated with both tested doses of free DOX (10 and 12.5 mg/kg) and SpHL-DOX at dose of 17.5 mg/kg

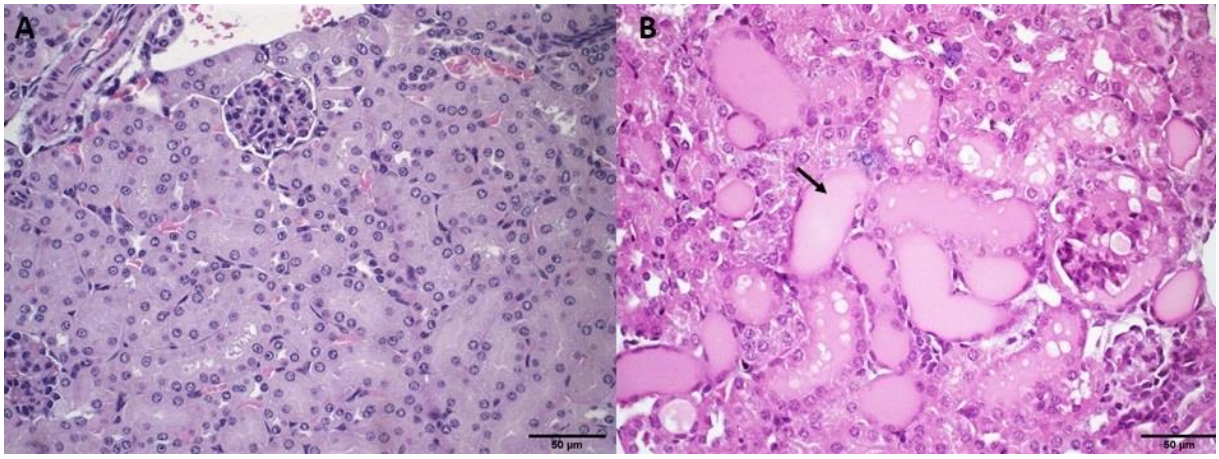

Arrow indicates the regions of tubule dilation. HE, scale bar = 50 µm.

Cardiac muscle analysis revealed that after DOX treatments areas of cardiomyocyte vacuolization were observed. Compared to the control group **(Figure 3A)** the treatment with free DOX (10 and 12.5 mg/kg) **(Figures 3B and 3C, respectively)** presented multifocal areas of cardiomyocyte vacuolization. The extent of the lesions was greater for the DOX treatment group at dose of 12.5 mg/kg. For SpHL-DOX (15 and 17.5 mg/kg) and ExoSpHL-DOX (15 and 17.5 mg/kg) treatment groups, discrete foci of cardiomyocyte vacuolization were observed **(Figure 3D)**. Evaluation of animals in all treatment groups revealed no evidence of bone marrow and lung toxicity (data not shown).

Figure 3: Histological sections of female Balb/c mice heart. (A) Represents the control group (HBS). (B) Represents the group treated with free DOX at dose of 10 mg/kg. Arrow indicates the areas of cardiomyocyte vacuolization. (C) Represents the group treated with free DOX at dose of 12.5 mg/kg. Arrow indicates the areas of cardiomyocyte vacuolization more intense than B. (D) Represents the groups treated with both doses of SpHL-DOX and ExoSpHL-DOX

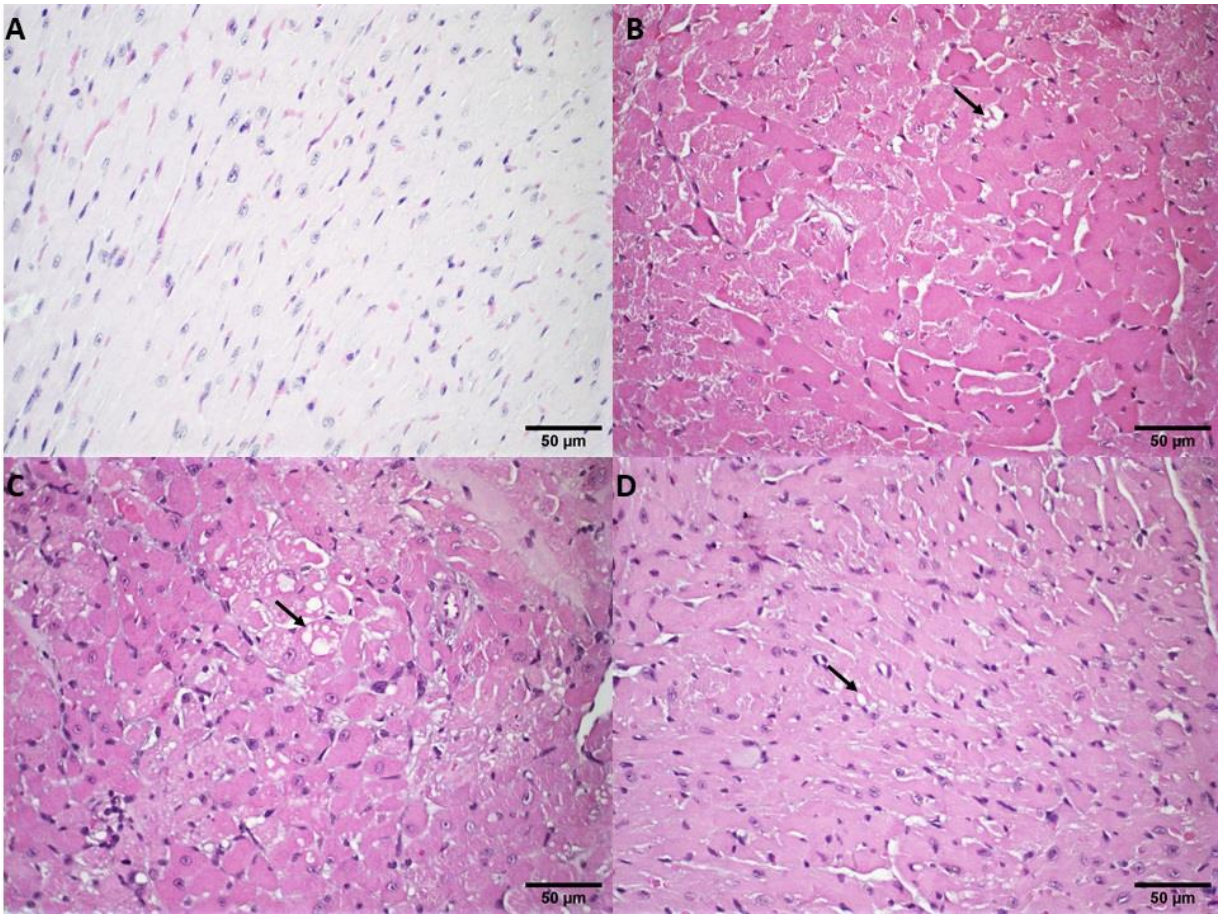

Arrow indicates the areas of discrete cardiomyocyte vacuolization. HE, scale bar = 50 µm.

3.3 Antitumor activity evaluation

The antitumor efficacy of free DOX, SpHL-DOX, and ExoSpHL-DOX treatments was evaluated in female Balb/c mice with 4T1 breast tumor by assessing the tumor volume variation over time. The tumor volume for ExoSpHL and HBS treatment groups increased rapidly over time and showed no significant difference, therefore, only HBS treatment group was expressed as a control. By contrast, significant differences in the tumor volume were observed among HBS treatment verses treatments with DOX, SpHL-DOX, and ExoSpHL-DOX at dose of 5.0 mg/kg **(Figure 4A)**. Tumor volume data were confirmed by the RTV values **(Table 3).** The treatments with formulations containing DOX significantly decreased the tumor growth compared to control group.

However, there was no significant difference between DOX, SpHL-DOX, and ExoSpHL-DOX treatments at cumulative dose of 25.0 mg/kg. In addition, the treatments showed similar TGI, close to 50% compared to the control group.

3.3.1 Evaluation of body weight loss

Body weight loss after treatments with DOX, SpHL-DOX, and ExoSpHL-DOX was evaluated in Balb/c female mice with 4T1 breast tumor**.** The results are presented in **Figure 4B**. Mice treated with HBS and ExoSpHL presented similar body weight gain, and therefore, only the HBS group was presented as the control group. By contrast, significant differences in the animal weight were observed among HBS treatment verses treatments with DOX, SpHL-DOX, and ExoSpHL-DOX. However, there was no significant difference in body weight loss for animals treated with DOX, SpHL-DOX, and ExoSpHL-DOX at cumulative dose of 25.0 mg/kg.

Figure 4: Antitumor efficacy evaluation of female Balb/c mice with 4T1 breast tumor. (A) Variation of the mice breast cancer tumor volume after treatment with HBS, DOX, SpHL-DOX, and ExoSpHL-DOX. Animals received intravenously five times, every 2 days, HBS (control), DOX at cumulative dose of 25 mg/kg, SpHL-DOX at cumulative dose of 25 mg/kg, or ExoSpHL-DOX at cumulative dose of 25 mg/kg. (B) Percentage of body weight variation, on day 10, after administration of HBS (control), DOX at cumulative dose of 25 mg/kg, SpHL-DOX at cumulative dose of 25 mg/kg, or ExoSpHL-DOX at cumulative dose of 25 mg/kg treatments

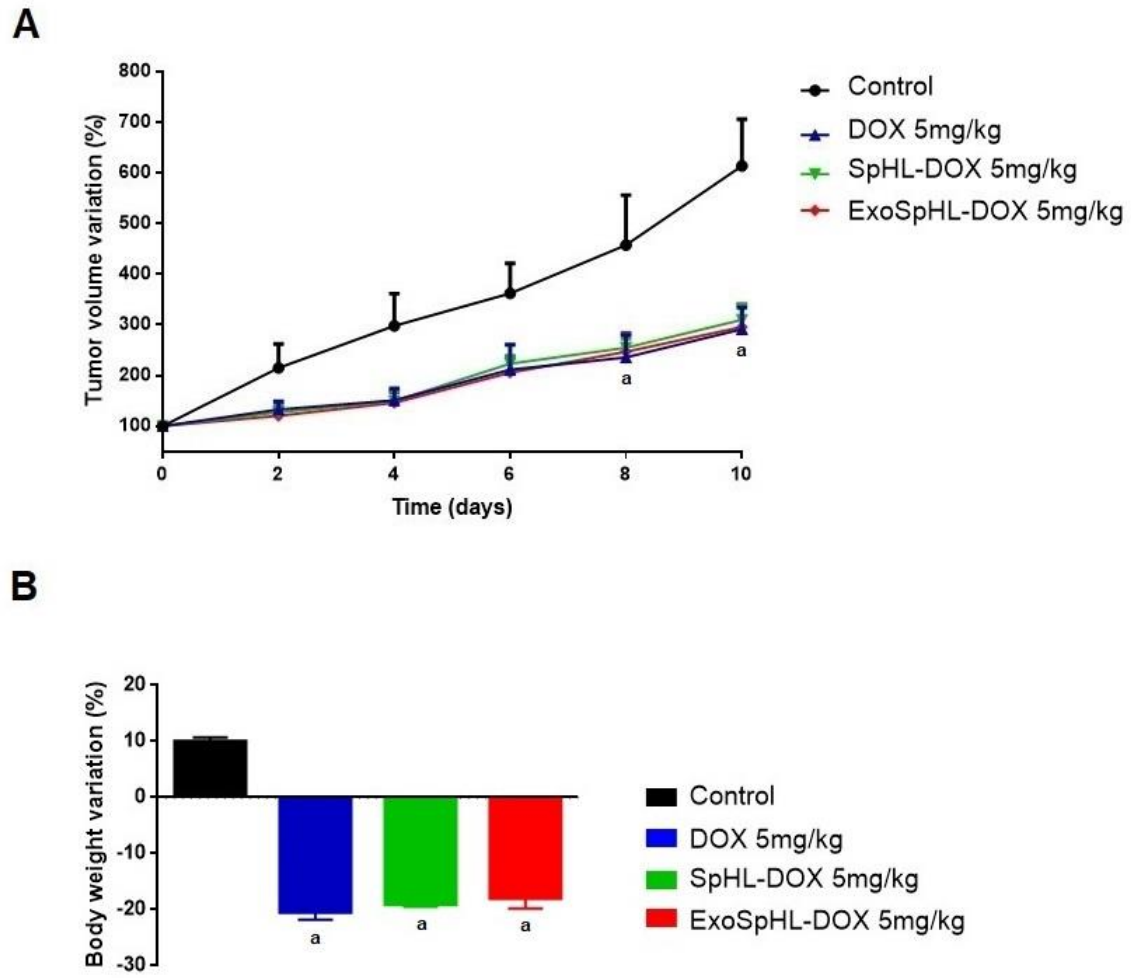

All data are presented as mean ± SEM, n = 6. [a] Statistical significance compared to control group (HBS) ($p<0.05$). Abbreviations: HBS: HEPES buffered saline; DOX: doxorubicin; SpHL-DOX: long-circulating and pH-sensitive liposomes containing doxorubicin; ExoSpHL-DOX: tumor-derived exosomes fused with long-circulating and pH-sensitive liposomes containing doxorubicin; SEM: standard error of the mean.

Table 3: Relative tumor volume and tumor growth inhibition after administration of HBS, free DOX, SpHL-DOX, and ExoSpHL-DOX by intravenous route

Treatment	RTV	TGI (%)
HBS (control)	6.1 ± 0.9	-
Free DOX 5 mg/kg	2.9 ± 0.4[a]	52.5
SpHL-DOX 5 mg/kg	2.8 ± 0.1[a]	54.1
ExoSpHL-DOX 5 mg/kg	2.7 ± 0.4[a]	55.7

The results are presented as mean ± standard error (n = 6). [a] Statistical significance compared to control (HBS) ($p < 0.05$).

3.3.2 Histological analysis

Histological analyses of the tumor and different organs were performed at the end of the treatment period. The 4T1 tumor cells grow in a solid arrangement. It was observed proliferation of pleomorphic cells and high mitotic index (GARCIA *et al.*, 2014). Mice treated with HBS or ExoSpHL presented tumors with necrosis only in the central region **(Figure 5A)**. On other hand, animals treated with DOX, SpHL-DOX or ExoSpHL-DOX presented extensive necrosis and few areas of viable cells due to the DOX-induced cell death **(Figure 5B)**.

Figure 5: Representative photomicrographs of histological sections of primary tumor of female Balb/c mice bearing 4T1 breast tumor treated with (A) HBS or ExoSpHL. (B) DOX, SpHL-DOX or ExoSpHL-DOX at cumulative dose of 25mg/kg.

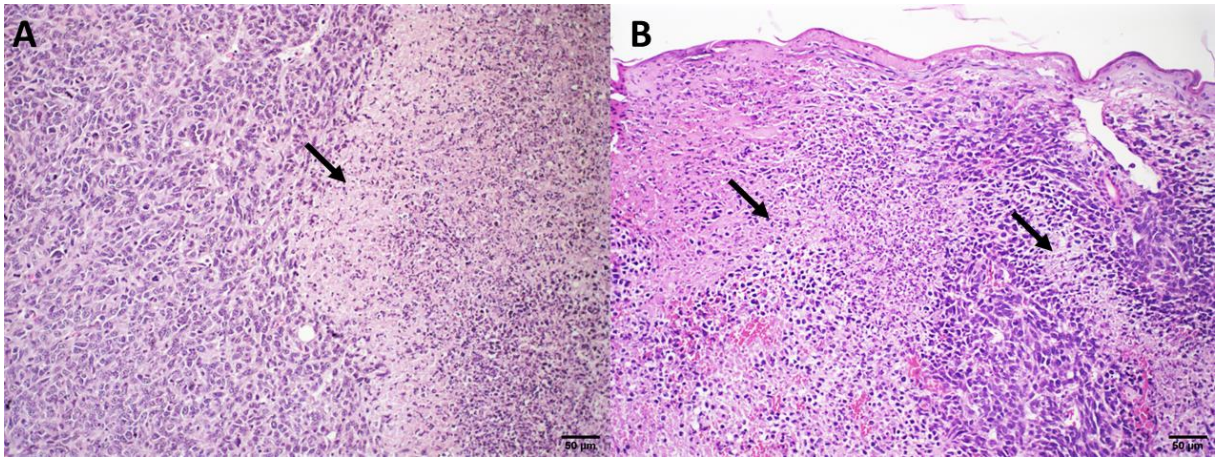

Arrows indicate tumor necrosis areas. HE, scale bar = 50 µm.

The 4T1 murine breast cancer is highly tumorigenic and invasive, where metastatic foci are observed in various organs (GARCIA *et al.*, 2014). Lung and liver are common organs for the appearance of 4T1 tumor metastases. Pulmonary histology revealed metastatic foci in animals in all treatment groups **(Figure 6A)**. The main difference was regarding the number of animals with pulmonary metastasis. In all animals treated with HBS, metastatic foci were observed. However, for animals treated with ExoSpHL, free DOX, SpHL-DOX or ExoSpHL-DOX rare metastatic foci were observed. Also, ExoSpHL-DOX treated group exhibited fewer metastatic foci in a semi-quantitative comparison with SpHL-DOX and free DOX treatments **(Table 4)**. Multiple metastatic foci in the liver were observed in animals treated with HBS or ExoSpHL, with no difference between them. Meanwhile, rare metastatic foci were observed in animals treated with DOX, SpHL-DOX, and ExoSpHL-DOX. However, in the liver there was no change between the groups treated with DOX, SpHL-DOX and, ExoSpHL-DOX **(Figure 6B)**.

Figure 6: Representative photomicrographs of metastatic foci in lung (A) and liver (B) of female Balb/c mice bearing 4T1 breast tumor treated with HBS (control), ExoSpHL (control), DOX at cumulative dose of 25mg/kg, SpHL-DOX at cumulative dose of 25mg/kg or ExoSpHL-DOX at cumulative dose of 25mg/kg

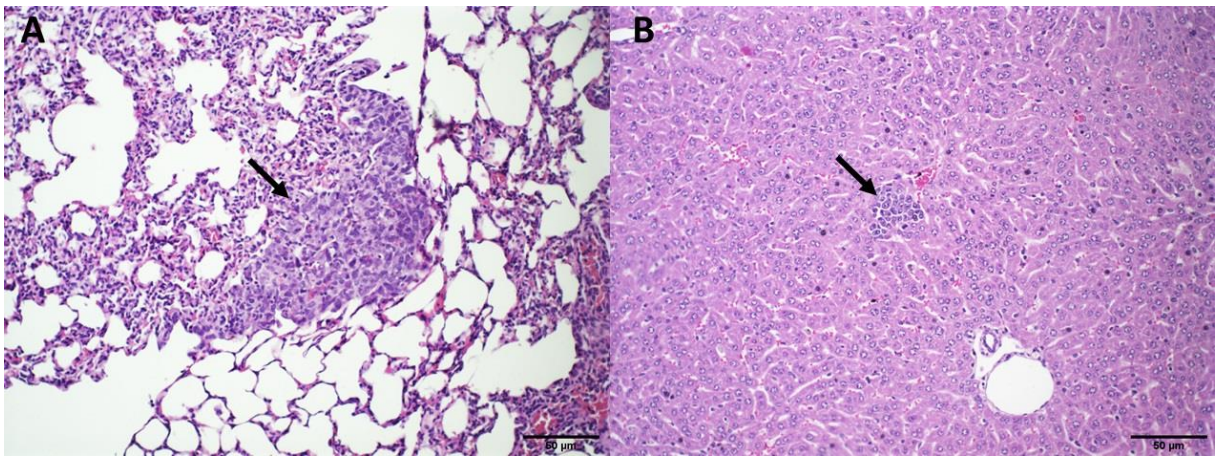

Arrows indicate tumor metastasis. HE, scale bar = 50 µm.

Table 4: Number of metastatic foci in the lungs of female Balb/c mice bearing 4T1 breast tumor treated with HBS, ExoSpHL, DOX, SpHL-DOX or ExoSpHL-DOX. Animals received each treatment intravenously five times, every 2 days, at a dose of 5 mg/kg

		HBS	ExoSpHL	DOX	SpHL-DOX	ExoSpHL-DOX
Score	Animal 1	+	+	0	+	0
	Animal 2	++	0	++	0	0
	Animal 3	+	+	+	+	+
	Animal 4	++	0	0	0	0
	Animal 5	++	0	0	+	0

Data were expressed by score: 0, no metastasis detected; +, 1-3 metastatic foci; ++, 4-7 metastatic foci.

Macroscopic analysis of the spleen showed splenomegaly in animals treated with HBS or ExoSpHL, which is commonly seen in mice with 4T1 murine breast cancer. For DOX, SpHL-DOX and, ExoSpHL-DOX treatments groups, spleen size was normal, indicating that the treatments were able to reverse splenomegaly. Regarding to histological analysis, the spleen tissue of animals treated with SpHL-DOX or ExoSpHL-DOX was preserved **(Figure 7A)**. The spleen of mice treated with HBS, ExoSpHL or DOX showed white and red pulp hyperplasia **(Figure 7B)**. Cardiac muscle analysis revealed that compared to the control **(Figure 7C)** after treatments with free DOX, SpHL-DOX, and ExoSpHL-DOX there were focal areas of degenerative hyalinization **(Figure 7D)**. Regarding the extent of the lesions, there was no significant difference and the pattern was similar to that found in the acute toxicity study**.** Evaluation of animals in all treatment groups revealed no changes in kidney tissue (data not shown).

Figure 7: Histological sections of spleen (A-B) and heart (C-D) of female Balb/c mice bearing 4T1 breast tumor. (A) Represents the groups treated with SpHL-DOX and ExoSpHL-DOX. Normal spleen. (B) Represents the groups treated with HBS, ExoSpHL and DOX. (C) Represents the groups treated with HBS and ExoSpHL. Normal heart. (D) Represents the groups treated with DOX, SpHL-DOX and ExoSpHL-DOX

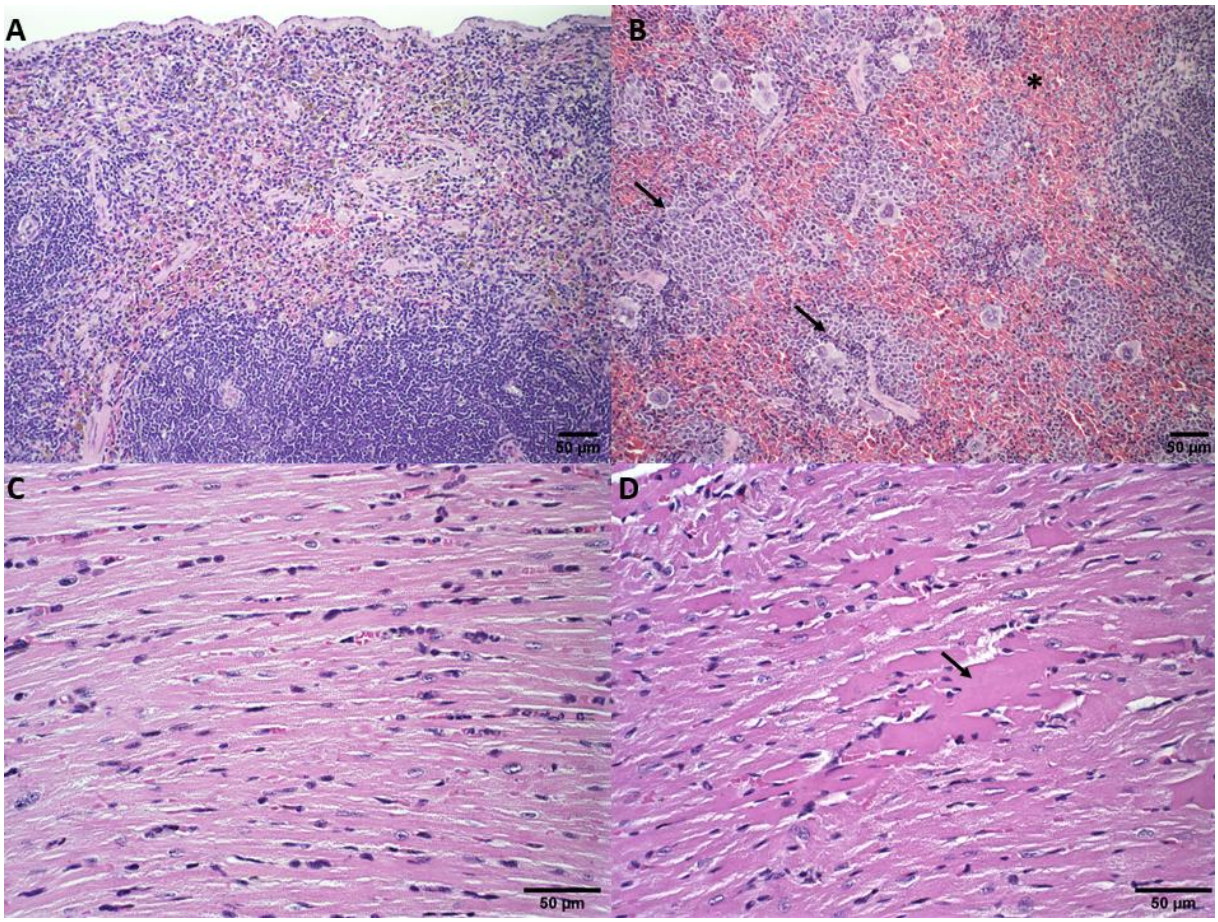

Asterisk indicate red pulp hyperplasia and arrows indicates the white pulp hyperplasia of the spleen. Arrow indicates the areas of degenerative hyalinization in the heart. HE, scale bar = 50 µm.

4 Discussion

Exosome-liposome hybrid nanocarriers have been developed to enhance drug delivery, improve treatment of metastatic cancer and, overcome chemoresistance in cancer (LV *et al.*, 2020; SUN *et al.,* 2021; LI *et al*., 2022). Based on these findings, our research group developed a hybrid nanocarrier of tumor-derived exosomes fused with long-circulating and pH-sensitive liposomes containing DOX (ExoSpHL-DOX) for the treatment of breast cancer. Our results showed that the developed formulation was

stable for 60 days, presented a high DOX encapsulation percentage, and a DOX release pH-dependent of the medium. Furthermore, our data showed the cytotoxic potential of ExoSpHL-DOX against 4T1 breast cancer cells (in press) (GOMES *at al.*, 2022). In this study, we investigated the acute toxicity and antitumor efficacy of ExoSpHL-DOX. The data obtained indicated that the LD50 for free DOX treatment is between 12.5 and 15 mg/kg. Meanwhile, for SpHL-DOX and ExoSpHL-DOX treatments, the LD50 is between 17.5 and 20 mg/kg. As expected, LD50 values were higher when DOX was administered encapsulated in liposomes or exosome-liposome hybrid nanocarrier than in the free form. Similar results were previously found by our research group, where female Balb/c mice treated with long-circulating and pH-sensitive liposomes containing DOX (SpHL-DOX) at dose of 15 mg/kg showed decrease in the morbidity and reduced renal, hepatic, and cardiac toxicity of DOX when compared to free DOX at dose of 15 mg/kg (SILVA *et al.*, 2018). Another study of acute toxicity of long-circulating and pH-sensitive liposomes containing paclitaxel (PTX):DOX at molar ratio of 1:10 administered in female Balb/c mice revealed a LD50 value between 28.9 and 34.7 mg/kg, while the free PTX:DOX treatment at molar ratio of 1:10 presented a LD50 between 20.8 and 23.1 mg/kg (ROQUE *et al.*, 2021). Even though the three animals had died after treatment with SpHL-DOX or ExoSpHL-DOX at a dose of 20 mg/kg, it is worth mentioning that treatment with SpHL-DOX caused twice as much weight loss as ExoSpHL-DOX. Hematological analysis showed leukocytosis and anemia in animals treated with free DOX at a dose of 12.5 mg/kg. Anemia is a frequent complication after chemotherapy treatment (TOBLLI *et al.*, 2014). However, the increase in white blood cells was not expected, since after DOX administration, leukopenia is common (SILVA *et al.*, 2018). In contrast, no changes were observed after treatment with both doses of SpHL-DOX and ExoSpHL-DOX, indicating no signs of toxicity in hematological parameters. Biochemical analyses revealed renal toxicity of free DOX treatment at a dose of 12.5 mg/kg, with an increase in plasmatic urea level. Renal damage was also confirmed by histopathology which showed tubule dilation and hyalinization of the glomeruli after treatments with both doses of free DOX and SpHL-DOX at dose of 17.5 mg/kg. On other hand, animals treated with both doses of ExoSpHL-DOX showed no signs of nephrotoxicity indicating that the presence of exosomes may alter the distribution of DOX and reduce kidney damage, even at the highest dose of the drug (TOFFOLI *et al.*, 2015). As an indicator of cardiac injury, CK-MB level was found increased after treatments with free DOX at

dose of 12.5 mg/kg, SpHL-DOX at dose of 17.5 mg/kg, and ExoSpHL-DOX at dose of 17.5 mg/kg. The increase of the CK-MB value was greater for free DOX treatment at dose of 12.5 mg/kg than liposomal and exosome-liposomal formulations at the highest dose. Cardiac damage by free DOX treatment was also confirmed by multifocal areas of cardiomyocyte vacuolization observed by histopathology in animals treated with both dose of free DOX (10 and 12.5 mg/kg). However, discrete cardiomyocyte vacuolization was observed for both doses of SpHL-DOX and ExoSpHL-DOX. These findings are in agreement with a previous study performed by our research group where female Balb/c mice were treated with free DOX at doses of 10 and 15 mg/kg and SpHL-DOX treatment at doses of 10 and 15 mg/kg (SILVA *et al.*, 2018) and can be explained by the lower accumulation of liposomes and exosomes in the heart, which has juxtaposed blood vessels and a well-developed lymphatic system (TOFFOLI *et al.*, 2015; DASA *et al.*, 2017). In this study, acute toxicity in the spleen and liver was also investigated. Due to the known uptake of liposomes by the liver and spleen, the monitoring the toxicity of these organs is very important (MONTEIRO *et al.*, 2018). Splenic toxicity was observed by histopathology only in the groups treated with free DOX. Histological analysis revealed liver damage in animals treated with both doses of free DOX and liposomal and exosome-liposomal at a dose of 17.5 mg/kg. However, there was no change in plasma levels of ALT and AST for all treatments. The antitumor efficacy of the ExoSpHL-DOX treatment was evaluated in Balb/c female mice with 4T1 breast tumor. Blank hybrid nanocarrier of tumor-derived exosomes fused with long-circulating and pH-sensitive liposomes did not inhibit tumor growth and showed no signs of toxicity, as did HBS treatment. From the obtained results of tumor volume growth and inhibition of the tumor volume growth, it was observed that the three treatments with DOX showed a higher antitumor effect compared to control group. However, in terms of efficacy, there was no superiority of the hybrid nanocarrier of tumor-derived exosomes fused with long-circulating and pH-sensitive liposomes compared to free DOX. Regarding the body weight of the animals, the three treatments containing DOX caused the same body weight loss, similar to another study performed by our research group in which female Balb/c mice received treatments of free DOX, SpHL-DOX and, long-circulating and pH-sensitive folate-coated liposomes containing DOX (SpHL-DOX-Fol) at cumulative dose of 20 mg/kg (SILVA *et al.*, 2019). To verify the antimetastatic activity of the ExoSpHL-DOX treatment, the organs common for the appearance of 4T1 tumor metastases were analyzed by histopathology. The hybrid

nanocarrier of tumor-derived exosomes fused with long-circulating and pH-sensitive liposomes reduced the number of metastatic foci in the lungs even when it did not contain DOX. Regarding liver metastasis, few metastatic foci were found after the treatments with formulations containing DOX and the blank hybrid nanocarrier of tumor-derived exosomes fused with long-circulating and pH-sensitive liposomes treatment did not inhibit the liver metastasis. Recent works in the literature have shown inhibition of metastasis after exosome treatment, but the reasons are still being explored. The innate organotropism capacity of exosomes, capture and neutralization of circulating tumor cells, in addition to the miRNA content of exosomes are probably involved in this ability to inhibit metastasis (NIE *et al*., 2020; WANG *et al.*, 2020). Therefore, hybrid nanocarrier of tumor-derived exosomes fused with long-circulating and pH-sensitive liposomes could serve as a promising nanocarrier for the inhibition of breast cancer metastases, mainly in the lung.

5 Conclusion

In conclusion, the results of the present study demonstrated that the toxicity of ExoSpHL-DOX treatment is lower than the free DOX treatment, proving exosome-liposome hybrid nanocarriers are capable of delivering higher doses of DOX without causing serious organ and tissue damage and with reduced adverse effects. In terms of antitumor efficacy, ExoSpHL-DOX treatment showed a higher antitumor effect compared to control group. Furthermore, ExoSpHL-DOX reduced the number of metastatic foci in the lungs even when the exosome-liposome hybrid nanocarrier did not contain DOX. These results indicate that ExoSpHL-DOX may be a promising nanocarrier for the treatment of breast cancer, reducing toxicity and inhibiting metastasis, mainly in the lungs.

4 DISCUSSÃO GERAL

Os lipossomas vêm sendo utilizados há algumas décadas para o tratamento de câncer. Essas vesículas são capazes de se acumular passivamente e ativamente no tumor, permitem modificações na superfície para aumentar o direcionamento para a região tumoral e liberação do fármaco mediante estímulos físicos fisiológicos e externos ao organismo (SINDHWANI *et al.*, 2020; FRANCO *et al.*, 2021; SHETH *et al.*, 2021). Recentemente, os exossomas começaram a ser estudados como nanocarreadores de quimioterápicos devido às suas características endógenas de reconhecimento e fusão preferencial com células de mesma origem e pelo menor reconhecimento dessas vesículas pelo sistema fagocitário mononuclear (HADLA *et* al., 2016; GONG *et al.*, 2019; QIAO *et al*., 2020). Para melhorar a entrega de fármacos, uma nova geração de nanossistemas tem sido desenvolvida a partir da fusão de lipossomas e exossomas, gerando os conhecidos nanocarreadores híbridos de exossoma-lipossoma (BUNGGULAWA *et al.*, 2018; MUKHERJEE *et al.*, 2022). Nesse estudo, lipossomas pH-sensíveis de circulação prolongada foram fundidos com exossomas secretados por células tumorais de mama murina 4T1 para encapsulação da doxorrubicina (ExoSpHL-DOX). Os exossomas secretados por células tumorais de mama murina 4T1 foram isolados por precipitação usando um kit comercial de extração de exossomas, seguido por etapa de centrifugação (ALZHRANI *et al.*, 2021). As vesículas extracelulares isoladas foram analisadas por NTA e apresentaram diâmetro médio de 115,8 nm, característico de exossomas (30 a 150 nm) (CHEN *et al.*, 2022). A análise por cryoTEM confirmou o tamanho e a forma dos exossomas isolados. O conteúdo total de proteínas nos exossomas foi determinado pelo ensaio de proteínas totais BCA e a presença da tetraspanina CD9 foi detectada por nanocitometria de fluxo (HUANG; LONG; HUO, 2010; ALZHRANI *et al.*, 2021; REZAKHANI *et al.*, 2021). O método escolhido para a fusão das membranas lipídicas foi hidratação de filme lipídico ou Bangham, que é uma técnica simples amplamente utilizada para preparo de lipossomas (BANGHAM; STANDISH; WATKINS, 1965). A DOX foi encapsulada remotamente por gradiente de sulfato de amônio. A porcentagem de encapsulação de DOX em ExoSpHL-DOX foi de 83,5%. Na encapsulação remota da DOX é formado sulfato de doxorrubicina, um sal insolúvel que se precipita no interior das vesículas (SILVA *et al.*, 2018; NOVAIS *et al*., 2021). ExoSpHL-DOX apresentou diâmetro médio das vesículas e índice de polidispersão

(IP) adequados para administração intravenosa. Ambas as técnicas DLS e NTA foram usadas para obter o valor médio do diâmetro para ExoSpHL-DOX e os resultados obtidos foram semelhantes. O diâmetro de ExoSpHL-DOX também foi confirmado por CryoTEM. O valor médio do potencial zeta (PZ) foi próximo da neutralidade, o que já era esperado devido à presença de PEG na formulação. Além de reduzir a mobilidade eletroforética das partículas, as moléculas de PEG impedem a agregação das vesículas devido à barreira estérica gerada (GOMES et al., 2018). ExoSpHL-DOX apresentaram estabilidade química e físico-química durante 60 dias de armazenamento a 4°C, sem alterações significativas no tamanho, IP, PZ e teor de DOX. A presença de moléculas de PEG e a precipitação da DOX no interior das vesículas podem justificar a estabilidade de ExoSpHL-DOX por 60 dias (GOMES *et al*., 2018; FRANCO *et al*., 2021; NOVAIS *et al*., 2021). O diâmetro médio, IP e PZ das vesículas foram avaliados após incubação em tampão HEPES (HBS) e meio biológico (RPMI). ExoSpHL-DOX mostrou estabilidade adequada em condições biológicas simuladas (pH, temperatura e teor de proteína) até 24h após a incubação. Portanto, ExoSpHL-DOX pode ser considerado adequado para ensaios *in vitro* e *in vivo*. Ensaios de BCA também foram realizados para quantificar o total de proteínas em ExoSpHL (HUANG; LONG; HUO, 2010; REZAKHANI *et al.*, 2021). A presença de proteínas foi confirmada nestas vesículas, o que sugere a fusão entre membranas de exossomas e lipossomas. ExoSpHL foram caracterizados por espectroscopia Raman e FTIR e comparados com SpHL, exossomas e uma mistura física de exossomas e SpHL. ExoSpHL apresentou sinais Raman e bandas características de FTIR de lipossomas e exossomas, que foram diferentes da mistura física exossomas+SpHL, sugerindo novamente a fusão entre as membranas de exossomas e lipossomas, durante o preparo de ExoSpHL (FARIED *et al*., 2019; KRUGLIK e*t al.*, 2019; HURVITZ *et al.*, 2019; MARTINS *et al.*, 2020). A caracterização de exossomas é comumente realizada pela identificação de CD9, CD63 e CD81, que são membros da família das tetraspaninas, abundantemente expressos na superfície dos exossomas (CHEN *et al.*, 2022; MUKHERJEE *et al.*, 2022). A presença de CD9, um marcador típico de exossomas, foi detectada na superfície de ExoSpHL usando nanocitometria de fluxo, confirmando a fusão de exossomas com lipossomas. O perfil de liberação *in vitro* de DOX de ExoSpHL-DOX foi avaliado por meio de estudos de diálise em HBS, à 37°C, pH 5 e 7,4, durante um período de 24 horas. O pH 7,4 foi avaliado como indicativo da liberação *in vivo*, na circulação sanguínea, uma vez que mimetiza o pH fisiológico e o

pH 5 como indicativo da liberação *in vivo* no tecido tumoral e interior dos endossomas. Após 24h, 97% de DOX foi liberada de ExoSpHL-DOX em pH 5.0, enquanto somente 70% de DOX foi liberada em pH 7.4. Além disso, foi observado aumento significativa no diâmetro das vesículas em pH 5,0, enquanto que não houve alteração no diâmetro das vesículas em pH 7,4. Quando exposto a um meio ácido, o grupo carboxila das moléculas de CHEMS que compõem as vesículas é protonado levando a uma transição de fase lamelar para hexagonal, e consequentemente, a liberação da DOX encapsulada (FRANCO *et al*., 2021). Esses resultados confirmam a pH-sensibilidade do nanocarreador híbrido e sugerem ExoSpHL-DOX como um sistema potencial para entrega de DOX à região tumoral, uma vez que serão capazes de liberar seu conteúdo quando em contato com o microambiente ácido da região tumoral e interior de endossomas (valores de pH entre 4,5 a 6,5) (SILVA *et al*., 2018; FRANCO *et al.*, 2021). Em relação à citotoxicidade frente à linhagem celular tumoral 4T1, os valores de IC_{50} foram semelhantes para os tratamentos com ExoSpHL-DOX, DOX livre e SpHL-DOX, o que indica que o efeito citotóxico da DOX não foi prejudicado com a fusão de lipossomas e exossomas. A toxicidade aguda de ExoSpHL-DOX foi avaliada em camundongos saudáveis. Os dados obtidos indicaram que a dose letal mediana (LD50) para tratamento com DOX livre está entre 12,5 e 15 mg/kg. Enquanto isso, para SpHL-DOX e ExoSpHL-DOX, a LD50 está entre 17,5 e 20 mg/kg. Como esperado, os valores de LD50 foram maiores quando a DOX foi administrada encapsulada em lipossomas ou nanocarreador híbrido de exossoma-lipossoma. Resultados semelhantes foram encontrados anteriormente por nosso grupo de pesquisa, onde camundongos Balb/c fêmeas tratados com lipossomas pH-sensíveis de circulação prolongada contendo DOX (SpHL-DOX) na dose de 15 mg/kg apresentaram diminuição na morbidade e redução de toxicidade renal, hepática e cardíaca em comparação com o grupo tratado com DOX livre na dose de 15 mg/kg (SILVA *et al*. 2018). Em outro estudo de toxicidade aguda, lipossomas pH-sensíveis de circulação prolongada contendo paclitaxel (PTX):DOX na razão molar de 1:10 administrados em camundongos Balb/c fêmeas apresentaram um valor de LD50 entre 28,9 e 34,7 mg/kg, enquanto a associação livre de PTX:DOX na razão molar de 1:10, apresentou LD50 entre 20,8 e 23,1 mg/kg (ROQUE *et al*. 2021). Com os dados da análise hematológica, foi observado leucocitose e anemia nos animais tratados com DOX livre na dose de 12,5 mg/kg, em relação ao grupo controle. A anemia é uma reação adversa muito comum associada ao uso de quimioterápicos (TOBLLI *et al.*,

2014). Porém, o aumento de glóbulos brancos não era esperado, pois após a administração de DOX é comum a ocorrência de leucopenia (SILVA *et al*. 2018). Em contraste, não foram observadas alterações hematológicas após o tratamento com ambas as doses de SpHL-DOX e ExoSpHL-DOX, indicando não haver sinais de toxicidade nos parâmetros hematológicos. As análises bioquímicas revelaram toxicidade renal da DOX livre na dose de 12,5 mg/kg, com aumento do nível plasmático de ureia. A lesão renal também foi confirmada por histopatologia que mostrou dilatação tubular e hialinização dos glomérulos após tratamentos com ambas as doses de DOX livre e SpHL-DOX na dose de 17,5 mg/kg. Por outro lado, os animais tratados com SpHL-DOX na dose de 15 mg/kg e ambas as doses de ExoSpHL-DOX não apresentaram sinais de nefrotoxicidade, indicando que os nanocarreadores híbridos podem alterar a distribuição de DOX e reduzir o dano renal, mesmo na dose mais elevada do fármaco (TOFFOLI *et al*., 2015). Como indicador de lesão cardíaca, o nível de CK-MB foi encontrado aumentado após tratamentos com DOX livre 12,5 mg/kg, SpHL-DOX e ExoSpHL-DOX na dose de 17,5 mg/kg. Vale ressaltar que o aumento de CK-MB foi maior após tratamento com DOX livre na dose de 12,5 mg/kg do que após o tratamento com ambas as formulações na dose mais elevada. O dano cardíaco por DOX livre também foi confirmado por áreas multifocais de vacuolização de cardiomiócitos observadas por histopatologia em animais tratados com ambas as doses de DOX livre (10 e 12,5 mg/kg). No entanto, discreta vacuolização dos cardiomiócitos foi observada para ambas as doses de SpHL-DOX e ExoSpHL-DOX. Esses achados estão de acordo com estudo prévio realizado pelo nosso grupo de pesquisa, no qual camundongos Balb/c fêmeas foram tratados com DOX livre e SpHL-DOX nas doses de 10 e 15 mg/kg (SILVA *et* al. 2018) e podem ser explicados pelo menor acúmulo de lipossomas e exossomas no coração, que tem vasos sanguíneos justapostos e um sistema linfático bem desenvolvido (TOFFOLI *et al*., 2015, DASA *et al*., 2017). Neste estudo, a toxicidade aguda no baço e fígado também foi investigada. Devido à conhecida captura de lipossomas pelo fígado e baço, a monitorização da toxicidade destes órgãos é muito importante (MONTEIRO *et al*., 2018). A análise histológica revelou toxicidade esplênica apenas nos grupos tratados com DOX livre e lesão hepática em animais tratados com ambas as doses de DOX livre e ambas as formulações na dose de 17,5 mg/kg. No entanto, não houve alteração nos níveis plasmáticos das enzimas alanina transaminase (ALT) e aspartato aminotransferase (AST) após nenhum dos tratamentos. Após avaliação da toxicidade aguda do

tratamento com ExoSpHL-DOX, foi realizado um experimento para investigação da eficácia antitumoral. O modelo tumoral utilizado foi camundongos Balb/c fêmeas portadores de tumor de mama 4T1. O nanocarreador híbrido de exossoma-lipossoma branco não inibiu o crescimento do tumor e não mostrou sinais de toxicidade, assim como o tratamento com HBS. A partir dos resultados obtidos de crescimento do volume tumoral e inibição do crescimento do volume tumoral, observou-se que os três tratamentos com DOX apresentaram maior efeito antitumoral em relação ao grupo controle. Em relação ao peso corporal dos animais, os tratamentos com DOX livre, SpHL-DOX e ExoSpHL-DOX causaram a mesma perda de peso corporal, semelhante a um estudo anterior realizado pelo nosso grupo de pesquisa no qual camundongos Balb/c fêmeas foram tratados com DOX livre, SpHL-DOX e lipossomas pH-sensíveis de circulação prolongada revestidos com folato contendo DOX (SpHL-DOX-Fol) em uma dose acumulativa de 20 mg/kg (SILVA *et al*., 2019). Para verificar a atividade antimetastática de ExoSpHL-DOX, os órgãos mais comuns de aparecimento de metástases dos tumores de mama foram analisados por histopatologia (KIM, 2021). ExoSpHL-DOX reduziu o número de focos metastáticos nos pulmões quando comparado aos outros tratamentos. Em relação à metástase hepática, poucos focos metastáticos foram encontrados no fígado após os tratamentos com DOX livre, SpHL-DOX e ExoSpHL-DOX. Curiosamente, mesmo quando não continha DOX, o nanocarreador híbrido de exossoma-lipossoma inibiu metástase pulmonar. Trabalhos recentes na literatura mostraram inibição de metástase após tratamento com exossomas, mas as razões ainda estão sendo exploradas. As prováveis explicações envolvem a capacidade inata de organotropismo dos exossomas, captura e neutralização de células tumorais circulantes, além do conteúdo de miRNA dos exossomas (NIE *et al*., 2020; WANG *et al.*, 2020).

5 CONCLUSÃO GERAL

Neste trabalho, foi preparado pela primeira vez um nanocarreador híbrido de exossoma-lipossoma obtido pela fusão de exossomas secretados por células tumorais 4T1 com lipossomas pH-sensíveis de circulação prolongada para encapsulação de doxorrubicina (ExoSpHL-DOX). Os resultados obtidos permitiram concluir que a formulação desenvolvida de ExoSpHL-DOX possui características químicas e físico-químicas adequadas para a sua administração endovenosa. As vesículas apresentaram estabilidade química e físico-química durante 60 dias de armazenamento a 4°C, sem alterações significativas no tamanho, IP, PZ e teor de DOX.

As caracterizações por espectroscopias Raman e infravermelho e a detecção do marcador típico de exossomas (CD9) por nanocitometria de fluxo comprovaram a fusão das membranas lipídicas de lipossomas e exossomas durante o preparo de ExoSpHL.

Os ExoSpHL-DOX apresentaram uma liberação de DOX dependente do pH. No meio de pH 7,4, a liberação de DOX após 24 horas foi de 70% e não houve alteração no tamanho das vesículas, enquanto no pH 5 a liberação foi de 97%, acompanhada de um aumento no tamanho de ExoSpHL-DOX.

Os resultados do ensaio de citotoxicidade demonstraram o potencial citotóxico dos ExoSpHL-DOX na linhagem de células tumorais de mama murina 4T1.

O estudo de toxicidade aguda confirmou que ExoSpHL-DOX reduziu a toxicidade induzida por DOX, uma vez que os valores de LD50 foram maiores para ExoSpHL-DOX comparado à DOX livre. Além disso, ExoSpHL-DOX foram capazes de reduzir o dano renal, quando comparado à DOX livre e SpHL-DOX.

Em relação à eficácia terapêutica, ExoSpHL-DOX foram capazes de inibir o crescimento tumoral. Adicionalmente, ExoSpHL-DOX inibiu a metástase pulmonar, até mesmo quando o nanocarreador híbrido exossoma-lipossoma não continha DOX.

Diante do exposto, os ExoSpHL-DOX apresentam-se como uma formulação promissora para o tratamento do câncer de mama, uma vez que são adequados para a administração endovenosa, apresentam estabilidade de armazenamento, demonstraram alto potencial citotóxico e atividade antitumoral em modelo de câncer

de mama 4T1, diminuição da toxicidade sistêmica da DOX e inibição de metástase pulmonar.

6 PERSPECTIVAS

Com base nos resultados do presente estudo, pode-se propor algumas perspectivas, a saber:

- Avaliação da captação celular de ExoSpHL-DOX por células tumorais de mama 4T1, com quantificação de DOX por citometria de fluxo.
- Avaliação da migração de células tumorais de mama 4T1, após tratamento com ExoSpHL-DOX.
- Estudos *in vitro* para investigação da cardiotoxicidade de ExoSpHL-DOX em cardiomiócitos humanos.
- Estudos *in vivo* para investigação da cardiotoxicidade de ExoSpHL-DOX em modelo animal experimental.

7 REFERÊNCIAS BIBLIOGRÁFICAS

AL-MALKY, H.S.; AL-HARTHI, S.E.; OSMAN, A.M. Major obstacles to doxorubicin therapy: cardiotoxicity and drug resistance. **Journal of Oncology Pharmacy Practice**, v. 26, n° 2, p. 434-444, 2020.

ALZHRANI, G.N. *et al.*, Exosomes: isolation, characterization, and biomedical applications. **Cell Biology International**, v. 45, 2021.

AMERICAN CANCER SOCIETY - ACS: Cancer facts and figures 2022. Disponível em: < https://www.cancer.org/content/dam/cancer-org/research/cancer-facts-and-statistics/annual-cancer-facts-and-figures/2022/2022-cancer-facts-and-figures.pdf. Acesso em 21 de janeiro de 2022.

BANGHAM, A.D.; STANDISH, M.M.; WATKINS, J.C. Diffusion of univalent ions across the lamellae of swollen phospholipids. **Journal of Molecular Biology**, v. 13, n°. 1, p. 238–252, 1965.

BOZZUTO, G.; MOLINARI, A. Liposomes as nanomedical devices. **International Journal of Nanomedicine,** v. 10, p. 975 – 999, 2015.

BRASILEIRO-FILHO, G.; PEREIRA, F.E.L.; GUIMARÃES, R.C. Distúrbios da proliferação e da diferenciação celulares. In: Brasileiro-Filho, G. **Bogliolo: Patologia.** 8° edição. Geraldo Brasileiro Filho. Rio de Janeiro: Guanabara Koogan, 2014, p. 219-276.

BUNGGULAWA, E.J. Recent advancements in the use of exosomes as drug delivery systems. **Journal of Nanobiotechnology**, v. 16, n° 81, p. 1-13, 2018.

CARVALHO, C. *et al.* Doxorubicin: the good, the bad and the ugly effect. **Current Medicinal Chemistry,** v. 16, p. 3267-3285, 2009**.**

CHEN, L. *et al.* Exosomes as drug carriers in anti-cancer therapy. **Frontiers in Cell and Developmental Biology**, v. 10, 2022.

DASA, S.S.K. *et al.* Evaluation of pharmacokinetic and pharmacodynamic profiles of liposomes for the cell type-specific delivery of small molecule drugs. **Nanomedicine: Nanotechnology, Biology and Medicine**, v. 13, n° 8, p. 2565-2574, 2017.

ExoCarta. Disponível em http://exocarta.org/index.html. Acesso em 13 de julho de 2022.

FARIED, M. *et al*. Membrane surface-enhanced Raman spectroscopy for cholesterol modified lipid systems: effect of gold nanoparticle size. **ACS Omega**, v.4, p. 13687-13695, 2019.

FERREIRA, D.S. *et al.* pH-sensitive liposomes for drug delivery in cancer treatment. **Therapeutic Delivery**, v. 4, nº 9, p. 1-24, 2013.

FERREIRA, D.S. *et al*. Development of a bone-targeted pH-sensitive liposomal formulation: physicochemical characterization, cytotoxicity, and biodistribution evaluation in a mouse model of bone metastasis. **International Journal of Nanomedicine**, v. 11, p. 3737-3751, 2016.

FISUSI, F.A.; AKALA, E.O. Drug combinations in breast cancer therapy. **Pharmaceutical Nanotechnology**, v.7, p.3-23, 2019.

FOX, C.B.; UIBEL, F.H.; HARRIS, J.M. Detecting Phase Transitions in Phosphatidylcholine Vesicles by Raman Microscopy and Self-Modeling Curve Resolution. **The Journal of Physical Chemistry B**, v. 111, p. 11428-11436, 2007.

FRAIX, A. *et al.* Overcoming doxorubicin resistance with lipid-polymer hybrid nanoparticles photoreleasing nitric oxide. **Molecular Pharmaceutics**, v.17, n° 6, p. 2135-2144, 2020.

FRANCO, M. S. *et al*. Triggered Drug Release From Liposomes: Exploiting the Outer and Inner Tumor Environment, **Frontiers in Oncology**, v. 11, 2021.

GABIZON, A. *et al.* Dose dependency of pharmacokinetics and therapeutic efficacy of pegylated liposomal doxorubicin (DOXIL) in murine models. **Journal of Drug Targeting.** v. 10, n. 7, p. 539-548, 2002.

GARCIA, C.M.S. *et al.* Morphological and Immunophenotipical Characterization of Murine Mammary Carcinoma 4T1. **Brazilian Journal of Veterinary Pathology**, v. 7, n° 3, p. 158-165, 2014.

GHANDHARIYOUN, N. *et al.* Reducing doxorubicin resistance in breast cancer by liposomal FOXM1 aptamer: *in vitro* and *in vivo*. **Life Sciences**, v. 262, 2020.

GOMES, E.R. *et al*. Long-circulating and fusogenic liposomes loaded with a glucoevatromonoside derivative induce potent antitumor response. **Biomedicine & Pharmacotherapy**, v. 108, p.1152-1161, 2018.

GOMES, E.R. *et al.*, Fusion of tumor-derived exosomes with long-circulating and pH-sensitive liposomes loaded with doxorubicin for the treatment of breast cancer. **AAPS PharmSciTech**, v. 23, n° 255, 2022.

GONG, C. *et al.* Functional exosome-mediated co-delivery of doxorubicin and hydrophobically modifed microRNA 159 for triple-negative breast cancer therapy. **Journal of Nanobiotechnology**, v. 17, n ° 93, 2019.

GUIMARÃES, D.; PAULO, A.C.; NOGUEIRA, E. Design of liposomes as drug delivery system for therapeutic applications. **International Journal of Pharmaceutics**, v. 601, 2021.

GURUNATHAN, S. *et al*. Review of the Isolation, Characterization, biological function, and multifarious therapeutic approaches of exosomes. **Cells**, v. 8, n° 307, p. 1-36, 2019.

GURUNATHAN, S.; KANG, M.H.; KIM, J.H. A comprehensive review on factors influences biogenesis, functions, therapeutic and clinical implications of exosomes. **International Journal of Nanomedicine**, v. 16, p. 1281-1312, 2021.

GYORGY, B. *et al.* Membrane vesicles, current state-of-the-art: emerging role of extracellular vesicles. **Cellular and Molecular Life Sciences**, v. 68, 16, p. 2667-2688, 2011.

HADLA, M. e*t al.* Exosomes increase the therapeutic index of doxorubicin in breast and ovarian cancer mouse models. **Nanomedicine**, v. 11, n° 18, p. 2431-2441, 2016.

HANAHAN, D. Hallmarks of cancer: new dimensions. **Cancer Discovery**, v. 12, n° 1, p. 31-46, 2022.

HAUCK, M.L. *et al.* Phase I trial of doxorubicin-containing low temperature sensitive liposomes in spontaneous canine tumors. **Clinical Cancer Research**, v. 12, n° 13, p. 4004-4010, 2006.

HUANG, T.; LONG, M.; HUO, B. Competitive binding to cuprous ions of protein and BCA in the bicinchoninic acid protein assay. **Open Biomedical Engineering Journal**, v. 4, p. 271-278, 2010.

HURVITZ, A.Z. *et al.* FTIR-based spectrum of salivary exosomes coupled with computational-aided discriminating analysis in the diagnosis of oral cancer. **Journal of Cancer Research and Clinical Oncology**, v. 145, n° 3, p. 685-694, 2019.

INSTITUTO NACIONAL DO CÂNCER – INCA. Disponível em: <https://www.inca.gov.br/institucional>. Acesso em 21 de janeiro de 2022.

JAMIALAHMADI, K.; ZAHEDIPOUR, F.; KARIMI, G. The role of microRNAs on doxorubicin drug resistance in breast cancer. **Journal of Pharmacy and Pharmacology**, v. 73, n°8, p. 997-1006, 2021.

KALLURI, R.; LEBLEU, V.S. The biology, function, and biomedical applications of exosomes. **Science**, v. 367, 2020.

KIM, J.Y. *et al.* The use of PEGylated liposomes to prolong circulation lifetimes of tissue plasminogen activator. **Biomaterials**, v. 30, p. 5751-5756, 2009.

KIM, M.S. *et al*. Engineering macrophage-derived exosomes for targeted paclitaxel delivery to pulmonary metastases: *in vitro* and *in vivo* evaluations. **Nanomedicine**, v. 14, n° 1, p. 195-204, 2018.

KIM, M.Y. Breast cancer metastasis. **Advances in Experimental Medicine and Biology**, v. 1187, p. 183-204, 2021.

KIZEK, R. e*t al.* Anthracyclines and ellipticines as DNA-damaging anticancer drugs: recent advances. ***Pharmacology & Therapeutics***, v. 133, p. 26–39, 2012.

KRAFT, J.C. *et al.* Emerging research and clinical development trends of liposome and lipid nanoparticle drug delivery systems. **Journal of Pharmaceutical Sciences**, v. 103, p. 29-52, 2014.

KRUGLIK, S.G. e*t al.* Raman tweezers microspectroscopy of circa 100 nm extracellular vesicles. **Nanoscale**, v.11, p. 1661-1679, 2019.

LAGES, E.B. *et al.* Co-delivery of doxorubicin, docosahexaenoic acid, and α-tocopherol succinate by nanostructured lipid carriers has a synergistic effect to enhance antitumor activity and reduce toxicity. **Biomedicine & Pharmacotherapy**, v.132, 2020.

LI, L. *et al.* Exosome-liposome hybrid nanoparticle codelivery of TP and miR497 conspicuously overcomes chemoresistant ovarian cancer, **Journal of Nanobiotechnology**, v.20, n° 50, 2022.

LIANG, Y. *et al.* Engineering exosomes for targeted drug delivery. **Theranostics**, v. 11, n° 7, p. 3183-3195, 2021.

LIU, J. *et al.* The biology, function, and applications of exosomes in cancer. **Acta Pharmaceutica Sinica B**, v. 11, n° 9, p. 2783-2797, 2021.

LOPES, W.A.; FASCIO, M. Esquema para interpretação de espectros de substâncias orgânicas na região do infravermelho. **Química Nova**, v. 27, n° 4, p. 670-673, 2004.

LV, Q. *et al.* Thermosensitive Exosome–Liposome Hybrid Nanoparticle-Mediated Chemoimmunotherapy for Improved Treatment of Metastatic Peritoneal Cancer. **Advanced Science**, 2000515, 2020.

MARTINS, T.S. *et al.* Potential of FTIR spectroscopy applied to exosomes for Alzheimer's disease discrimination: a pilot study. **Journal of Alzheimer's Disease**, v. 74, p. 391-405, 2020.

MAUGHAN, K.L.; LUTTERBIE, M.A.; HAM, P.S. Treatment of breast cancer. **American Family Physician**, v. 81, n° 11, p.1339-1346, 2010.

MEREDITH, A.M.; DASS, C.R. Increasing role of the cancer chemotherapeutic doxorubicin in cellular metabolism. **Journal of Pharmacy and Pharmacology**, v. 68, n° 6, p. 729-741, 2016.

MIHÁLY, J. *et al.* Characterization of Extracellular Vesicles by IR spectroscopy: fast and simple classification based on amide and CH stretching vibrations. **Biochimica et Biophysica Acta – Biomembranes**, v. 1859, n° 3, p. 459-166, 2016.

MONTEIRO, L.O.F. *et al.* Paclitaxel-loaded folate-coated long-circulating and pH-sensitive liposomes as a potential drug delivery system: A biodistribution study. **Biomedicine & Pharmacotherapy**, v. 97, p. 489-495, 2018.

MONTEIRO, N. *et al.* Liposomes in tissue engineering and regenerative medicine. **Journal of the royal society Interface**, v. 11, 2014.

MUKHERJEE, A. *et al.*, Current advances in the use of exosomes, liposomes, and bioengineered hybrid nanovesicles in cancer detection and therapy. **Acta Pharmacologica Sinica,** 2022.

NASCIMENTO, R.G.; OTONI, K.M. Histological and molecular classification of breast cancer: what do we know? **Mastology**, v. 30, 2020.

NGAN, Y.H.; GUPTA, M. A comparison between liposomal and nonliposomal formulations of doxorubicin in the treatment of cancer: an updated review. **Archives of Pharmacy Practice**, v. 7, 2016.

NIE, H. *et al.* Use of lung-specific exosomes for miRNA-126 delivery in non-small cell lung cancer, **Nanoscale**, v.12, p. 877-887, 2020.

NOVAIS, M.V.M. *et al*. Liposomes co-encapsulating doxorubicin and glucoevatromonoside derivative induce synergic cytotoxic response against breast cancer cell lines, **Biomedicine & Pharmacotherapy**, v. 136, 2021.

NSAIRAT, H. *et al*., Liposomes: structure, composition, types, and clinical applications. **Helyon**, v. 8, n° 5, 2022.

NÚÑEZ, C. *et al*. An overview of the effective combination therapies for the treatment of breast cancer. **Biomaterials**, v. 97, p. 34 – 50, 2016.

OECD. Test No. 423: Acute Oral toxicity - Acute Toxic Class Method, OECD Guidelines for the Testing of Chemicals, Section 4, OECD Publishing, Paris, 2002.

PADDA, R.S. *et al.* Nanoscale flow cytometry to distinguish subpopulations of prostate extracellular vesicles in patient plasma, **The Prostate**, v. 79, n° 6, p. 592–603, 2019.

QIAO, L. *et al.* Tumor cell-derived exosomes home to their cells of origin and can be used as Trojan horses to deliver cancer drugs. **Theranostics**, v. 10, n° 8, p. 3474, 3487, 2020.

RAWAT, P.S. *et al.* Doxorubicin-induced cardiotoxicity: An update on the molecular mechanism and novel therapeutic strategies for effective management. **Biomedicine & Pharmacotherapy**, v. 139, 2021.

RAYAMAJHI, S. *et al.* Macrophage-derived exosome-mimetic hybrid vesicles for tumor targeted drug delivery. **Acta Biomaterials**, v. 94, p. 482-494, 2019.

REZAKHANI, L. *et al.*, Isolation and characterization of crab haemolymph exosomes and its effects on breast cancer cells (4T1). **Cell Journal**, v. 6, p. 658-664, 2021.

ROLLAND, C. L. *et al*. Inhibition of vascular endothelial growth factor reduces angiogenesis and modulates immune cell infiltration of orthotopic breast cancer xenografts. **Molecular Cancer Therapeutics***,* v. 8, p. 1761-1771, 2009.

ROMANÒ, S. *et al.*, Fourier transform infrared spectroscopy as a useful tool for the automated classification of cancer cell-derived exosomes obtained under different culture conditions. **Analytica Chimica Acta**, v.1140, p. 219-227, 2020.

ROQUE, M.C. *et al.* Preclinical toxicological study of long-circulating and fusogenic liposomes co-encapsulating paclitaxel and doxorubicin in synergic ratio. **Biomedicine & Pharmacotherapy**, v. 144, 2021.

SHETH, V. *et al.*, Strategies for Delivering Nanoparticles across Tumor Blood Vessels. **Advanced Functional Materials,** v. 31, n° 8, 2021.

SILVA, J.O. *et al.* Toxicological study of a new doxorubicin-loaded pH-sensitive liposome: A preclinical approach. **Toxicology and Applied Pharmacology,** v. 352, p.162-169, 2018.

SILVA, J.O. *et al.* Folate-coated, long-circulating and pH-sensitive liposomes enhance doxorubicin antitumor effect in a breast cancer animal model. **Biomedicine & Pharmacotherapy**, v. 118, 2019.

SINDHWANI, *et al.*, The entry of nanoparticles into solid tumours. **Nature Materials**, v. 19, p. 566-575, 2020.

SONGBO, M. *et al.* Oxidative stress injury in doxorubicin-induced cardiotoxicity. **Toxicology Letters**, v. 1, n° 307, p. 41-48, 2019.

SUN, L. *et al.* Clodronate-loaded liposomal and fibroblast-derived exosomal hybrid system for enhanced drug delivery to pulmonary fibrosis, **Biomaterials**, v. 271, 2021.

SUNG, H. *et al.* Global cancer statistics 2020: GLOBOCAN Estimates of Incidence and Mortality Worldwide for 36 Cancers in 185 Countries. **CA: A Cancer Journal for Clinicians**, v. 71, n°3, p. 209–249, 2021.

TACAR, O.; SRIAMORNSAK, P.; DASS, C. R. Doxorubicin: an update on anticancer molecular action, toxicity and novel drug delivery systems. **Journal of Pharmacy and Pharmacology**, v. 65, n°2, p. 157-170, 2013.

TAK, W.Y. *et al*. Phase III heat study adding lyso-thermosensitive liposomal doxorubicin to radiofrequency ablation in patients with unresectable hepatocellular carcinoma lesions. **Clinical Cancer Research**, v. 24, n° 1, p. 73-83, 2018.

TANG, Y.T. *et al.* Comparison of isolation methods of exosomes and exosomal RNA from cell culture medium and serum. **International Journal of Molecular Medicine***,* v. 40, p. 834–844, 2017.

TARDI, P. G.; BOMAN, N. L.; CULLIS, P. R. Liposomal doxorubicin. **Journal of Drug Targeting**, v. 4, n. 3, p. 129-140, 1996.

TOBLLI, J.E. *et al.* Ferric carboxymaltose-mediated attenuation of doxorubicin-induced cardiotoxicity in an iron deficiency rat model. **Chemotherapy Research and Practice**, v. 2014, 570241, 2014.

TOFFOLI, G. *et al*. Exosomal doxorubicin reduces the cardiac toxicity of doxorubicin. **Nanomedicine**, v. 10, n° 19, p. 2963- 2971, 2015.

TORCHILIN, V.P. Recent advances with liposomes as pharmaceutical carriers. **Nature**, v. 4, p. 145-160, 2005.

TRAYES, K.P.; COKENAKES, S.E.H. Breast cancer treatment. **American Family Physician**, v. 104, n°2, p. 171-178, 2021.

TSANG, J.Y.S.; TSE, G.M. Molecular Classification of Breast Cancer, **Advances in Anatomic Pathology**, v. 27, n° 1, 2020.

VICHAI, V; KIRTIKARA, K. Sulforhodamine B colorimetric assay for cytotoxicity screening, **Nature Protocols**, v. 1, n° 3, p. 1112–1116, 2006. DOI: 10.1038/nprot.2006.179.

VINCENT, T.L.; GATENBY, R.A. An evolutionary model for initiation, promotion, and progression in carcinogenesis. **International Journal of Oncology**, v.32, p.729-737, 2008.

WANG, J.; ZHENG, Y.; ZHAO, M. Exosome-based cancer therapy: implication for targeting cancer stem cells. **Frontiers in Pharmacology**, v.7, n° 533, 2016.

WANG, K. *et al.* An exosome-like programmable-bioactivating paclitaxel prodrug nanoplatform for enhanced breast cancer metastasis inhibition, **Biomaterials**, v. 257, 2020.

WHO, Classification of Tumors Editorial Board, ed. WHO classification of tumors, 5th edition – Breast tumors. Lyon: International Agency for Research on Cancer 2019.

WHO, 2021. Breast cancer. Disponível em: https://www.who.int/news-room/fact-sheets/detail/breast-cancer. Acesso em 29 de junho de 2022.

WHO, 2022. Disponível em: http://https://www.who.int/health-topics/cancer#tab=tab_1/. Acesso em 29 de junho de 2022.

YANG, F. *et al*. Doxorubicin, DNA torsion, and chromatin dynamics. **Biochimica et Biophysica Acta (BBA) – Reviews on Cancer**, v. 1845, n. 1, p. 84-89, 2014.

YIN, L. *et al.*, Triple-negative breast cancer molecular subtyping and treatment progress. **Breast Cancer Research**, v. 22, n° 61, 2020.

ZHAO, N.; WOODLE, M.C.; MIXSON, A.J. Advances in delivery systems for doxorubicin. **Journal of Nanomedicine & Nanotechnology**, v. 9, n° 5, 2018.

PRODUÇÕES RELACIONADAS À TESE

Pedido nacional de Invenção, Modelo de Utilidade, Certificado de Adição de Invenção e entrada na fase nacional do PCT

Número do Processo: BR 10 2021 024659 6

Dados do Depositante (71)

Depositante 1 de 2

Nome ou Razão Social: UNIVERSIDADE FEDERAL DE MINAS GERAIS
Tipo de Pessoa: Pessoa Jurídica
CPF/CNPJ: 17217985000104
Nacionalidade: Brasileira
Qualificação Jurídica: Instituição de Ensino e Pesquisa
Endereço: Av. Antônio Carlos, 6627 - Unidade Administrativa II - 2º andar- sala 2011
Cidade: Belo Horizonte
Estado: MG
CEP: 31270-901
País: Brasil
Telefone: (31) 3409-6430
Fax:
Email: patentes@ctit.ufmg.br

Depositante 2 de 2

Nome ou Razão Social:	FUNDAÇÃO DE AMPARO À PESQUISA DO ESTADO DE MINAS GERAIS - FAPEMIG
Tipo de Pessoa:	Pessoa Jurídica
CPF/CNPJ:	21949888000183
Nacionalidade:	Brasileira
Qualificação Jurídica:	Instituição de Ensino e Pesquisa
Endereço:	Av. José Cândido da Silveira, n. 1500, Bairro Horto
Cidade:	Belo Horizonte
Estado:	MG
CEP:	31035-536
País:	BRASIL
Telefone:	
Fax:	
Email:	

Dados do Pedido

Natureza Patente:	10 - Patente de Invenção (PI)
Título da Invenção ou Modelo de Utilidade (54):	COMPOSIÇÃO FARMACÊUTICA CONTENDO DOXORRUBICINA ENCAPSULADA EM VESÍCULAS HÍBRIDAS DE EXOSSOMAS TUMORAIS E LIPOSSOMA pH-SENSÍVEL, PROCESSO E USO
Resumo:	A presente tecnologia trata de uma composição farmacêutica contendo o fármaco doxorrubicina (DXR) encapsulado em vesículas híbridas de exossomas derivados de células de mama tumorais fundidos com lipossomas pH-sensíveis de circulação prolongada. A tecnologia trata ainda do processo de produção e do uso dessa composição para a produção de medicamentos para o tratamento de câncer.
Figura a publicar:	3

AAPS PharmSciTech (2022) 23:255
https://doi.org/10.1208/s12249-022-02349-y

RESEARCH ARTICLE

Fusion of Tumor-Derived Exosomes with Long-Circulating and pH-Sensitive Liposomes Loaded with Doxorubicin for the Treatment of Breast Cancer

E. R. Gomes[1] · A. T. Carvalho[2] · T. C. Barbosa[3] · L. L. Ferreira[4] · H. D. R. Calado[4] · A. P. Sabino[5] · M. C. Oliveira[1]

Received: 5 April 2022 / Accepted: 28 June 2022

Abstract

Doxorubicin (DOX) is a chemotherapeutic agent that has been used in the treatment of breast cancer. However, serious toxic effects have limited its use, mainly cardiotoxicity. To minimize the adverse effects, liposomal preparations containing DOX have been developed. These preparations can reach the target in the tumor region as well as bypass the resistance-related problems. An alternative to increased therapeutic efficacy may be the fusion of liposomes with exosomes released from tumor cells to facilitate membrane and fusion interactions, achieving greater cell uptake. Thus, the purpose of this study was the fusion of exosomes derived from breast tumor cells with long-circulating and pH-sensitive liposomes loading DOX (ExoSpHL-DOX) for the treatment of breast cancer. The mean diameter of ExoSpHL-DOX was 100.8 ± 7.8 nm, the polydispersity index was 0.122 ± 0.004, and the encapsulated DOX content was equal to 83.5 ± 2.5%. The fusion of exosomes with long-circulating and pH-sensitive liposomes was confirmed by Fourier transform infrared spectroscopy, Raman spectroscopy, and nano-flow cytometry. The physicochemical characteristics of ExoSpHL-DOX were maintained for 60 days, at 4 °C. The study of the release of DOX from ExoSpHL-DOX in dilution media with different pH values showed the pH sensitivity characteristic of the nanosystem, since 96.6 ± 0.2% of DOX was released from ExoSpHL-DOX at pH 5.0, while at pH 7.4, the release was 70.1 ± 1.7% in the medium. The cytotoxic study against the breast cancer cell line demonstrated that ExoSpHL-DOX treatment significantly reduced the cancer cell viability.

Keywords Breast cancer · Liposomes · Exosomes · Fusion · Doxorubicin

Introduction

Anthracycline antibiotics, such as doxorubicin (DOX), are of great importance being used in the treatment of breast cancer [1, 2]. However, the high toxicity, mainly cardiac, related to DOX, as well as the resistance mechanisms developed by cells to this drug, has limited its use [2–5]. To minimize the adverse effects of DOX, nanocarriers, such as liposomes, are in development for delivering the antitumor drug [2, 4, 6].